Bio-Inspired Plastics

Derived from Aquaculture By-product

A thesis

submitted in partial fulfilment

of the requirements for the degree

of

Master of Science (Research)

Materials and Processing

at

The University of Waikato

by

Zachary J. Howarth

THE UNIVERSITY OF
WAIKATO
Te Whare Wānanga o Waikato

2023

This page is deliberately left blank

.

Abstract

The deliberate cultivation of seafood through aquaculture is expanding with a focus on environmental sustainability, specifically decreasing global emissions and waste. In New Zealand this industry is growing at a rapid pace with intentions to scale up the farming of species such as salmon, pacific oysters and Greenshell™ Mussels.

During processing by-products such as mussel shell are produced and often sent to land fill. Greenshell™ mussel shells consisted of approximately 90% calcium carbonate (Hamester, Balzer, & Becker, 2012) making it a valuable resource.

This study focuses on the creation of polymer composites and foams which have been inspired by the marine environment and the materials in it such as calcium carbonate from mussel shells. It specifically aimed to incorporate mussel shell powder (0-30wt% for composites and 0-10wt % for foams) into polylactic acid (PLA) and low-density polyethylene (LDPE). These polymers were chosen for their bioderived nature and degree of recyclability respectively. This work creates, characterises, and tests these materials to determine potential applications.

Composite materials were successfully extruded and then processed into 3D printing filaments to extend the applications of these materials. These samples were tensile tested, and granulated composites were used for thermal analysis. PLA composites showed far superior tensile strength and stiffness over LDPE samples, reaching 60.69 MPa yield stress and 3748 MPa Youngs' modulus at 8wt% of mussel shell powder, with LDPE composites reaching 8.9 MPa yield stress and 197 MPa Youngs' modulus. At 30wt% of mussel shell both PLA and LDPE samples showed less plastic deformation with PLA + 30wt% sample reaching failure almost instantly.

Thermal stability of PLA and LDPE composites showed varying properties. The most notable difference between the two polymers was the change in thermal degradation temperature as the weight percentage of mussel shell powder was increased. PLA samples showed a reduction in thermal degradation temperature due to the introduction of moisture and hydrolysis as the weight percentage of mussel shell powder increased, decreasing from 340℃ (0wt%) to 287℃ (30wt%). LDPE samples showed an increase in thermal degradation temperature due to the high volumes of ceramic mussel shell powder and no hydrolysis.

Thermal degradation of LDPE composites was seen to increase by 22°C between the control sample to 30wt% samples.

Extruded foams were moulded into small blocks for compression and microscopy. PLA foams showed higher expansion ratios than LDPE foams and much lower density. PLA 0.5wt% reached three times the expansion of un-foamed PLA and showed the highest expansion ratio of all samples tested. The expansion of PLA foams decreased between 0.5wt% and 10wt% as expected while the compressive strength showed a good improvement from 5 MPa to 20 MPa. Overall, LDPE foams had both lower compressive stress (13 MPa) and expansion (1.5) than the PLA samples. LDPE samples showed far greater recovery at 70%, which was 40% higher than PLA foams.

In summary, PLA displayed best reinforcement at 8wt%, best thermal properties between 0-2wt% and best foam nucleation results at 0.5wt%. Finally, LDPE samples showed comparable results with best reinforcement at 8wt%, best thermal properties between 20-30wt% and best foam nucleation results at 0.5-1wt%.

This thesis has thoroughly investigated composites and foams that could be introduced into a circular economy, resulting in a beneficial impact on the environment. Options for biodegradable (PLA) and recyclable (LDPE) polymers were shown while valuable by-product material (mussel shell) was introduced to composites and foams as a method of reducing stress on landfills and improving the properties of these materials. These materials could be made into complex containers, sandwich composites, and equipment in the medical, automotive, and aerospace industries.

Acknowledgments

I would like to start off with a massive thanks to my supervisor Chanelle Gavin. Firstly, I cannot express how grateful I am for your patience, wisdom, knowledge, and feedback throughout every stage of this experience. Secondly, I would like to thank you for your support outside of this project, including help in other papers and checking on my general wellbeing throughout the last year and a half, especially when the lab equipment was playing up. Lastly, I would like to thank you for avoiding 9am meetings 90% of the time and choosing optimal learning hours after 12pm. Also, thanks for allowing me to have a cheeky holiday halfway through the year.

Additionally, I would like to extend a huge thanks to the University of Waikato and the Engineering and Science departments for allowing me to use their facilities and most of all the scholarship and funding of this research. Thanks to Whakatōhea Mussels Limited for providing waste material that could be repurposed in an effort to develop biodegradable and sustainable biomaterials that can be implemented into a circular economy.

I am also grateful to Jonathan van Harselaar, Sophia Rodrigues and Helen Turner for teaching and helping me with experimental processes and troubleshooting. Thank you to Rob Torrens for suppling me with a part time job teaching first years. Thank you also for your help and advice when Chanelle was unavailable.

Thank you to my peers in the materials engineering and LSL WESMO groups for help and advice throughout my time working with you guys. Thanks for the friendly chats as well as allowing me to use the lab instruments when I forgot to book them.

A special thanks to my beautiful partner Olivia Whorskey for supporting me through this journey. I appreciate the unwavering love and patience you have shown me. Your encouragement has been a constant source of motivation to help me complete this thesis.

Lastly, I would like to mention a thanks to my family and friends for the support and keeping me on track. Thank you to my parents Nicky Howarth and Wayne Howarth for the support and encouragement to perform at my best throughout university. Thanks to my sister Jesse Howarth for competitively pushing me to excel to my greatest academic potential. Cheers, to all my friends for supporting me especially Charles Johnson, Jared Steel, Levi Clothier, Nash Smith, Rohan Lewis, Royden Thony, and Zach Clothier for always and listening to my constant rants, enragement and complaining about what is going wrong in my work.

Table of contents

Abstract ..... **i**

Acknowledgments ..... **iii**

List of figures ..... **viii**

List of tables ..... **xi**

Introduction **1**

Chapter one: Literature review **3**

What is aquaculture? 3

New Zealand aquaculture 5

Aquaculture farming techniques 8

Offshore and nearshore farming 8

Onshore farming 9

Species 10

Mussels 10

Kingfish 11

Paua 12

Oyster 13

Sustainability in aquaculture 14

Aquaculture waste from processing 15

Mussel waste 16

Research in aquaculture waste 17

What does bio-inspired mean? 19

Applications 19

Materials 20

Plastic production 21

Plastic waste 21

Types of plastics 22

Fossil-based plastics 22

Bio-based and biodegradable plastics 24

Low density polyethylene 26

Polylactic acid 26

Specialist materials 27

Composite plastics 27

Polymer foams 30

Conclusion 32

Aims and objectives **34**

References **36**

Chapter two: Methodology **48**

Characterisation of mussel shell powder 48

Creation of mussel shell powder 48

Cleaning and disinfection 48

Crushing and milling 48

By-product characterisation 49

Optical microscopy 49

Scanning electron microscopy 49

Thermal gravimetric analysis 49

Hydroscopic analysis 50

Particle size analysis 50

Experimental 50

Plastic grades 51

PLA 3052D 51

LD 2420D 51

Weight percentage 51

Sample preparation 51

Extrusion 52
Granulation 53
Filament extrusion 53
3D printing 53
Sample characterisation and testing 53
Optical microscopy 53
Scanning electron microscopy 54
Thermal gravimetric analysis 54
Tensile testing 54
Compression testing 54
Foam density and expansion 55
Experimental plans 55
Chapter 3 - Characterisation outline 55
Chapter 4 - Experiment one outline 55
Chapter 5 - Experiment two outline 56
References **57**
Chapter three: Characterisation **58**
Mussel waste characterisation 58
Shell characterisation 58
SEM and optical microscopy 59
Particle analysis of mussel shell powder 61
Hydroscopic behaviour of mussel shell powder 62
Simultaneous thermal analysis 63
References **65**
Chapter four: Experiment one **66**
Filament composites 66
Tensile testing 69

Microscopy/SEM 75

Thermal analysis 77

Thermogravimetric analysis 78

Differential scanning calorimetry 85

3D printing 91

References **93**

Chapter five: Experiment two **95**

Density and Expansion Ratios 96

SEM/microscopy 99

Compression 102

Cyclic compression 106

Compression summary 106

References **110**

Chapter six: Applications **111**

PLA composites 111

PLA foams 112

LDPE composites 113

LDPE foams 114

References **115**

Chapter seven: Conclusion and recommendations **117**

Appendices **120**

Appendix A: Brief history of fisheries 120

Appendix B: Plastic processing profile 121

Appendix C: Particle size analysis 123

Appendix D: Tensile graphs 124

Appendix E: Compression graphs 135

List of figures

Figure 1: Effective number of species in large aquaculture countries/territories, 2018. Reproduced from: (Cai, Yan, & Leung, 2022) 4
Figure 2: World aquaculture production of aquatic animals and algae, 1990-2018. Reproduced from: (FAO, n.d.) 5
Figure 3:New Zealand mussel farming. Reproduced from: (Broekhuzen, n.d.) 6
Figure 4: Recirculating Aquaculture System. Reproduced from: NIWA (n.d). 9
Figure 5: Lifecycle of Greenshell™ Mussel. Reproduced from: NIWA (n.d.). 11
Figure 6: Kingfish at the Northland Aquaculture Centre (Mackay, n.d) 12
Figure 7: Lifecycle of Pacific Oysters, Reproduced from: NIWA (n.d). 13
Figure 8: Common types of Fossil-Based Plastics 23
Figure 9: Experimental Flowchart 50
Figure 10: Half mussel shells a) outside and b) inside 58
Figure 11: Mussel shell x5 magnification 59
Figure 12: a) Mussel shell fracture surface x5 magnification, b) Mussel shell fracture SEM. 60
Figure 13: a) Calcium carbonate powder made from mussel shell x5 magnification, b) Calcium Carbonate powder made from mussel shell SEM. 60
Figure 14: Cumulative distribution of mussel shell powder particle size. 61
Figure 15: Hydroscopic behaviour of mussel shell powder 62
Figure 16: TGA for mussel shell 63
Figure 17: DSC for mussel shell 63
Figure 18: Filament process, a) Filament cooling fans, b) Filament measurement system, c) Filament spool collection. 67
Figure 19: LDPE + 30wt% filament during tensile testing 68
Figure 20: Tensile results for PLA 0-2wt% samples 69
Figure 21: Tensile results for PLA 4-10wt% samples 70
Figure 22: Tensile results for PLA 10-30wt% samples 70
Figure 23: Tensile results for LDPE 0-2wt% samples 71
Figure 24: Tensile results for LDPE 4-10wt% samples 72
Figure 25: Tensile results for LDPE 10-30wt% samples 72
Figure 26: Yield stress of PLA and LDPE composites in relation to weight percentage of filler. 74

Figure 27: Youngs' modulus of PLA and LDPE composites in relation to weight percentage of filler. 74
Figure 28: Ultimate tensile stress of PLA and LDPE composites in relation to weight percentage of filler. 75
Figure 29: Tensile images a) control b) 2wt% c) 10wt% d) 30wt%. [note: the top sample in each image is LDPE and the bottom sample in each image is PLA] 76
Figure 30: SEM tensile images a) PLA control, b) LDPE control, c) PLA 2wt%, d) LDPE 2wt%, e) PLA 10wt%, f) LDPE 10wt%, g) PLA 30wt%, h) LDPE 30wt%. 77
Figure 31: TGA of PLA 0-2wt% samples showing thermal degradation. 79
Figure 32: TGA of PLA 4-10wt% samples showing thermal degradation. 80
Figure 33: TGA of PLA 10-30wt% samples showing thermal degradation. 81
Figure 34: TGA of LDPE 0-2wt% samples showing thermal degradation. 82
Figure 35: TGA of LDPE 4-10wt% samples showing thermal degradation. 83
Figure 36: TGA of LDPE 10-30wt% samples showing thermal degradation. 84
Figure 37: Thermal degradation temperatures of PLA and LDPE composites in relation to weight percentage of filler. 85
Figure 38: DSC of PLA 0-2wt% samples showing thermal peaks. 85
Figure 39: DSC of PLA 4-10wt% samples showing thermal peaks. 87
Figure 40: DSC of PLA 10-30wt% samples showing thermal peaks. 88
Figure 41: DSC of LDPE 0-2wt% samples showing thermal peaks. 89
Figure 42: DSC of LDPE 4-10wt% samples showing thermal peaks. 90
Figure 43: DSC of LDPE 10-30 wt% samples showing thermal peaks. 90
Figure 44: PLA tensile bars a) 0-10wt% bars, b) close view of tensile bars. 91
Figure 45: PLA foam compression blocks (0.5wt%), b) LDPE foam compression blocks (0.5wt%), c) PLA foam compression blocks (8wt%), d) LDPE foam compression blocks (8wt%) 96
Figure 46: Expansion ratio of PLA and LDPE with increasing nucleating agent 96
Figure 47: Density of PLA and LDPE with increasing nucleating agent 98
Figure 48: Foam images at 1x stereo microscope: a) PLA control, b) LDPE control, c) PLA + 2wt%, d) LDPE + 2wt%, e) PLA + 10wt%, f) LDPE +10wt%. 100
Figure 49: SEM images of foam a) PLA control, b) LDPE control, c) PLA + 2wt%, d) LDPE + 2wt%, e) PLA + 10wt%, f) LDPE +10wt%. 101
Figure 50: PLA foam compression 0-2wt% (low weight percentage) 102
Figure 51: PLA foam compression 4-10wt% (medium weight percentage) 102

Figure 52: LDPE foam compression 0-2wt% (low weight percentage) 103
Figure 53: LDPE foam compression 4-10wt% (medium weight percentage) 103
Figure 54: Compressive stress of PLA and LDPE with various expansion ratios 104
Figure 55: Relative stiffness of PLA and LDPE for relative density 105
Figure 56: Cyclic compression of PLA and LDPE 106

List of tables

Table 1: Some potential species for aquaculture in the Bay of Plenty Region. Reproduced from: Bay of Plenty Regional Council Aquaculture Group (2011). 8
Table 2: Plastics used in mussel farms and general use in New Zealand 17
Table 3: Types of Fossil-Based Plastics. Reproduced from WasteMINZ (2022). 23
Table 4: Types of Bio-Based Plastics, Reproduced from WasteMINZ (2022). 25
Table 5: Powder for low weight percentages 51
Table 6: Powder for medium and high weight percentages 51
Table 7: Composite and foam extrusion processing profile 52
Table 8: Plastic processing profile 52
Table 9: PLA foam properties 107
Table 10: LDPE foam properties 108

Introduction

The global decline in ocean stocks, the increased demand for seafood, and our growing population are driving growth in the aquaculture industry. The deliberate cultivation of seafood species will reduce ocean harvest, reducing pressure on wild populations (Naylor et al., 2000). Therefore, aquaculture has begun to pave the way for more environmentally friendly and biologically efficient farming with much lower global average emissions (MacLeod et al., 2020). New Zealand has a large coastline making aquaculture an attractive option. Consequently, the New Zealand government has committed to growing this industry to $3 billion by 2035, with significant growth expected in the Bay of Plenty region, and a focus on sustainable farming practices.

Although aquaculture is seen as inherently sustainable a substantial portion of waste, specifically by-products such as shell, protein, by-catch and plastics are produced from aquaculture cultivation. As most of the waste ends its life cycle in landfill, there is little contribution to a circular economy. Efforts to minimise these waste streams can include incorporating them into new materials, while inspiration can be taken from the marine environment itself leading to bio-inspired materials. The aim of materials development is to create materials for applications which have higher levels of sophistication, are recyclable, and benefit the environment (Sanchez, Arribart, & Guille, 2005).

This project will focus on waste minimization of Greenshell™ mussel shells, while drawing inspiration from the marine environment. The shells which are mainly calcium carbonate will be incorporated into composite and foamed plastics, mimicking structures observed in nature. This study builds upon previous literature which has shown calcium carbonate is an effective filler and nucleating material. Previous studies which have examined alternative sources of calcium carbonate included eggshell and other mollusc shells but not Greenshell™ mussels.

This work builds upon preliminary work previously conducted at the University of Waikato. Therefore, the scope of this master's thesis is to continue to develop and trial bio-inspired composites and foams. It specifically studies polylactic acid (PLA), a bioderived and biodegradable thermoplastic, and compares this to materials made with low-density polyethylene (LDPE), a conventional plastic which does not biodegrade.

Key research questions:

- What is the optimum weight percentage of mussel shell powder which can be included in a PLA or LDPE bio-composite as a filler?
- Can mussel shell powder effectively nucleate polymer foams at low percentages and provide reinforcement within PLA and LDPE foams at higher weight percentages?

The broad scope of this study is to enable these composites and foams to be evaluated as potential future products and to identify where further research is required.

This thesis is structured as follows:

Chapter one covers previous academic studies relating to the aquaculture industry, specifically New Zealand aquaculture, in addition to previous bio-inspired materials and their applications, and PLA/LDPE composites and foams containing calcium carbonate. Chapter two includes the methods used to make mussel shell powder and the production of the polymer composites and foams, along with experimental methods. The experimental chapters cover properties of mussel shell, PLA/LDPE composites and PLA/LDPE foams. The characterisation of these samples was conducted using light microscopy, scanning electron microscopy, thermal analysis, tensile and compression tests, and the results are reported in chapters three to five. The next chapter evaluates potential applications for the PLA/LDPE composites and foams studied in this thesis. The last chapter concludes the findings of this study and makes recommendations as to future work.

Chapter one: Literature review

Previous studies at the University of Waikato have tested the feasibility of incorporating aquaculture waste into various polymers. It was determined that a polymer composite and foam could be produced from a bio-based plastic (polylactic acid) and calcium carbonate (mussel shell). This work continues from there and looks at the research and findings from other academics on similar topics. With many options of calcium carbonate fillers worldwide the research was narrowed down to waste produced sustainably and locally through aquaculture in New Zealand.

This literature review provides a background to the wider aquaculture industry, the species cultivated and farming methods. It then covers other types of aquaculture waste before focusing on mussel shells and previous studies which have used calcium carbonate as a filler in bio-composites or a nucleating agent in foams.

What is aquaculture?

Aquaculture is the cultivation of marine, freshwater or hatchery-based animals and plants (*Aquaculture*, n.d). Aquaculture is set to reduce pressure on fisheries, improve water quality, and strengthen aquatic biodiversity (Frankic & Hershner, 2002). Therefore, aquaculture is the most rapidly growing industry worldwide, increasing by approximately 10-15% in volume every year since 1996. Globally the consumption of fish and shellfish is projected to increase by more than 27% by 2030, with the aquaculture sector expected to increase by 62% by weight to help meet the demand (Reverter et al., 2020). Aquaculture is currently led by Asia, which contributes 89% of aquaculture production worldwide by volume. Within this region, China cultivated 66 million tonnes in 2018, making up a total of 27% of global production (Cai, Yan, & Leung, 2022). Countries in Oceania, such as New Zealand have been increasing in volume, but still produce very little in comparison to the leading countries, only 0.1 million tonnes.

An indicator of diversity within the aquaculture industry is the effective number of species (ENS). This relates to both the number of different species farmed and the proportions of these species. The left column on the graph shows the country and mass of annual cultivation. The right column on the graph shows the effective number of species in an aquaculture system. It is notable that China has the highest ENS value of over 27, where most countries average 3-5 (Figure 1).

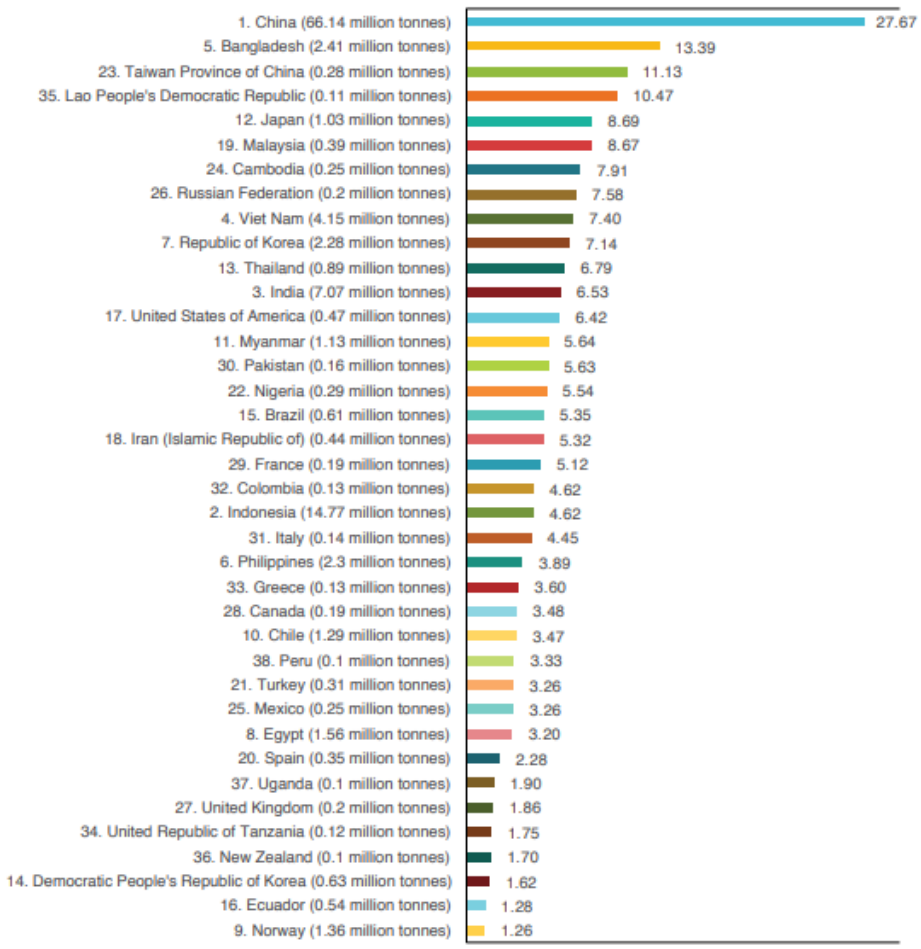

Figure 1: Effective number of species in large aquaculture countries/territories, 2018. Reproduced from: (Cai, Yan, & Leung, 2022).

Currently there are over 220 species farmed globally which can be categorised as finfish, crustaceans, and shellfish. Most species tend to be salmon, shrimp, carp, mussels, and giant clams. According to the Food and Agriculture Organization (FAO) the combination of freshwater and saltwater finfish production has been the leading species to farm in aquaculture (Figure 2). This is a consequence of crustacean farming (crabs, crayfish, prawns, and shrimp) being dependent on a concentrated and highly strict diet (Naylor et al., 2000), limiting production to 9.4 million tonnes in 2018 (FAO, 2020). Recently there has been growing opportunities towards species of molluscs (clams, mussels, and oysters) as an alternative to finfish. Figure 2 shows a large increase of 12 million tonnes for molluscs between 1990 and 2018, reaching a total of 17.3 million tonnes of production by weight in 2018.

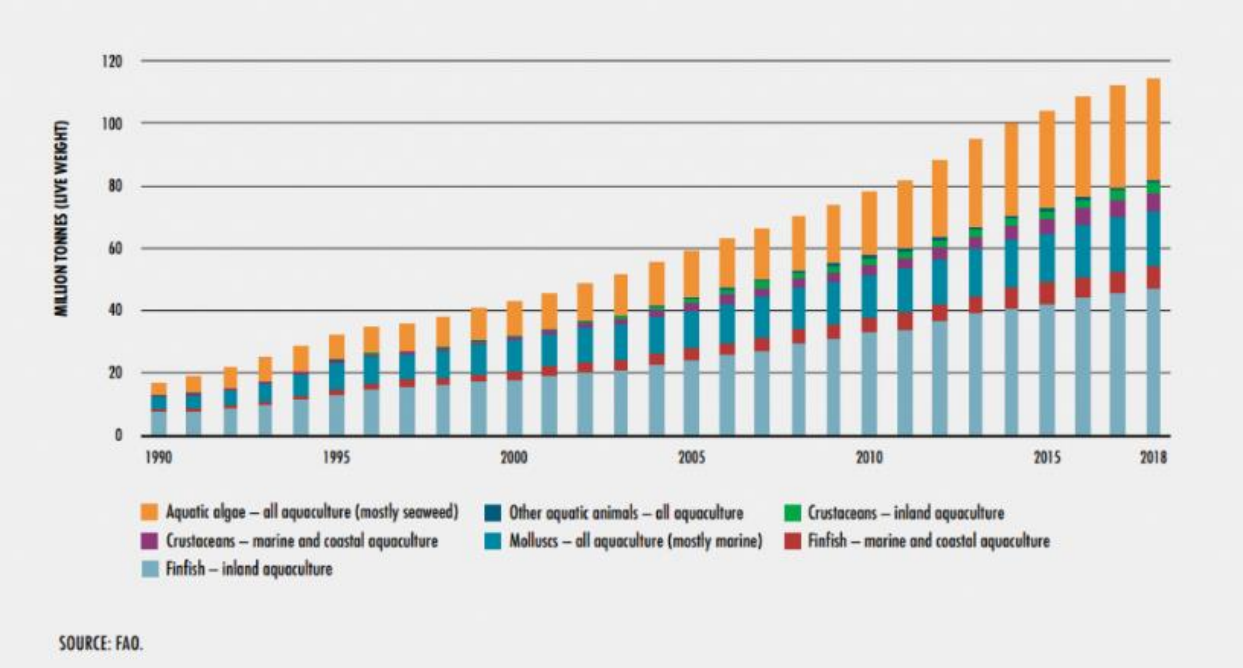

Figure 2: World aquaculture production of aquatic animals and algae, 1990-2018. Reproduced from: (FAO, n.d.).

It should also be noted that large volumes of aquatic algae including seaweed are produced globally in aquaculture however, it is not a focus of this review.

New Zealand aquaculture

Aquaculture is an ideal opportunity for New Zealand due to the extensive coastal area of over 4 million square kilometres, making it the fourth largest in the world. Additionally, the Bay of Plenty region has the most productive waters for commercial farming and makes up 44% of the coastal areas for aquaculture in New Zealand, with a major export port, the Port of Tauranga in a close vicinity (*Bay of Connections Aquaculture Strategy 2013*, 2013). In New Zealand the most common species farmed in aquaculture are mussels (Figure 3), paua, oysters and kingfish.

Figure 3:New Zealand mussel farming. Reproduced with permission from NIWA: (Broekhuzen, n.d.).

The New Zealand Government Aquaculture Strategy (2019) states that “development through innovation and best practice can enrich our communities and our global reputation”, while producing seafood and products that are “sustainable, healthy and highly valued.” The strategy defines its challenges as meeting consumer demand sustainability and to reduce the increasing pressure on the natural ecosystem due to climate change. It also notes that the increase in the global population has deemed the majority of capture fisheries at or near capacity. This means that aquaculture is essential as a viable and proven option to increase sustainability within the earth’s environmental limits. The strategy document reviews developments in land-based and offshore aquaculture systems to increase growth in the sector to reach an annual sales goal of $3 billion by 2035 (New Zealand Government, 2019). Currently, the New Zealand Government has financially assisted in developing the Opotiki farms with the opening of the Whakatohea mussel processing factory and the mussel reef restoration in the Marlborough Sounds (New Zealand Government, 2022). Cultivation of mussels in New Zealand has been limited to high subtidal and sheltered inshore areas (Martínez-García, González-Fonteboa, Martínez-Abella, & López, 2017), such as coastal estuaries which are partially enclosed bodies of water (NIWA, 2001). These are known to

be suitable for growth for the native mussel species (Martínez-García, González-Fonteboa, Martínez-Abella, & López, 2017).

This industry was recognised as a priority for the Bay of Plenty as early as 2009, when a strategy for aquaculture farming in the Bay of Plenty was launched to create an integrated and sustainable aquaculture industry. This strategy was implemented to mitigate pressure on the industry and to help the breeding and growth of animals and plants in the aquatic environment (*Aquaculture*, n.d). During this time, there was a 3,300ha aquaculture farm in Opotiki, with proposals for larger developments to substantially contribute to the economy. Research into the appropriate species and conditions to farm in aquaculture is being progressed with many opportunities looking viable (Table 1) (Bay of Plenty Regional Council Aquaculture Group, 2011). The aquaculture strategy was further updated in 2013, with the vision of the Bay of Plenty being a world-class aquaculture region and the continuation of the goal to grow an integrated and sustainable aquaculture industry with export sales of $250 million by 2025. Over the years between 2009 and 2013 the Bay of Connections have established collaboration between Waikato University, Bay of Plenty Polytechnic, and local Iwi-led mussel farms (Bay of Connections, 2013). Currently, the focus is on continued support for the Opotiki Harbour and proposed expansion of the Coastal Marine Field Station at Sulphur Point, with the idea to promote and advocate for marine science, technology, education and training, for the future growth of the aquaculture industry (Bay of Connections, 2018).

Table 1 shows a few species that could potentially be cultivated in aquaculture in the Bay of Plenty Region. Although there are hatcheries for these species elsewhere in New Zealand, there are processes to develop farms in the Bay of Plenty Region. Waikawa Point and Mamaku facilities are in development and trialling black-foot paua operations. Ohiwa Harbour has three operational oyster farms of approximately 2ha each. Opotiki is the largest farm, producing mussels, scallops, pacific oysters, and flat oysters, with current commercial trials underway (Bay of Plenty Regional Council Aquaculture Group, 2011).

Table 1: Some potential species for aquaculture in the Bay of Plenty Region. Reproduced from: Bay of Plenty Regional Council Aquaculture Group (2011).

Species	Temperature Range (Ideal)	Saltwater/ Freshwater	Comments
Kingfish	>15°C	Saltwater	The global kingfish aquaculture industry is steadily growing. Increasing market demand from Japan and USA. Kingfish farming has yet to achieve commercial success in New Zealand.
Mussels	Natural temperature range ~15°C	Saltwater	Grow in waters throughout the country and is an established industry in New Zealand. Growth trials at offshore sites in Opotiki have shown favourable results.
Pacific Oyster	15-18°C	Saltwater	Established industry in New Zealand. Currently farmed on a small scale in Ohiwa Harbour.
Paua	Optimal: 16°C	Land-based saltwater	Established aquaculture and wild catch industries in New Zealand, with two small farms in Bay of Plenty. High costs associated with pumping seawater onto land.

Aquaculture farming techniques

The process of cultivating fish and shellfish depends on the species and location. Naylor et al. (2000) states that generally molluscs are farmed on coastlines or in wild hatcheries, while crustaceans are farmed in coastal ponds. For species to thrive the ideal conditions must be met which match the species natural habitat. Similarly, the conditions in the enclosure hatchery system must be artificially controlled to do the same.

Offshore and nearshore farming

Offshore and nearshore aquaculture are defined by certain parameters including water depth, distance from shore and wave exposure (Gentry, et al., 2017). Offshore aquaculture farms are located in open water and tend to reside within sight of the shoreline in fairly sheltered waters at depths of 10-50m (Holmer, 2010), where nearshore aquaculture farms are located neighbouring bays, shores or coastlines (Gentry et al., 2017; Troell et al., 2009). Both styles can include fish-cage aquaculture which use a flow-through net-pen system (Troell et al., 2009). While fish can be farmed in both environments' shellfish are predominately restricted to nearshore farming due to the lower harvesting depths.

Onshore farming

Onshore aquaculture has adapted land-based tanks to reduce coastal habitat depletion and to mitigate global climate change. Each farm has the addition of a water filtering process to remove sludge and increase the water quality of each tank (Tal et al., 2009). East Land Aquaculture Ltd built a recirculating aquaculture system in 2003 which was found to promote rapid growth rates in paua. The design was built in collaboration with Bream Bay Aquaculture Park and NIWA's recirculating aquaculture systems (RAS) tanks. Further species have been trialled in New Zealand since 2003 (NIWA, 2006).

The Northland Marine Research Centre in New Zealand currently have two recirculating aquaculture system (RAS) one of which is 6x5 m^3 and the other 2×25 m^3 consisting of three side by side tanks (Figure 4). These tanks are land based and utilize water treatment systems that reduce the water usage, with ideally 100% of the water in the tanks being reused. Varying species of aquatic organisms and finfish have been produced, with the RAS systems capable of being changed based on the species growth and functionality (NIWA, n.d.).

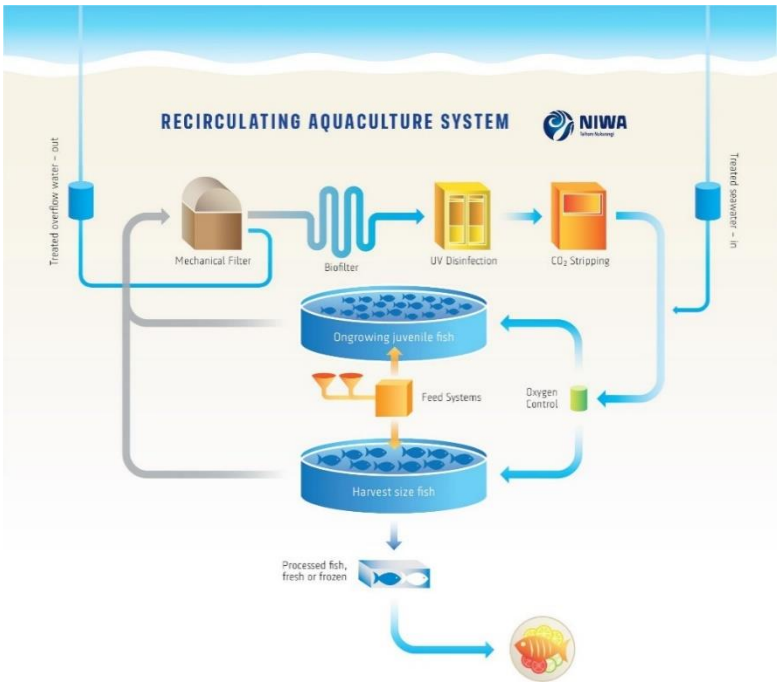

Figure 4: Recirculating Aquaculture System. Reproduced from: NIWA (n.d).

Species

As mentioned previously in New Zealand the most common species farmed in aquaculture are mussels, paua, oysters and kingfish. This section looks at the most common species in New Zealand aquaculture, basic lifecycles of these species and the methods used for cultivation.

Mussels

Currently in New Zealand the main species being farmed in aquaculture is Greenshell™ Mussel which is also known as the Green lipped mussel, or scientifically speaking *Perna canaliculus* (Jeffs et al., 2018). Aquaculture mussel beds in New Zealand have been implemented to compensate for the loss of natural habitats caused by dredging, trawling and sedimentation. These mussel beds now support vast ecosystems that were once abundant (Broekhuizen & Stenton-Dozey, 2019). Figure 5 shows the lifecycle of mussels in a farmed environment where New Zealand farms utilise a method known as a longline culture system (Woods et al., 2012). Long line culture uses buoyed lines that are approximately 110m long and run along the sea-surface with dropper lines that run towards the ocean floor. The dropper lines have crop mussels seeded onto them once past the metamorphic larvae stage (NIWA, n.d.). The majority of New Zealand aquaculture farms are located in estuaries, bays and coastlines; specifically, in the Firth of Thames, Marlborough Sounds and Bay of Plenty. (Longdill et al., 2008).

Export volumes of green lipped mussels reached 100,000 tonnes/year in 2005, which showed a double in exports from 1995 (Longdill, Healy, & Black, 2008). The Bay of Plenty has a specialised factory which deals with locally grown aquaculture products. North Island Mussel Ltd (NIML) has a factory capable of processing up to 100 green weight tonnes (GWT) of mussels per day (Bay of Plenty Regional Council Aquaculture Group, 2011). New Zealand exports this native species of mussel to approximately sixty countries (Martínez-García, González-Fonteboa, Martínez-Abella, & López, 2017).

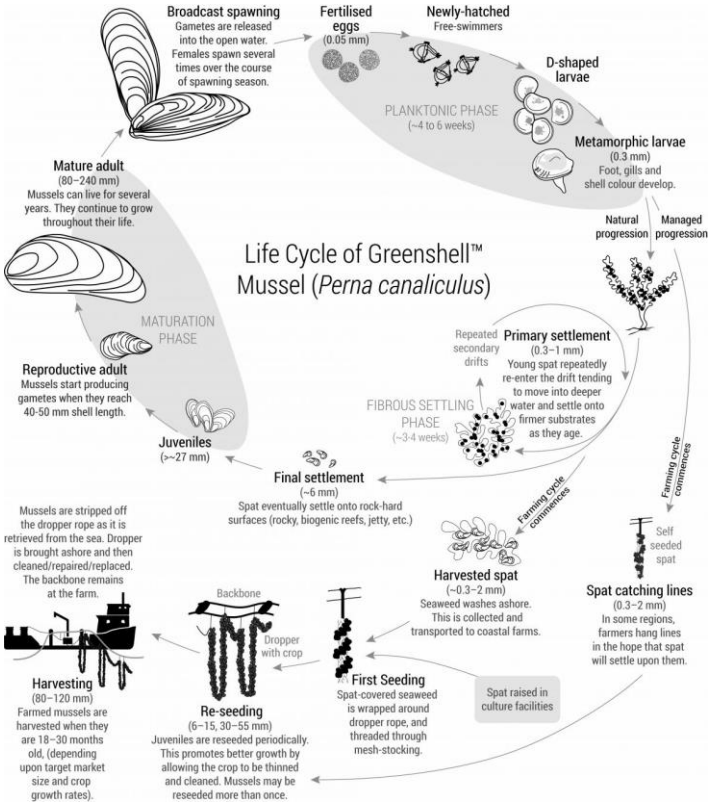

Figure 5: Lifecycle of Greenshell™ Mussel. Reproduced with permission from: NIWA (n.d.).

Kingfish

Historically, farming species of kingfish (*Seriola*) in sea cages has been successful in Japan, producing approximately 150,000 tonnes per annum. Kingfish hatcheries have been established in countries such as Australia, Chile, and Mexico, that have improved broodstock conditioning, controlled spawning, larval rearing, and juvenile production. European countries (Denmark and Netherlands) have implemented land-based tanks to attempt to increase harvest size (NIWA, 2020).

Figure 6: Kingfish at the Northland Aquaculture Centre. Reproduced with permission from NIWA (Mackay, n.d).

Yellowtail kingfish is ideal for aquaculture farming due to the rapid growth rate, high market value and the quality of the product for consumption (NIWA, 2020). Kingfish are found in the open coastal waters, rocky outcrops, and reefs around northern New Zealand (Ministry for Primary Industries, n.d). Yellowtail kingfish aquaculture farms are currently being trialled at the Northland Marine Research Centre (Figure 6) where there is a commercial based prototype hatchery which is expected to sustainably produce up to 3,000 metric tonnes of kingfish.

Paua

Paua in New Zealand is also being farmed in various locations. Water is pumped from the ocean into land-based hatcheries, with Paua taking up to four years to reach commercial sizes for consumption. Currently only black foot Paua is being farmed in New Zealand, but there are also naturally growing yellow foot and white foot Paua in the ocean (*Land Based Aquaculture Assessment Framework*, n.d). Paua reproduce by broadcast spawning, where microscopic larvae which float around in the water and eventually sink to the bottom. Once settled the larvae begin to develop shells. This breeding process is often unreliable with a very low survival rate. (The Paua Industry Council, n.d) During the 90's the Paua aquaculture industry set a production goal to reach 100 tonnes per year, but was only breaking 2 tonnes per year in 2001 (Heath, 2006) equating to approximately $80 million (The Paua Industry Council, n.d). From 2002 better development

processes have been researched, with a flow-through seawater system in Mahanga Bay, showing a 50% increase in Paua growth rates (Heath, 2006).

Oyster

Although New Zealand has a native species of oyster the pacific oysters were introduced into New Zealand in the 1960s. Oysters follow similar growth patterns to mussels, but do not re-attach to the environment after the spat stage. Instead of been permanently attached in contrast to mussels, oysters settle on the ocean floor or freely drift. Therefore, the farming mechanics for oysters are different to that of mussels. Figure 7 shows how pacific oysters (*Crassostrea gigas*) are currently being farmed in aquaculture, collecting spat and placing them in wooden racks to grow in a hatchery. Another method is single-seed oyster harvesting which includes various systems of trays, baskets, long-line, and cages in subtidal or intertidal areas. This process benefits the breeding process but is considered more labour intensive (NIWA, n.d)

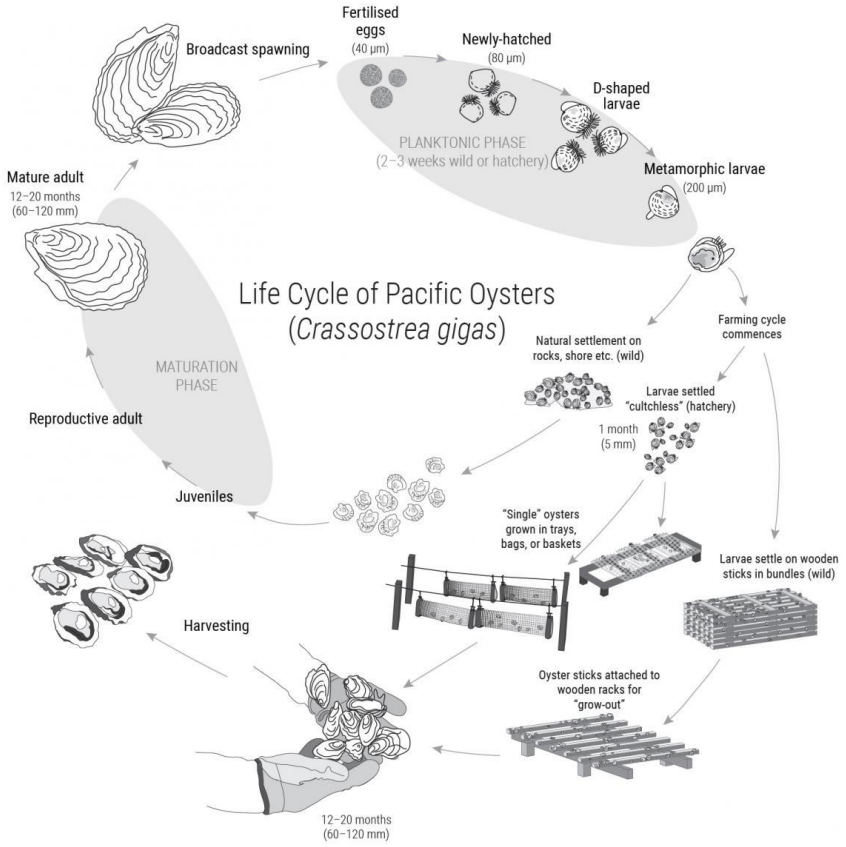

Figure 7: Lifecycle of Pacific Oysters, Reproduced with permission from NIWA (n.d).

Sustainability in aquaculture

"*Environmental sustainability is the ability to maintain the qualities that are valued in the physical environment"* (Sutton, 2004). According to Longdill et al. (2008), factors that influence sustainable aquaculture are economic sustainability, environmental sustainability and conflicting uses and constraints. To consider an aquaculture system to be viable it must survive throughout human ventures (population changes, global warming etc.) and multiple generations of both humans and species. Therefore, there is a limit as to what demand can be met without compromising natural resources, exceeding natural capacities, and degrading the ecosystem.

Environmental sustainability needs to consider how efficiently natural resources are being used and the waste generated in aquaculture farms. Other key considerations for aquaculture farming include whether the nutrients and resources used are sustainable. These resources include the total amount of water, land and energy (Valenti et al., 2011). Lastly, contaminated waste such as effluent and uneaten feed has had negative environmental impacts.

Aquaculture systems based on a monoculture of species fed on concentrated commercial diets is inefficient. They are inadequate due to the loss of material with only 20% being transferred into biomass, the rest is wasted. With on average an 80% loss it shows there is an unsustainable approach to certain aquaculture farming techniques that needs rectifying (Valenti et al., 2011). A way to combat uneaten feed waste is the addition of bottom filter feeders (shellfish) making up a multitrophic system. Bottom filter feeders convert this form of waste into body mass, creating another farming opportunity, pushing aquaculture towards sustainable and environmentally acceptable approaches (Chávez-Crooker & Obreque-Contreras, 2010).

Although aquaculture has been seen to benefit the fisheries industry by relieving the demand and sustainability pressure there has been some negative impacts that need attention. Prolonged damage from shrimp and salmon farming has been observed through habitat destruction. In some cases, aquaculture developments have been the reason for the removal of large quantities of mangroves and wetlands, which results in an ecosystem loss because mangroves and wetlands are essential and predominantly reduce coastal erosion and sedimentation (Naylor et al., 2000).

On occasions, shellfish farms tend to cause damage to the marine ecosystem, but it has been noted that with correct restoration shellfish habitats produce filtration, denitrification and

stabilization of sediments around shorelines (Alleway et al., 2019). In New Zealand the addition of mussel farms using the correct methods have shown restoration to once depleted reefs (Broekhuizen & Stenton-Dozey, 2019).

A key environmental concern is global warming and the contribution to greenhouse gases and carbon emissions using the cradle-to-gate method. This method includes emissions from transport, production of feed, water usage etc (MacLeod et al., 2020). Pollution from aquaculture farms can be produced by total suspended solids, biochemical oxygen demand (BOD), chemical oxygen demand (COD) and the total amount of greenhouse gas emissions released into the atmosphere (Valenti et al., 2011). It is important that for aquaculture to be sustainable mitigations must be put into place to reduce pollution in all waste streams including residual waste products such as bone, shell, and other unused products from production.

Rijn (2013) states that waste management is a crucial challenge faced in aquaculture. Biochemical oxygen demand (BOD) is an arguably challenging task that has been seen to stem from uneaten feed from overfeeding. If left unmanaged an accumulation of solid waste can undoubtedly increase the BOD, resulting in increased levels of organic matter and causing oxygen in the water to rapidly deplete (Rijn, 2013; Cao, et al., 2007).

Aquaculture waste from processing

Aside from feed waste there is also production waste from processing fish, crustacean and shellfish waste. Globally, fish waste in aquaculture has reached upwards of 32 million tonnes, with 50% of the net weight becoming waste. The overall waste of fish aquaculture is an accumulative of heads, frames, tails, skin, lugs, bones, fins, and viscera, which tends to be disposed of in landfills or is converted to a source of biofuel such as biomethane or biodiesel. Alternatively, fish waste has been developed into a bio fertilizer using specialised methods (Pędziwiatr, Zawadzki, & Michalska, 2017).

Mollusc waste in northwest Spain has reached +80,000 tons per year in shell waste with even more waste coming from residual meat. Calcium carbonate accounts for 95-99% of shell waste by weight (Barros, Bello, Bao, & Torrado, 2009). Molluscs waste tends to vary from region to region, mussels, clams, and scallops can be sold or exported in full shell, half shell or without shells. European countries tend to import with shells on whereas Asian countries prefer canned or

frozen without shells (Summa, Lanzoni, Castaldelli, Fano, & Tamburini, 2022). Although exported waste from shell may vary between demographic region it could likely be arguably concluded that the majority of the waste ends up in landfills. Therefore, efforts have been made since the 1980s to incorporate calcium carbonate into materials as a filler, with Japanese researchers exploring a range of construction materials using calcium carbonate obtained from oyster shells (Barros, Bello, Bao, & Torrado, 2009).

In addition to solid waste, wastewater from these processing facilities can also have a major effect on the environment if it is not discharged correctly. Raw wastewater from aquaculture systems can contain high concentrations of nitrogen, phosphorus, and organic contents. Unprocessed discharge of raw wastewater can result in infectious diseases and serious health issues (Cao, et al., 2007).

Mussel waste

Mussel waste can be categorized under three sections: solid waste, wastewater, and other waste. Solid waste can be broken down into crushed solid remains of shells, mussels' tissue, byssus, and whole mussels that have been rejected for consumption. Wastewater includes water used and produced during the mussel cooking process, organic residues, and water from other manufacturing processes. Other waste includes packaging materials used in the supply chain as well as odours and atmospheric emissions (Uzcátegui, Vergara, & Bordes, 2021).

A large portion of waste in mussel aquaculture is shells, byssus threads and residual meat, with only one third of a metric tonne for current mussels being processed meat for human consumption (Uzcátegui, Vergara, & Bordes, 2021). With 100,000 tonnes per year being exported (Longdill, Healy, & Black, 2008) that leads us to believe up to 200,000 tonnes per year becomes waste. Approximately 65% of waste is shells, with the remaining 35% being organic mussel waste (Iribarren, Moreira, & Feijoo, 2010). Mussel shells equate to more than 70% of the shellfish, with over 90% of the shell consisting of calcium carbonate ($CaCO_3$). Due to the filter feeding nature of mussels other components are related to what the shellfish has absorbed. In some cases, it has been noted that in poor and polluted water conditions that the composition of the mussel shells was found to contain traces of heavy metals such as mercury (Hg), lead (Pb) and in some cases large quantities of iron oxide (Fe_2O_3) (Hamestera, Balzer, & Becker, 2012). The current method for

waste management of shells is typically through the process of crushing and milling waste shells into a fine power, then disposing in landfills (Uzcátegui, Vergara, & Bordes, 2021).

Alternatively, the nutritional waste can be used for biomass or fertilizers (Uzcátegui, Vergara, & Bordes, 2021). The growth of blue mussels tends to be a common addition to green lipped mussel farms and are typically seen as waste. Residual blue mussel flesh has been broken down into a high protein ingredient for salmon feed, to reduce waste and develop a new stream of products (Stenton-Dozey, Heath, Ren, & Zamora, 2021).

A variety of plastic is used in aquaculture from specific farming equipment to personal protective equipment (PPE) which contributes to waste from mussel farms. Plastic is the chosen material due to its resistance to abrasion, durability, and non-corrosive properties. The most used plastic is high density polyethylene (HDPE), which is used for floats, baskets, polystyrene foam-filled sea pen collars, polymer-coated net pens and plastic harvest bins (Sustainable Business Network, 2020). Table 2 shows some of the common uses for plastic in the mussel farming industry and some more general uses in the aquaculture industry has a collective.

Table 2: Plastics used in mussel farms and general use in New Zealand.

Specific Farm Items	**Long Term Single Use Items**	**Personal Protective Equipment (PPE)**	**Processing and Distribution**
Floats	Barge refurbishment	Gloves	Ice packs
Ropes/nets	Dive gear	Hardhats	Poly boxes
Processing bags	Boats	Wet weather gear	Tape
Mussock (Cotton with PE blend)	Processing machinery (conveyors, tubing, cables, etc)	Aprons	Pallets
Strops		Gumboots	Wrap
Buoys		Hairnets	Plastic box liners
Ties/Lashings (PP)			Bags

Research in aquaculture waste

A large amount of research has already been done to investigate the management of aquaculture waste, specifically looking at converting waste into biomass, biofuels (e.g., biodiesel) and fertilizer.

Biodiesels are formed from fatty acid alkyl esters in linear long chains obtained from vegetable oils or animal fats through transesterification reaction with an alcohol and a suitable catalyst. Calcium oxide is a popular catalyst that is found in egg and mollusc shells that is low in cost, non-corrosive and highly reusable. The use of calcium oxide has been noted to reach a biodiesel yield of 98% (Rezaei, Mohadesi, & Moradi, 2013).

Other research takes aquaculture fish waste from RAS systems to make liquid fertilizer through aerobic digestion (Khiari, Kaluthota, & Savidov, 2019). Although the waste stream in this study was fish manure and not waste slurry the research looks at minimising biodegradable waste in aquaculture and improving existing management practices.

Other alternatives of interest have been the addition of aquaculture waste into concrete, usually using bones and shells as filaments or fibre reinforcement (Mo, Alengaram, Jumaat, Yap, & Lee, 2016). A study on concrete incorporating cockle shells showed that the best results were obtained with 30% shell and 70% cement, making a feasible concrete component (Prusty & Patro, 2015).

Little research has investigated the use of aquaculture waste in the development of plastics. With the use of aquaculture waste as fibre reinforcement in concrete there is certainly an application for it in the reinforcement of a range of plastics from fossil-based plastics to bioplastics. Research by Gigante, et al (2020) which investigated mussel shell and polylactic acid showed increased tensile properties. The addition of calcium carbonate to polylactic acid showed an increase in Youngs' Modulus from neat polylactic acid. Although, natural fibres and fillers can reduce the maximum strength of a composite due to incompatibility with the polymeric matrix and potentially creating stress concentrators within the composite if the reinforcing additives are too large (Gigante, et al., 2020). More research into bioplastics needs to be done with the addition of natural fibres and/or fillers from aquaculture by-waste in efforts to combat this problem. Research should be continued in the attempt to reduce waste and increase an understanding of bio-based plastics.

Having understood the aquaculture industry, species farmed in NZ and the waste they generate this literature review will now focus on bio-inspired materials, bio composites and polymer foams to provide a background to this work.

What does bio-inspired mean?

Bio-inspired applications, materials and products are inspired or based on biological structures or processes in the natural environment (Merriam-Webster, n.d.). Bio-inspiration has slightly varied definitions across different areas of study. Notably, these differentiations were derived between biologists and engineers. Helms, Vattam, & Goel, (2009) states that "*biologists in general seek to understand designs occurring in nature while design engineers generally seek to generate designs for new problems, they typically use different methods of investigation and often have different perspectives on design."* Materials engineering takes advantage of the natural world and the materials that appear in nature. The behaviour of materials in the natural environment inspires many properties and developments in sophistication, resistance, and adaptability (Sanchez, Arribart, & Guille, 2005).

Typically, the use of wood, cotton, silk, bone, and shell have been used in textiles, tools, and weapons. New requirements such as the discontinued manufacture of single use plastics (New Zealand Government, 2022) have been set to decrease environmental effects steering away from the stereotypical use of these materials. The ideal aim is to develop materials and applications such as bio-inspired composites and foams that have higher levels of sophistication that are recyclable and benefit the environment (Sanchez, Arribart, & Guille, 2005). Unquestionably, synthetic materials lack the properties of natural materials found in biological systems, resulting in a desire to mimic natural materials. Although mimicking natural materials has been somewhat successful, with engineering methods capable of generating materials in a matter of hours, they do not always match the performance of the natural materials (Braun, 2003). Many scientific problems have been solved by taking inspiration from solutions within nature, e.g., the development of high-performance materials such as those which use the well-known honeycomb structure (Zhang, et al., 2015).

Applications

Ceramic composites and bio-glasses have been the more common approach to bio-inspired applications, where implants tend to be the most notable functions developed from ceramics (Dujardin & Mann, 2002). Research has found similar comparisons between proteins in dental enamel and final stages of paua (abalone) shell. However, while there is an ability to recreate the structure of paua shell as a potential dental application, the synthetic recreation could not compare

to that of the natural paua shell (Braun, 2003). Applications surrounding aviation technologies have taken into account various birds and insects in the development of new aircraft developing bio-inspired properties such as miniaturization, stabilization, autonomy, intelligence and aerodynamics (Han, Hui, Tian, & Chen, 2021).

Materials

Selecting the appropriate material for the required task is an important factor in materials engineering. Various structures have been noted to follow a clear pattern of sophistication, with many naturally occurring composites being observed in mollusc shells, bone, and teeth tissues in vertebrates. Research into the nature of these properties helps understand aspects such as "self-assembly, phase separation, confinement, chirality in complex systems, possibly in relation to external stimuli or fields and the use of genetically engineered proteins." These themes help to overcome challenges in many inorganic applications developing products and materials which are bio-inspired (Sanchez, Arribart, & Guille, 2005). Hybrid materials have been derived from molecular crystals, micelles, and membranes in naturally occurring materials and organisms with the combination of organic or inorganic materials to develop hybrid composite materials (Sanchez, Arribart, & Guille, 2005). Calcium phosphate, calcium carbonate and silica continue to be biologically relevant minerals that present growth and form in bio-inspired materials. (Dujardin & Mann, 2002). Alternatively, paua shells consisting of alternating layers which aids the strength of the shell (Braun, 2003), have already been based into other forms of materials such as composites, sandwich composites and multi-axial materials. Bio inspired foams have been studied due to the porous and lightweight properties with thin-walled structures and axially graded thickness (Yao, et al., 2022). Additionally, bio inspired materials need to be reliable and consume less energy. This can be achieved by doing a cradle to gate lifecycle analysis (LCA), showing areas where energy usage and pollution can be reduced to make a 'greener' material. Products using biodegradable materials and incorporating a circular economy show more effective LCA, usually producing less waste, pollution, and energy. This process can be developed through materials that are based on objects or material following the basic building ideologies of living organisms (Sanchez, Arribart, & Guille, 2005). Hence drawing inspiration from these naturally occurring composite and foams investigations can be conducted incorporating natural fillers and bio-based polymers.

Plastic production

Plastics have revolutionised the past decades, being applied in many applications (Thompson, Swan, Moore, & Saal, 2009). Polymers are formed by creating bonds between a selection of monomers to create a larger polymer to manufacture a plastic which meets the desired properties (The Society of the Plastics Industry, 1991). Plastics can be amorphous (Mekonnen, Mussone, Khalil, & Bressler, 2013) or semi-crystalline polymers (Quan, Li, Yang, & Huang, 2005) and can be manufactured into a diverse array of products. The wide range of versatility and cost-efficient production of plastic makes it an extremely valued material (Mekonnen, Mussone, Khalil, & Bressler, 2013). The ability for the material to be extruded, moulded, cast, spun, or applied as a coating makes it desirable in many manufacturing processes (Thompson, Swan, Moore, & Saal, 2009). The manufacturing of plastic is the second largest use of petroleum after energy with almost one-third of that plastic being used for packaging (Mekonnen, Mussone, Khalil, & Bressler, 2013). Approximately 90% of plastics are synthesized from non-renewable fossil fuels, with 35% being used for packaging worldwide (Al-Salem, Lettieri, & Baeyens, 2009).

Plastic waste

In 2020 over 400Mt of plastic was produced, resulting in less than 10% of that plastic being recycled. Poorly managed landfills equate to 4.8 billion tons of plastic pollution in the environment. With the ever-increasing amount of plastic being used it is predicted to reach 1000 Mt at the current rate by 2050. Within that same time span, the annual greenhouse gas emissions are expected to rise to 6.5 Gt of CO_2 directly related to the life-cycle of plastics (Tiso, et al., 2021).With decreasing space in landfills there is a push towards the treatment of plastics, whether it is recovery or recycling. Methods in the last decade saw 388,000 tonnes of discarded waste polyethylene recycled to produce various types of textiles. Other varieties of plastics have been recycled into automobile parts, appliances, mulches, and films. Other methods have converted waste plastic into oils, chars, and sources of power/energy (Al-Salem, Lettieri, & Baeyens, 2009). Plastic waste in New Zealand is typically exported overseas to be recycled, but regrettably, most unrecyclable plastics end up in landfills causing long term environmental effects (Perrot & Subiantoro, 2018).

However, another viable option for minimising plastic waste is the introduction of bio-based plastics which can be made from renewable resources and recyclable or biodegradable plastics that can be composted and ideally, return to the natural environment without pollution.

Overall, the focus of this study is to create materials for the circular economy by incorporating aquaculture waste (mussel shell) into plastics in a way which enables them to be viable options for current and future applications.

Types of plastics

Plastics lie within three polymer categories that convey various mechanical properties. Many conventional plastics fall into the class of thermoplastics, due to the ability to re-melt the material without severely degrading the molecular structure. Thermoplastics can have either an amorphous or crystalline structure. They consist of long chains of molecule with linear bonding with inter-chain bonding consisting of secondary Van Der Waals bonds. At high temperatures thermoplastic materials become a viscous liquid where secondary bonds break and the primary chains can move over each other. During cooling the secondary bonds can reform and the material can again transition into a rigid state, allowing recyclability. Thermosets have amorphous structures predominately consisting of long molecular chains that are attached to each other by covalent bonds. The cross-linked structure allows the material to hold its shape but, reduces the ability to re-melt and recyclability. Elastomers follow a similar structure to thermosets with long molecular chains that exist in the form of amorphous linear bonding with occasional cross-links, but in this case at room temperature the Van Der Waals bonds have been overcome by the level of excitation of the molecular chains. Post deformation, the cross-links give the material the ability to revert the molecular structure back to the original shape (University of New South Wales, n.d).

Fossil-based plastics

Most commonly known plastics are derived from fossil-based resources, which use hydrocarbon monomers to create a long synthetic polymer chain. Fossil-based plastics tend to be manufactured as a by-product during the process of refining oil. During this process ethylene in the form of gas is produced, resulting in a by-product that has been reused in the production of polymers (Plastics NZ, 2022). The abundance of fossil-based plastic material synthesised from hydrocarbons such as oil and gas show notably little degradability due the resilient chemical structure. The most common polymers produced by fossil-based hydrocarbons are polyethylene (PE), polypropylene (PP), polyvinyl chloride (PVC), polyethylene terephthalate (PET) and polystyrene (PS) (Figure 8), each with various and differing material characteristics and chemical structures (Pivato, et al., 2022).

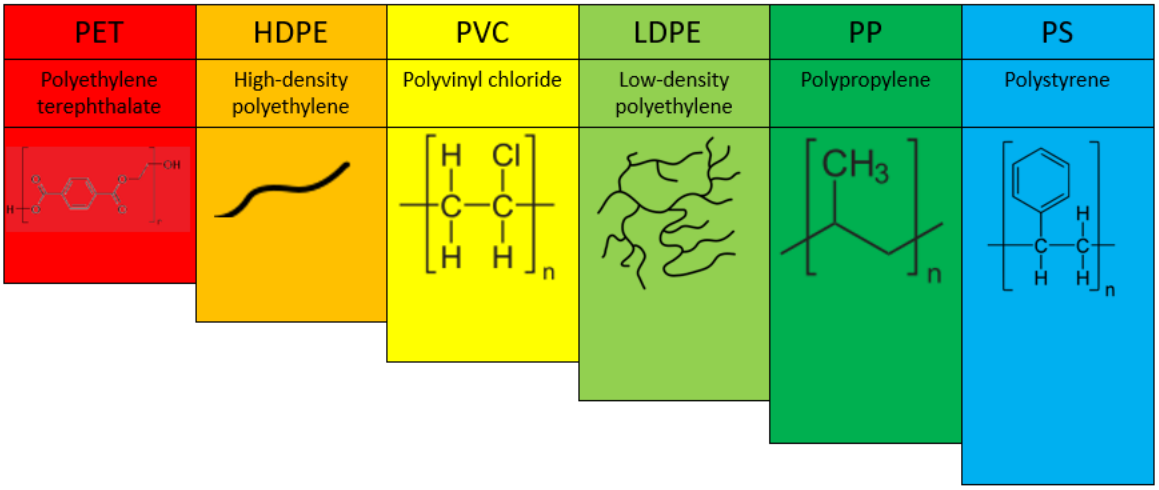

Figure 8: Common types of Fossil-Based Plastics.

Table 3: Types of Fossil-Based Plastics. Reproduced from WasteMINZ (2022).

Plastic	**Composition**	**Can be recycled in curbside**	**Can be certified biodegradable in commercial or home composting**	**Common applications**
CA (Cellulose Acetate)	CA can be fully or partially made from fossil fuel. *CA can be fully or partially made from plants	No	Yes	Bio-degradable cellophane
HDPE (high density polyethylene)	HDPE can be fully or partially made from fossil fuel. *HDPE can be fully or partially made from plants	Yes	No	Plastic bottles and piping
LDPE (low density polyethylene)	LDPE is fully made from fossil fuel.	Yes	No	Plastic bottles
PBAT (polybutylene adipate-co-terephthalate)	PBAT is fully derived from fossil-fuel but can be combined with a plant-based plastic such as PLA.	No	Yes	Some certified home compostable bags are made from a mixture of PBAT and PLA and cornstarch
PBS (Polybutylene succinate)	PBS can be fully or partially made from fossil fuel.	No	Yes	Service ware and packaging

	*PBS can be fully or partially made from plants		
PCL (Polycaprolactone)	PCL is fossil-fuel derived	No	Yes Bags
PEF (polyethylene fuanorate)	PEF can be fully or partially made from fossil fuel. *PEF can be fully or partially made from plants	No	No Beverage bottles
PHA (polyhydroxyalkanoate) and PHB (polyhydroxybutyrate)	PHA and PHB can be fully or partially made from fossil fuel. *PHA and PHB can be fully or partially made from plants	No	Yes Service ware and packaging
PP (polypropylene)	PP is fully made from fossil fuel.	Yes	NoPlastic bottles

Table 3 depicts common types of fossil-based plastics used in New Zealand along with the composition, recyclability, and common uses. Fossil-based plastics such as HDPE, LDPE and PP cannot be certified as biodegradable in commercial or home composting but are all recyclable plastics. These plastics are used in the most common types of applications such as plastic bottles and more advanced applications such as packaging and piping.

Bio-based and biodegradable plastics

Mekonnen, Mussone, Khalil, & Bressler (2013) state that "over the coming few decades bioplastic materials are expected to complement and gradually replace some of the fossil-based materials". With greater consumer pressure for environmentally sustainable products and a decreased carbon footprint, steering away from fossil-based polymers as an "environmentally friendly" solution has become more evident. Recently, there has been an increased demand for bio-based materials and more so, for the development of bio-based polymers (Murariu & Dubois, 2016).

There tends to be a miscommunication between bioplastics and the term biodegradable, where it is notable that not all bioplastics are biodegradable or compostable. Renewable bio-based

plastics can be sorted into two categories: biodegradable and non-biodegradable plastics. Some types of plastics cannot be recycled with conventional polymers. For example, PET can have a negative effect on existing plastic recycling processes and are susceptible to hydrolysis. Non-biodegradable plastics are defined as polymers partly or fully made of natural or renewable resources, bio-based but non-biodegradable, manufactured the same way as fossil-based plastic, designed to be identical to fossil-based plastics and are recyclable in the same ways as fossil-based plastics (Plastics NZ, 2022).With a large commercial push in the direction of bioplastics, environmental challenges and sustainability issues could be overcome. Furthermore, resulting in the reduced production and disposal of synthetic or fossil-based plastics (Mekonnen, Mussone, Khalil, & Bressler, 2013).

Table 4 depicts common types of bio-based plastics used in New Zealand along with the composition, recyclability, and common uses.

Table 4: Types of Bio-Based Plastics, Reproduced from WasteMINZ (2022).

Plastic	**Composition**	**Can be recycled in curbside**	**Can be certified biodegradable in commercial or home composting**	**Common applications**
CA (Cellulose Acetate)	CA can be fully or partially made from plants. *CA can be fully or partially made from fossil fuel	No	Yes	Bio-degradable cellophane
HDPE (Bio-PE) (high density polyethylene)	HDPE can be fully or partially made from plants. *However, currently most commercial production of HDPE is fossil-based	Yes	No	92% Sugar cane HDPE
PBS (Polybutylene succinate)	PBS can be fully or partially made from plants. *PBS can be fully or partially made from fossil fuel	No	Yes	Service ware and packaging
PEF (polyethylene fuanorate)	PEF can be fully or partially made from plants.	No	No	Beverage bottles

	*PEF can be fully or partially made from fossil fuel			
PHA (polyhydroxyalkanoate) and PHB (polyhydroxybutyrate)	PHA and PHB can be fully or partially made from plants. *PHA and PHB can be fully or partially made from fossil fuel	No	Yes	Service ware and packaging
PLA (polylactic acid)	PLA is full plant-based. *But can be combined with other fossil-fuel based plastics such as PBAT.	No	Yes	Bags

For this study LDPE and PLA have been chosen because each material individually shows unique properties that can be beneficial to the environment. LDPE is a vastly recyclable material that can contribute to sustainability through recycling and a circular economy. PLA is a bioplastic that can be industrially biodegraded in as little as six weeks (Rosenboom, Langer, & Traverso, 2022).

Low density polyethylene

Low density polyethylene (LPDE) is a common thermoplastic synthesised from fossil fuels and is manufactured by free radical polymerization of the single monomer ethylene at high pressures (Gupta, 1987). LDPE was one of the first plastics to be commercialised in 1933. LDPE is a unique plastic with long chain branching that improves both shear and extension of the polymer (Maraschin, 2001). LDPE shows a yield stress of 9 MPa and a Youngs' modulus of approximately 200 MPa (Zapata, et al., 2019) and is a widely recycled polymer.

Polylactic acid

Polylactic acid is a polyester-based plastic that displays biodegradable properties and is produced from renewable resources (Murariu & Dubois, 2016). PLA is typically made from fermented starch and obtained by synthesis of lactic acid (Yang, Wu, Yang, & Yang, 2008). PLA is one of the most favourable bioplastics/biopolymers in the up-and-coming market for bio-based materials, being desired in applications such as biomedical, packaging, textile fibres and technical items; with

further products being developed (Murariu & Dubois, 2016). PLA is desirable for medical purposes as it is non-toxic and often compared to the performance properties of conventional thermoplastics and has similar physical properties to polystyrene (Mekonnen, Mussone, Khalil, & Bressler, 2013). PLA has improved mechanical properties, currently displaying a distinctly high tensile strength (62 MPa) and Young's modulus (50 MPa), with concordantly good flexural strength (108MPa). Although with these characteristics, which are respectively higher than that of fossil-based polymers such as Polyethylene (PE), Polypropylene (PP) and Polyethylene terephthalate (PET), the bioplastic cannot compete with the petrochemical counterpart (Murariu & Dubois, 2016). This is due to the materials susceptibility to brittle failure and lack of plastic deformation. PLA becomes brittle due to conventional condensation polymerization of lactic acid, where the molecular weight of the polymer is relatively low (Liang, Zhou, Tang, & Tsui, 2013). Due to these disadvantages, there becomes a limit to the desired applications in bio-based polymers that are less common in the fossil-based thermoplastics (Murariu & Dubois, 2016).

Specialist materials

Composite plastics

Composite materials are the addition of two or more materials with varying physical characteristics, contributing to more desirable properties (Merriam-Webster, n.d.). The addition of both fibres and particles to a plastic can be used to make a composite material (Edwards, 1998; Gigante, et al., 2020). Composite plastics have been integrated into high stress environments due to the high specific stress and specific stiffness. The use of plastic in high stress environments allows for a greater potential of design, with the ability to shape a material to almost endless results similar to the likes of metals (Murariu & Dubois, 2016). Murariu & Dubois (2016) expressed that the introduction of fibres in a material is relatively common.

Fibre composites are influenced by variables such as, fibre types, alignment of the fibres, distribution of the fibres, fibre/matrix interfaces, size, and shape of the fibres and, loading direction (Edwards, 1998). Another addition to make a composite material is using fillers in the form of powder or particulates (Gigante, et al., 2020). Using natural fibres/fillers is a cost efficient, renewable, and sustainable way of creating bio-based composites, while increasing other properties. It is not necessary when making a composite polymer to use all bio-based or all fossil-based materials, the addition of renewable and/or bio-based fibres are desirable when reinforcing

bioplastics as the composite remains bio derived and/or biodegradable. Likewise adding a natural filler to a conventional plastic to produce more desirable properties can combine the benefits of the fossil-based plastic with renewable, bio derived and/or biodegradable resources.

Research by Edwards (1998) showed E-glass fibres had a Youngs' modulus of 45 GPa, Kevlar had a tensile strength of 75 GPA, and carbon fibre had a tensile strength of 140-220 GPa. The fibres were tested as 60% unidirectional fibre reinforced plastic. Other materials such as steel, aluminium and titanium had tensile strengths of 200 GPa, 73 GPa and 100 GPa.

Alternately, a study by Gigante, et al. (2020) using natural fillers from mussel shell (10wt%) mixed with PLA/PBAT (3:1) showed an elastic modulus of 2.35 GPa and maximum stress of approximately 38 MPa.

The addition of calcium carbonate from the shell powder to polylactic acid showed an increase in Youngs' Modulus/stiffness from neat polylactic acid, reaching values of 75GPa. Natural fibres and fillers tend to reduce the maximum strength of a composite due to inconsistencies between the polymeric matrix and fibres/fillers potentially creating stress concentrators within the composite if the reinforcing particulates are too large, occurring at weight percentages of 15wt% (Gigante, et al., 2020).

Calcium carbonate is a sought-after material that has been an additive filler in many polymer composites for a long time. Calcium carbonate can be formed as calcite, aragonite and vaterite, with calcite being the most common phase found in the natural environment. Micron-sized ground calcite has been used in several studies involving enhancing mechanical properties in polypropylene samples. In a study conducted by Osman, et al. (2004) LDPE was mixed with 0.1 or 0.2 volume fraction of calcium carbonate filler and stearic acid. The study found that the use of $CaCO_3$ and stearic acid linearly increased the modulus and yield stress of LDPE but reduced its tensile strength, yield strain, and ultimate elongation. Youngs' modulus increased approximately 50% to 530 MPa, with the yield stress increasing from 10.9 MPa to 12.7 MPa. The change in values occurred between the neat plastic sample and the 0.2 volume fraction sample (Osman, Atallah, & Suter, 2004).

Calcium carbonate is predominantly used as a filler in plastics due to the high chemical purity, degree of whiteness, low abrasiveness and good dispersibility. In a study by Piekarska,

Piorkowska, & Bojda (2017) calcium carbonate in the form of chalk was introduced into polylactic acid, which stated that 5wt% of filler increased tensile strength and tensile impact strength, while maintaining a similar crystallinity level to neat PLA. Tensile strength averaged at approximately 55 MPa for the PLA samples containing 5wt% $CaCO_3$.The addition of calcium carbonate fillers did not affect the glass transition temperature of PLA but resulted in an intensified cold crystallization, due to nucleation in the composite matrix (Piekarska, Piorkowska, & Bojda, 2017).

Research on calcium carbonate in the form of vaterite and polylactic acid composites showed interesting properties. The study used 30wt% of vaterite calcium carbonate filler which improved the elastic modulus by 3.5-6 GPa, resulting in a polylactic acid composite that did not show brittle properties compared to neat PLA (Kasuga, et al., 2003).

Recent research has studied the introduction of calcium carbonate from eggshells as an additive in polylactic acid. Eggshell consists of 95% calcium carbonate which supports the hardness in the material and demonstrates desirable properties as a composite additive. XRD patterns confirm the addition of highly crystalline calcium carbonate powder accelerates crystallization of polylactic acid by acting as a nucleating agent. It has been noted that 4wt% eggshell showed ideal tensile strength of 49.29 MPa (Sivagnanamani, Begum, Siva, & Kumar, 2021), which should be noted when working with mussel shell as both types of shell have similar calcium carbonate content.

Other research has studied mussel shell particulates in epoxy resins such as bisphenol-A type epoxy (NPEK), PU modified epoxy (NPER 133L) and CTBN (carboxyl-terminated poly (butadiene-*co*-acrylonitrile)) modified epoxy (NPER 450). Obtaining the following tensile results of 86 MPa, 56 MPa and 43 MPa using 40wt% of mussel shell. In this paper it was expressed that epoxies are less ductile than thermoplastics due to the degree of cross-linking in the polymer matrix and that as the mussel shell wt% increased so did the hardness of the materials, resulting in the reduction of the elongation capabilities of the samples during tensile testing (Kocaman, Ahmetli, Cerit, Yucel, & Gozukucuk, 2016). Further research on calcium carbonate fillers determined that the viscosity and pseudo-plasticity of the epoxy resin decreased when the filler was added (Ivanov, Cheshkov, & Natova, 2001).

It has been noted that previous research shows that when adding natural fibres/fillers to PLA it is important to ensure that the materials must be dried to evaporate any potential moisture

due to the hydrophilic nature of the material. PLA remains sensitive to hydrolysis creating a potential problem if adequate steps are not taken (Murariu & Dubois, 2016).

Polymer foams

The matrix of a polymer foam is filled with many tiny air pockets which allow the material to have a low density, good heat insulation, good sound insulation effects, high specific strength, high corrosion resistance (Jin, Zhao, Park, & Park, 2019), high impact strength, high toughness and great stiffness to weight ratios (Liao, Yu, & Zhou, 2010). These properties make polymer foams widely utilized in the industrial environments for applications such as packaging and insulation.

There are three main ways to produce polymer foams. The methods include mechanical, physical, and chemical foaming. The polymers are typically processed using industrial techniques including foam extrusion and foam injection moulding (Jin, Zhao, Park, & Park, 2019).

During the process of plastic foaming there are three stages that take place (nucleation, bubble/cell growth, and stabilization). The material must undergo nucleation with a lower viscosity of the polymer at high temperatures, flowed by bubble growth, then the increase from low to high viscosity results in stabilisation (Gavin, Verbeek, & Lay, 2019). The cell size and distribution are highly dependent on the kinetics of nucleation and bubble growth (Ruiz, et al., 2015). Bubble growth is aided by the introduction of a blowing agent, physical or (Gavin, Verbeek, & Lay, 2019). Heterogeneous nucleation results in desirable growth, size, and distribution properties of bubbles throughout the foam (Shaft, Joshi, & Flumerfelt, 1997). Cells within the molten polymer can grow, with bubbles becoming pressurised and joining together making larger cells and decreasing the total number of cells (Jin, Zhao, Park, & Park, 2019). With a decreasing temperature and gas concentration, the polymer undergoes the final stage of stabilization as it lowers below the glass transition temperature creating the air pockets observed in a polymer foam (Gavin, Verbeek, & Lay, 2019).

Polypropylene has been foamed using carbon dioxide as the blowing agent, with calcium carbonate as a nucleating agent. It was found that low weight percentages of calcium carbonate introduced homogeneous distribution of particles throughout the polymer (Ding, Ma, Song, & Zhong, 2013). This is because particulates aid the development of bubbles during nucleation within

thermoplastics. Microbubbles on the surface of particulates increase in size and join under pressure and at the right temperature (Feng & Bertelo, 2004). Therefore, adding mussel shell powder directly will contribute to the nucleation process.

The most common endothermic blowing agents used in polymer foaming tend to be sodium bicarbonate and zinc bicarbonate, which results in either a chemical reaction or thermal decomposition to produce a known gas. Multiple studies have focused on analysing the dependence of the solubility of carbon dioxide (CO_2) in polypropylene. Although, during decomposition nitrogen (N_2) or carbon dioxide (CO_2) is produced (Ruiz, et al., 2015) and in some cases water (H_2O) is produced due to hydrolysis of esters and polycarbonates (Kmetty, Litauszki, & Réti, 2018).

Exothermic blowing agents include carbon monoxide (CO), carbon dioxide (CO_2) and ammonia (NH_3). Exothermic blowing agents are typically used in low temperature applications and widely used in rubber foams (Heck III, 1998).

Previously, chlorofluorocarbons (CFCs) and hydrochlorofluorocarbons (HCFCs) were used as foaming agents in polymers. Freons tend to cause negative environmental effects, including depletion of the tropospheric ozone layer contributing to the tragic green-house effect around our planet (Grolier & Randzio, 2012) and so have been phased out.

Research shows that cell morphology in polylactic acid can be influenced by temperature during foaming. At lower temperatures (70°C) cell nucleation tends to increase, with cell size reducing and total number of cells increasing. At higher temperatures (110°C) the opposite happens, with cell size increasing and total number of cells decreasing. The addition of calcium carbonate in foamed PLA was noted to also increase the storage modulus of the polymer to 1.6 GPa in a glassy state. The increase indicates that reinforcing of the polymer matrix also occurred due to the calcium carbonate creating a nanocomposite (Mahdavi, Yousefzade, & Garmabi, 2018).

Foam PLA has shown good tensile strength and high modulus but has a low elongation at-break and is very brittle which limits its applications in many fields in materials science. Foam blends of PLA/PBAT of 15 and 20wt% of PBAT shows an increase in plastic deformation noted by necking of the samples during tensile testing. The study theorises that necking could occur in tensile tests under tension due to the addition of PBAT as it localises stress and promotes micro

voids to occur in the PLA matrix. With the increase of ductility in the material the tensile strength of the foam blend tends to decrease but still shows results of 48 MPa at a 20wt% (Wei, Shicheng, & Hongfu, 2018).

Research using plastic derived from corn starch and eggshell powder as a nucleating agent to target bubble growth and stabilization was conducted by Xu and Hanna (2007). Eggshell acted as a nucleating agent decreasing cell size and increasing the total amount of cells in the matrix, showing desirable results. Eggshell samples of 0-6wt% showed a decrease in expansion ratio and compressibility. Notably, compressibility decreases from 7.37 MPa to 2.63 MPa over the range of 0-6wt% and finally increased to 5.28 MPa once reaching 10wt%. Overall, the foaming properties were noted to be better using smaller particle sizes than what was exhibited by the larger particle sizes of eggshell powder (Xu & Hanna, 2007).

Conclusion

As a growing industry, aquaculture is benefiting from continued research relating to aquaculture farming, especially towards species and methods. There has been various New Zealand based projects by NIWA regarding aquaculture farming of species such as mussels, kingfish, and oysters. These projects have shown that aquatic animals can be cultivated in near-shore farms and on shore hatcheries. Other research by Chávez-Crooker & Obreque-Contreras (2010) introduces sustainable methods that relied on multitrophic systems, where bottom feeders such as molluscs are introduced to reduce waste feed from primary farmed aquatic animals. The ability to cultivate sustainably is beneficial for the improvement of the environment as it reduces waste (Chávez-Crooker & Obreque-Contreras, 2010).

Currently, aquatic animals are being harvested and processed for consumption with waste materials commonly being exported to landfills (Pędziwiatr, Zawadzki, & Michalska, 2017). Regardless of sustainable growing practices this waste is inevitable. Incorporating this waste into an alternative application provides opportunities to create a circular economy (Chávez-Crooker & Obreque-Contreras, 2010).

Structures like polymers foams and composites are present in nature and therefore, there is a desire to replicate synthetic versions of these materials and structures. Waste from natural or

biological materials can inspire complex structures that can be used to produce synthetic versions of these materials.

Calcium carbonate is commonly used as a filler in polymers such as LDPE and is usually mined from large quarries. With calcium carbonate naturally occurring in mussel shells it poses an opportunity for an alternative source.

Unpublished scoping work has already shown that it is possible to use calcium carbonate in various materials, including but not limited to the use of mussel shell fillers in PLA composites and LDPE composite, as well as polymer foams using the same materials (Walshe, 2022). While the changes in performance were not quantified during the scoping work by Walshe the addition of calcium carbonate has shown increased tensile strength and Youngs' Modulus in bio-based plastics such as PLA between 1-5wt% (Sivagnanamani, Begum, Siva, & Kumar, 2021). The maximum filler composition observed in literature was 30% by weight using calcium carbonate in the form of vaterite. While other studies have investigated using calcium carbonate from mussels or other mollusc shells, they usually report a range from 1-20wt% but lack testing above this.

Literature regarding polymer foams tend to study how calcium carbonate fillers affect the properties of the polymer and the process of foaming. Therefore, it is important to further study how these fillers affect nucleating during foaming and subsequent foam morphology. Research in the past has studied PLA foams consisting of up to 10wt% eggshell and up to 20wt% of calcium carbonate to study expansion ratio and compressibility.

Little research has introduced mussel shell into polymer foams as either a filler or nucleating agent and while some existing research in standard composites has already been conducted, a higher wt% has not been reported. Both composites and foams are essentially used in packaging, for protection (foam) and plastic boxes/trays (composites) creating opportunities for a circular economy. The bioinspired nature of this work is shown in the replication of these structures for new applications and will be extended by the production of a 3D printing PLA composite filament with the intention that this filament will enable future development of bioinspired designs as a specific application has not yet been identified.

Aims and objectives

The scope of this master's thesis is to continue to develop and trial a bio-inspired composites and foams containing mussel shell, a form of aquaculture waste. This work is therefore broken down into two sections. The first section studies composites and the second section studies polymer foams.

1.0 Composites:

Aim: To produce 3D printable PLA and LDPE polymer composites with the addition of mussel shell powder as a reinforcing material between 2-30wt%.

Hypothesis: That incorporating mussel shell into these materials at high weight percentages will still result in a material which is 3D printable and that an increase in tensile strength can be achieved by incorporating this additive at a high level due to the reduction in elongation due to the properties of the ceramic material.

Specific objectives:

1.1 To determine the most optimal weight percentage of mussel shell powder that can be added to PLA to produce a bio-composite. With PLA being susceptible to moisture, this research aims to introduce a high weight percentage while trying to minimise hydrolysis.

1.2 To determine the most optimal weight percentage of mussel shell powder that can be added to LDPE to produce a composite for comparison with the PLA bio-composite.

1.3 To study the thermal and mechanical properties of PLA and LDPE composites to determine the most significant weight percentage of mussel shell powder. Theses composites will have up to 30% mussel shell added.

1.4 To examine the printability of these filaments as a method of extending the usability of these composites.

2.0 Foams:

Aim: To utilise low percentages of mussel shell as a nucleating agent and high percentages as a reinforcement within PLA and LDPE foams.

These samples will be foamed PLA and LDPE polymer with the addition of mussel shell powder as a nucleating or reinforcing material. The mechanical properties of PLA and LDPE foams will be determined to establish the optimum weight percentage of mussel shell powder. Further research into the foaming properties of the polymers with the addition of mussel shell powder will be conducted.

Hypothesis: Particulates in foam are likely to act as stress concentrators rather than reinforcement due to the minimal thickness of plastic between cells. Although tensile stress may drop the particulates will increase cell nucleation in the polymers. An increase in cells within a foam will improve the compressibility on the polymer foam.

Specific objectives:

2.1 To determine the most optimal weight percentage of mussel shell powder that can be added to PLA to produce a bio-foam. With PLA being susceptible to moisture, this research aims to introduce a high weight percentage of 10wt% while trying to minimise hydrolysis.

2.2 To determine the most optimal weight percentage of mussel shell powder that can be added to LDPE to produce a foam for comparison with the PLA foam.

References

Alleway, H. K., Gillies, C. L., Bishop, M. J., Gentry, R. R., Theuerkauf, S. J., & Jones, R. (2019, January). The Ecosystem Services of Marine Aquaculture: Valuing Benefits to People and Nature. *BioScience*, 69(1), 59-68. https://doi.org/10.1093/biosci/biy137

Al-Salem, S., Lettieri, P., & Baeyens, J. (2009, October). Recycling and recovery routes of plastic solid waste (PSW): A review. *Waste Management*, 29(10), 2625-2643. https://doi.org/10.1016/j.wasman.2009.06.004

Andraka, S., Mug, M., Hall, M., Pons, M., Pacheco, L., Parrales, M., . . . Vogel, N. (2013, April). Circle hooks: Developing better fishing practices in the artisanal longline fisheries of the Eastern Pacific Ocean. *Biological Conservation,* 160, 214-224. https://doi.org/10.1016/j.biocon.2013.01.019

Aquaculture. (n.d.). *Bay of Plenty Regional Council* https://www.boprc.govt.nz/environment/coast-and-ocean/aquaculture#:~:text=The%20Bay%20of%20Plenty%20Aquaculture,of%20%24250%20million%20by%202025

Barros, M., Bello, P., Bao, M., & Torrado, J. (2009). From waste to commodity: transforming shells into high purity calcium carbonate. *Journal of Cleaner Production*, 17(3), 400-407. https://doi.org/10.1016/j.jclepro.2008.08.013

Bay of Connections. (2013, March). *Bay of Connections Aquaculture Strategy 2013*. Bay of Connections. https://atlas.boprc.govt.nz/api/v1/edms/document/A3887860/content

Bay of Connections. (2018). *Aquaculture Strategy 2018*. Bay of Connections. www.bayofconnections.com/: https://www.bayofconnections.com/downloads/070819_-FINAL-DOC_SPR18016-Aquaculture-PAGES1.pdf

Bay of Plenty Regional Council Aquaculture Group. (2011). *A REGION WIDE KNOWLEDGE BASE FOR THE AQ*. http://www.toi-eda.co.nz/getattachment/About-Toi-Eda/Bay-of-Connections-strategies/FINAL_BoP_Aqua_Audit_150811.pdf.aspx

Bostock, J., McAndrew, B., Richards, R., Jauncey, K., Telfer, T., Lorenzen, K., . . . Corner, R. (2010). Aquaculture: global status and trends. *Philosophical Transactions of the Royal Society B*, 365(1554). https://doi.org/10.1098/rstb.2010.0170

Braun, P. V. (2003). Natural Nanobiocomposites, Biomimetic Nanocomposites and Biologically *Inspired Nanocomposites*. https://doi.org/10.1002/3527602127.ch3

Broekhuizen. (n.d) *Greenshell™ mussel,* NIWA, Dropper with a developing crop of mussels https://niwa.co.nz/aquaculture/aquaculture-species/greenshell-mussel

Broekhuizen, & Stenton-Dozey. (2019). *HEALTHY COASTAL ECOSYSTEMS: ECOLOGICAL BENEFITS OF MUSSEL FARMS IN THE MARLBOROUGH SOUNDS.* NIWA. https://niwa.co.nz: https://drive.google.com/file/d/1Qs8r8EpxL4nCVWIPLwjA96xh4uIVCPSF/view

Cai, J., Yan, X., & Leung, P. (2022). Benchmarking species diversification in global aquaculture. *FOOD AND AGRICULTURE ORGANIZATION OF THE UNITED NATIONS.* https://www.fao.org/3/cb8335en/cb8335en.pdf

Cao, L., Wang, W., Yang, Y., Yang, C., Yuan, Z., Xiong, S., & Diana, J. (2007). Environmental Impact of Aquaculture and Countermeasures to Aquaculture Pollution in China. *Env Sci Pollut Res*, 14(7), 452-462. http://dx.doi.org/10.1065/espr2007.05.426

Chávez-Crooker, P., & Obreque-Contreras, J. (2010, June). Bioremediation of aquaculture wastes. *Current Opinion in Biotechnology*, 21(3), 313-317. https://doi.org/10.1016/j.copbio.2010.04.001

Dauda, A. B., Ajadi, A., Tola-Fabunmi, A. S., & Akinwole, A. O. (2019, May). Waste production in aquaculture: Sources, components, and managements in different culture systems. *Aquaculture and Fisheries*, 4(3), 81-88. Retrieved from https://doi.org/10.1016/j.aaf.2018.10.002

Ding, J., Ma, W., Song, F., & Zhong, Q. (2013). Effect of nano-Calcium Carbonate on microcellular foaming of polypropylene. *Journal of Materials Science*, 48, 2504-2511. https://doi.org/10.1007/s10853-012-7039-1

Dujardin, E., & Mann, S. (2002). Bio-inspired Materials Chemistry. *Advanced Materials*, 14(11), 775-788. https://doi-org.ezproxy.waikato.ac.nz/10.1002/1521-4095(20020605)14:11%3C775::AID-ADMA775%3E3.0.CO;2-0

Edwards, K. (1998, February 1). An overview of the technology of fibre-reinforced plastics for design purposes. *Materials & Design*, 19(1-2), 1-10. Retrieved from https://doi.org/10.1016/S0261-3069(98)00007-7

FAO. (2020). *The State of World Fisheries and Aquaculture*. FAO. https://www.fao.org/3/ca9229en/ca9229en.pdf

FAO. (n.d.). *Fisheries and Aquaculture*. FAO. https://www.fao.org/fishery/en/aquaculture/en

Feng, J. J., & Bertelo, C. A. (2004). Prediction of bubble growth and size distribution in polymer foaming based on a new heterogeneous nucleation model. *Journal of Rheology*, 48(2). https://doi.org/10.1122/1.1645518

FOA. (2008). *Climate change implications for fisheries and aquaculture: Overview of current scientific knowledge.* FAO. https://www.ipcinfo.org/fileadmin/user_upload/newsroom/docs/FTP530.pdf

Frankic, A., & Hershner, C. (2002, November 19). Sustainable aquaculture: developing the promise. *Aquculture International.* 11, 517-530 https://link.springer.com/content/pdf/10.1023/B:AQUI.0000013264.38692.91.pdf

Gavin, C., Verbeek, C. J., & Lay, M. C. (2019). The role of plasticizers during protein thermoplastic foaming. *Journal of Applieed Polymer Science,* 136(30). https://doi-org.ezproxy.waikato.ac.nz/10.1002/app.47781

Gentry, R. R., Lester, S. E., Kappel, C. V., White, C., Bell, T. W., Stevens, J., & Gaines, S. D. (2017). Offshore aquaculture: Spatial planning principles for sustainable development. *Ecology and Evolution*. 7(2), 733-743. https://doi.org/10.1002/ece3.2637

Gigante, V., Cinelli, P., Righetti, M. C., Sandroni, M., Tognotti, L., Seggiani, M., & Lazzeri, A. (2020, July 28). Evaluation of Mussel Shells Powder as. *International Journal of Molecular Sciences*. 21(15). https://doi.org/10.3390/ijms21155364

Goulletquer, P., & Heral, M. (1997). Marine Molluscan Production Trends in France: From Fisheries to Aquaculture. https://books.google.co.nz/books?hl=en&lr=&id=jo5RAQAAIAAJ&oi=fnd&pg=PA137&dq=wild+fisheries+vs+aquaculture&ots=FIXi4gAa9D&sig=pCLMyutBGUzfybDfTnrvblE8yIM&redir_esc=y#v=onepage&q=wild%20fisheries%20vs%20aquaculture&f=false

Grolier, J.-P. E., & Randzio, S. L. (2012). Simple gases to replace non-environmentally friendly polymer foaming agents. A thermodynamic investigation. *The Journal of Chemical Thermodynamics*, 46, 42-56. https://doi.org/10.1016/j.jct.2011.07.017

Gupta, S. K. (1987). LOW DENSITY POLYETHYLENE (LDPE) POLYMERIZATION — A REVIEW. *Current Science,* 56(19), 979-984. https://www.jstor.org/stable/24090114

Hamester, M. R., Balzer, P. S., & Becker, D. (2012). Characterization of Calcium Carbonate Obtained from Oyster and Mussel Shells. *Materials Research.,* 15(2), 204-208. 10.1590/S1516-14392012005000014

Han, J., Hui, Z., Tian, F., & Chen, G. (2021, July). Review on bio-inspired flight systems and bionic aerodynamics. *Chinese Journal of Aeronautics,* 34(7), 170-186. https://doi.org/10.1016/j.cja.2020.03.036

Heath, P. (2006, September 1). *Creating the right conditions for paua*. NIWA. https://niwa.co.nz/publications/wa/vol14-no3-september-2006/creating-the-right-conditions-for-paua

Heck III, R. L. (1998). A review of commercially used chemical foaming agents for thermoplastic foams. *Journal of Vinyl and Additive Technology*, 4(2).

Helms, M., Vattam, S. S., & Goel, A. K. (2009). Biologically inspired design: process and products. *Design Studies*, 30(5), 606-622. https://doi.org/10.1016/j.destud.2009.04.003

Holmer, M. (2010). Environmental issues of fish farming in offshore. *AQUACULTURE ENVIRONMENT INTERACTIONS,* 1(57-70). 10.3354/aei00007

Iribarren, D., Moreira, M. T., & Feijoo, G. (2010). Revisiting the Life Cycle Assessment of mussels from a sectorial perspective. *Journal of Cleaner Production*, 18(2), 101-111. https://doi.org/10.1016/j.jclepro.2009.10.009

Ivanov, Y., Cheshkov, V., & Natova, M. (2001). SOLID MECHANICS AND ITS APPLICATIONS: *Polymer Composite Materials - Interface Phenomena & Processes* (Vol. 90). Kluwer Academic Publishers.

Jeffs, A. G., Delorme, N. J., Stanley, J., Zamora, L. N., & Sim-Smith, C. (2018, March 10). Composition of beachcast material containing green-lipped mussel (Perna canaliculus) seed harvested for aquaculture in New Zealand. *Aquaculture*, 488, 30-38. https://doi.org/10.1016/j.aquaculture.2018.01.024

Jin, F.-L., Zhao, M., Park, M., & Park, S.-J. (2019, June). Recent Trends of Foaming in Polymer Processing: A Review. *Polymers,* 11(6). https://doi.org/10.3390%2Fpolym11060953

Kasuga, T., Maeda, H., Kato, K., Nogami, M., Hata, K.-i., & Ueda, M. (2003). Preparation of poly(lactic acid) composites containing calcium carbonate (vaterite). *Biomaterials,* 24(19), 3247-3253. https://doi.org/10.1016/S0142-9612(03)00190-X

Khiari, Z., Kaluthota, S., & Savidov, N. (2019, February 1). Aerobic bioconversion of aquaculture solid waste into liquid fertilizer: Effects of bioprocess parameters on kinetics of nitrogen mineralization. *Aquaculture*, 500, 492-499. https://doi.org/10.1016/j.aquaculture.2018.10.059

Kmetty, Á., Litauszki, K., & Réti, D. (2018). Characterization of Different Chemical Blowing Agents and Their Applicability to Produce Poly(Lactic Acid) Foams by Extrusion. *Applied Sciences*, 8(10), 1960. https://doi.org/10.3390/app8101960

Kocaman, S., Ahmetli, G., Cerit, A., Yucel, A., & Gozukucuk, M. (2016). Characterization of Biocomposites Based on Mussel Shell Wastes. World Academy of Science, Engineering and Technology: *International Journal of Materials and Metallurgical Engineering*, 10(4), 438-444.

Land Based Aquaculture Assessment Framework. (n.d.). *Paua*. http://www.lbaaf.co.nz/nz-aquaculture-species/modelled-species/paua/

Liang, J.-Z., Zhou, L., Tang, C.-Y., & Tsui, C.-P. (2013). Crystalline properties of poly(L-lactic acid) composites filled with nanometer calcium carbonate. *Composites Part B: Engineering*, 45(1), 1646-1650. https://doi.org/10.1016/j.compositesb.2012.09.086

Liao, R., Yu, W., & Zhou, C. (2010). Rheological control in foaming polymeric materials: I. Amorphous polymers. *Polymer*, 51(2), 568-580. https://doi-org.ezproxy.waikato.ac.nz/10.1016/j.polymer.2009.11.063

Longdill, P. C., Healy, T. R., & Black, K. P. (2008). An integrated GIS approach for sustainable aquaculture management area site selection. *Ocean & Coastal Management*, 51(8-9). https://doi.org/10.1016/j.ocecoaman.2008.06.010

Mackay, S. (n.d). Yellowtail kingfish. NIWA. https://niwa.co.nz/aquaculture/species/yellowtail-kingfish

MacLeod, M. J., Hasan, M. R., Robb, D. H., & Mamun-Ur-Rashid, M. (2020). Quantifying greenhouse gas emissions from global aquaculture. *Scientific Reports.* https://doi.org/10.1038/s41598-020-68231-8

Mahdavi, M., Yousefzade, O., & Garmabi, H. (2018). A simple method for preparation of microcellular PLA/calcium carbonate nanocomposite using super critical nitrogen as a blowing agent: Control of microstructure. *Advances in Polymer Technology*, 37(8), 3017-3026. https://doi.org/10.1002/adv.21972

Maraschin, N. (2001). Ethylene Polymers, LDPE. *In Encyclopedia of Polymer Science and Technology.* https://doi.org/10.1002/0471440264.pst121

Martínez-García, C., González-Fonteboa, B., Martínez-Abella, F., & López, D. C. (2017, May 15). Performance of mussel shell as aggregate in plain concrete. *Construction and Building Materials*, 139, 570-583. https://doi.org/10.1016/j.conbuildmat.2016.09.091

Mekonnen, T., Mussone, P., Khalil, H., & Bressler, D. (2013). Progress in bio-based plastics and plasticizing modifications. *Journal of Materials Chemistry A*, 1, 13379-133398. https://doi.org/10.1039/C3TA12555F

Merriam-Webster. (n.d.). Bioinspired. Retrieved from Merriam-Webster.com dictionary: https://www.merriam-webster.com/dictionary/bioinspired

Merriam-Webster. (n.d.). Composite. Retrieved from Merriam-Webster.com dictionary: https://www.merriam-webster.com/dictionary/composite

Ministry for Primary Industries. (n.d). *Kingfish status and information.* MPI. https://www.mpi.govt.nz/https://www.mpi.govt.nz/https://www.mpi.govt.nz/

Mo, K. H., Alengaram, U. J., Jumaat, M. Z., Yap, S. P., & Lee, S. C. (2016, March 20). Green concrete partially comprised of farming waste residues: a review. *Journal of Cleaner Production*, 117, 122-138. https://doi.org/10.1016/j.jclepro.2016.01.022

Murariu, M., & Dubois, P. (2016, December 15). PLA composites: From production to properties. *Advanced Drug Delivery Reviews*, 107, 17-46. https://doi.org/10.1016/j.addr.2016.04.003

Naylor, R. L., Goldburg, R. J., Primavera, J. H., Kautsky, N., Beveridge, M. C., Clay, J., . . . Troell, M. (2000, June 29). Effect of aquaculture on world fish supplies. *Nature.* https://doi.org/10.1038/35016500

New Zealand Geographic. (n.d.). *Science & Environment: Aquaculture*. NZGEO. https://www.nzgeo.com/stories/aquaculture/

New Zealand Government. (2019). *The New Zealand Government Aquaculture Strategy*. https://drive.google.com/file/d/1gLidnTyUSu1my4URexhNOOvELL1Jbf-0/view

New Zealand Government. (2022). *Aquaculture Strategy: 2022 implementation plan*. www.mpi.govt.nz: https://www.mpi.govt.nz/dmsdocument/50570/direct

New Zealand Government. (2022). *Waste Minimisation (Plastic and Related Products) Regulations 2022*. Ministry for the Environment. https://legislation.govt.nz/regulation/public/2022/0069/13.0/whole.html

NIWA. (2001). *Estuaries.* NIWA. www.niwa.co.nz: https://niwa.co.nz/education-and-training/schools/students/estuaries#:~:text=An%20estuary%20is%20a%20partially,%2C%20sounds%2C%20wetlands%20and%20swamps.

NIWA. (2006, September 1). *Creating the right conditions for paua*. NIWA. https://niwa.co.nz/publications/wa/vol14-no3-september-2006/creating-the-right-conditions-for-paua

NIWA. (2020). *Yellowtail kingfish.* NIWA. https://niwa.co.nz/aquaculture/species/yellowtail-kingfish

NIWA. (n.d.). *Greenshell™ mussel*. NIWA. https://niwa.co.nz/aquaculture/aquaculture-species/greenshell-mussel

NIWA. (n.d.). *Our facilities.* NIWA. https://niwa.co.nz/aquaculture/our-services/our-facilities

NIWA. (n.d.). *Pacific oyster.* NIWA. https://niwa.co.nz/aquaculture/species/pacific-oyster

Osman, M. A., Atallah, A., & Suter, U. W. (2004, February). Influence of excessive filler coating on the tensile properties of LDPE–calcium carbonate composites. *Polymer,* 45(4), 1177-1183. https://doi.org/10.1016/j.polymer.2003.12.020

Pędziwiatr, P., Zawadzki, D., & Michalska, K. (2017). AQUACULTURE WASTE MANAGEMENT. *Acta Innovations* (ISSN 2300-5599), 22, 20-29. https://www.proakademia.eu/gfx/baza_wiedzy/421/nr_22_20_29_2.pdf

Perrot, J.-F., & Subiantoro, A. (2018). Municipal Waste Management Strategy Review and Waste-to-Energy Potentials in New Zealand. *Sustainability*, 10(9). https://doi.org/10.3390/su10093114

Piekarska, K., Piorkowska, E., & Bojda, J. (2017, Sptember). The influence of matrix crystallinity, filler grain size and modification on properties of PLA/calcium carbonate composites. *Polymer Testing*, 62, 203-209. https://doi.org/10.1016/j.polymertesting.2017.06.025

Pivato, A. F., Miranda, G. M., Prichula, J., Ligabue, R. A., Seixas, A., & Trentin, D. S. (2022, April). Hydrocarbon-based plastics: Progress and perspectives on consumption and biodegradation by insect larvae. *Chemosphere*, 293. https://doi.org/10.1016/j.chemosphere.2022.133600

Plastics NZ. (2022). *Bioplastics & Degradables*. Plastics NZ. https://www.plastics.org.nz/environment/bioplastics-degradables

Plastics NZ. (2022). *Plastics & Environment*. Plastics NZ. https://www.plastics.org.nz/environment/plastics-environment

Prusty, J. K., & Patro, S. K. (2015, May 1). Properties of fresh and hardened concrete using agro-waste as partial replacement of coarse aggregate – A review. *Construction and Building Materials*, 82, 101-113. https://doi.org/10.1016/j.conbuildmat.2015.02.063

Quan, H., Li, Z.-M., Yang, M.-B., & Huang, R. (2005, June). On transcrystallinity in semi-crystalline polymer composites. Composites Science and Technology, 65(7-8), 999-1021. Retrieved from https://www.sciencedirect.com/science/article/pii/S0266353804003677#!

Reverter, M., Sarter, S., Caruso, D., Avarre, J.-C., Combe, M., Pepey, E., . . . Gozlan, R. E. (2020, April 20). Aquaculture at the crossroads of global warming and antimicrobial resistance. *Nature Communications*, 11(1870). https://doi.org/10.1016/j.compscitech.2004.11.015

Rezaei, R., Mohadesi, M., & Moradi, G. R. (2013, July). Optimization of biodiesel production using waste mussel shell catalyst. *Fuel*, 109, 534-541. https://doi.org/10.1016/j.fuel.2013.03.004

Rijn, J. v. (2013, March). Waste treatment in recirculating aquaculture systems. *Aquacultural Engineering*, 53, 49-56. https://doi.org/10.1016/j.aquaeng.2012.11.010

Rosenboom, J.-G., Langer, R., & Traverso, G. (2022). Bioplastics for a circular economy. *Nature Reviews - Materials*, 7, 117-137. https://doi.org/10.1038/s4157-021-00407-8

Ruiz, J. A., Vincent, M., Agassant, J.-F., Sadik, T., Pillon, C., & Carrot, C. (2015). Polymer foaming with chemical blowing agents: Experiment and modeling. *Polym Eng Sci*, 55, 2018-2029. https://doi.org/10.1002/pen.24044

Sanchez, C., Arribart, H., & Guille, M. M. (2005). Biomimetism and bioinspiration as tools for the design of innovative materials and systems. *Nature Materials*, 4(4), 277-288. https://doi.org/10.1038/nmat1339

Shaft, M. A., Joshi, K., & Flumerfelt, R. W. (1997). Bubble size distributions in freely expanded polymer foams. *Chemical Engineering Science*, 52(4), 635-644. https://doi.org/10.1016/S0009-2509(96)00433-2

Sivagnanamani, G. S., Begum, S. R., Siva, R., & Kumar, M. S. (2021, 12 1). Experimental Investigation on Influence of Waste Egg Shell Particles on Polylactic Acid Matrix for Additive Manufacturing Application. *Journal of Materials Engineering and Performance*, 31, 3471–3480. https://doi.org/10.1007/s11665-021-06464-y

Stenton-Dozey, J. M., Heath, P., Ren, J. S., & Zamora, L. N. (2021). New Zealand aquaculture industry: research, opportunities, and constraints for integrative multitrophic farming.

New Zealand Journal of Marine and Freshwater Research, 55(2), 265-285. https://doi-org.ezproxy.waikato.ac.nz/10.1080/00288330.2020.1752266

Summa, D., Lanzoni, M., Castaldelli, G., Fano, E. A., & Tamburini, E. (2022). Trends and Opportunities of Bivalve Shells' Waste Valorization in a Prospect of Circular Blue Bioeconomy. *Resources*, 11(5), 48. https://doi.org/10.3390/resources11050048

Sustainable Business Network. (2020). *Tackling plastic waste in New.* MPI. https://www.mpi.govt.nz/dmsdocument/41121-Tackling-plastic-waste-in-NZ-aquaculture-FINAL-Full-Report

Sutton, P. (2004). *A Perspective on environmental sustainability?* https://www.donboscogozo.org/images/pdfs/energy/A-Perspective-on-Environmental-Sustainability.pdf

Tacon, A. G. (2020). Trends in Global Aquaculture and Aquafeed Production: 2000-2017. *Reviews in Fisheries Science and Aquaculture*, 28, 43-56. https://doi.org/10.1080/23308249.2019.1649634

Tal, Y., Schreier, H. J., R.Sowers, K., Stubblefield, J. D., Place, A. R., & Zohar, Y. (2009, January). Environmentally sustainable land-based marine aquaculture. *Aquaculture*, 286(1-2), 2843-2850. https://doi.org/10.1016/j.aquaculture.2008.08.043

The Paua Industry Council. (n.d). *About Paua*. https://paua.org.nz/about-paua/

The Society of the Plastics Industry. (1991*). Plastics Engineering Handbook (Fifth ed.).* https://books.google.co.nz/books?hl=en&lr=&id=FzPEJyDTqtEC&oi=fnd&pg=PR5&dq=plastics&ots=xFJUcoiVC6&sig=T_V8yR2pAvA8JrZVg4u41e4ZWtA&redir_esc=y#v=onepage&q=plastics&f=false

Thompson, R. C., Swan, S. H., Moore, C. J., & Saal, F. S. (2009). Our plastic age. *Phil. Trans. R. Soc. B*, 364(1526), 1973-1976. https://doi.org/10.1098/rstb.2009.0054

Thurstan, R. H., Brockington, S., & Roberts, C. M. (2010). The effects of 118 years of industrial fishing on UK bottom trawl fisheries. *Nature Communications*, 1(15). https://doi.org/10.1038/ncomms1013

Tiso, T., Winter, B., Wei, R., Hee, J., Witt, J. d., Wierckx, N., . . . Blank, L. M. (2021, December). The metabolic potential of plastics as biotechnological carbon sources – Review and targets for the future. *Metabolic Engineering.* https://doi.org/10.1016/j.ymben.2021.12.006

Troell, M., Joyce, A., Chopin, T., Neori, A., Buschmann, A. H., & Fang, J.-G. (2009, December). Ecological engineering in aquaculture — Potential for integrated multi-trophic aquaculture (IMTA) in marine offshore systems. *Aquaculture*, 297(1-4), 1-9. https://doi.org/10.1016/j.aquaculture.2009.09.010

University of New South Wales. (n.d). *Polymer Types. Retrieved from School of Materials Science and Engineering* https://www.materials.unsw.edu.au/study-us/high-school-students-and-teachers/online-tutorials/polymers/structure-and-form/polymer-types

Uzcátegui, L. U., Vergara, K., & Bordes, G. M. (2021, March 5). Sustainable alternatives for by-products derived from industrial mussel processing: A critical review. *Waste Management & Research: The Journal for a Sustainable Circular Economy*, 40(2), 123-138. https://doi.org/10.1177/0734242X21996808

Valenti, W. C., Kimpara, J. M., & Preto, B. d. (2011). Measuring aquaculture sustainability. *World Aquaculture,* 43(3), 26-30. https://www.caunesp.unesp.br/Home/publicacoes/fa_valenti_measuring-aquaculture.pdf

Walshe, A. (2022). Aquaculture Derived Composite. *Unpublished manuscript.*

wasteMINZ. (2022). *Plastics used in compostable products and packaging*. https://www.wasteminz.org.nz/projects/compostable-packaging-2/plastics-used-in-compostable-products-and-packaging/

Wei, L., Shicheng, H., & Hongfu, Z. (2018). Preparation and properties of flexible poly(lactic acid) blend foams. *Cellular Polymers*, 37(4-6), 189-205. https://doi.org/10.1177/0262489318797514

Woods, C. M., Floerl, O., & Hayden, B. J. (2012). Biofouling on Greenshell™ mussel (Perna canaliculus) farms: a preliminary assessment and potential implications for sustainable aquaculture practices. *Aquaculture International*, 537-557. https://doi.org/10.1007/s10499-011-9484-2

Xu, Y., & Hanna, M. (2007). Effect of Eggshell Powder as Nucleating Agenton the Structure, Morphology and FunctionalProperties of Normal Corn Starch Foams. *PACKAGING TECHNOLOGY AND SCIENCE*, 20, 165-172. 10.1002/pts.751

Yang, S.-l., Wu, Z.-H., Yang, W., & Yang, M.-B. (2008, December). Thermal and mechanical properties of chemical crosslinked polylactide (PLA). *Polymer Testing*, 27(8), 957-963. https://doi.org/10.1016/j.polymertesting.2008.08.009

Yao, R., Pang, T., He, S., Li, Q., Zhang, B., & Sun, G. (2022). A bio-inspired foam-filled multi-cell structural configuration for energy absorption. *Composites Part B: Engineering*, 238. https://doi.org/10.1016/j.compositesb.2022.109801

Zapata, P. A., Palza, H., Díaz, B., Armijo, A., Sepúlveda, F., J. A., . . . Oyarzún, C. (2019). Effect of CaCO3 Nanoparticles on the Mechanical and Photo-Degradation Properties of LDPE. *Molecules*, 24(1), 126. https://doi.org/10.3390/molecules24010126

Zhang, Q., Yang, X., Li, P., Huang, G., Feng, S., Shen, C., . . . Lu, T. J. (2015). Bioinspired engineering of honeycomb structure – Using nature to inspire human innovation. *Progress in Materials Science*, 74, 332-400. https://doi.org/10.1016/j.pmatsci.2015.05.001

Chapter two: Methodology

This section outlines the experimental plans, methods and characterisation techniques used in this study. This includes the analysis of raw materials, creation of a powder from mussel shell waste and the production of polylactic acid and polyethylene composites (experiment one) and foams (experiment two).

Characterisation of mussel shell powder

Raw mussel waste provided by Whakatōhea Mussels Limited consists predominately of mussel shells. Characterisation techniques were used to determine the structure and properties of the shell before and most importantly after the mussel shells had been crushed and milled into a fine powder. The particulates in the powder are typically less than 600 μm depending on geometry.

Creation of mussel shell powder

The creation of the mussel shell powder had two stages. The first stage involved cleaning and disinfecting of the mussel shell, which prepared the samples for crushing and milling. Crushing and milling broke down the larger shells into a fine mussel shell powder.

Cleaning and disinfection

Frozen by-product containing predominantly mussel shells was firstly defrosted to room temperature and prepared for cleaning and disinfection. This process was necessary to remove any potential bacteria and cleaning agents used in the mussel processing facility. The use of a brush was also occasionally required to remove any loose barnacles and tissue from the mussel shells. In this case warm soapy water was used to clean and partially disinfect the shells. After disinfection, the by-product was placed in a drying oven at 100-105°C for approximately 24 hours to dry and kill any remaining micro-organisms.

Crushing and milling

The dried mussel shells were crushed into pieces (1-2 cm^2) using a hammer before being milled into a fine powder using a Fritsch Planetary Mono Mill Pulverisette 6 Mill. A steel cylinder used in the milling process was filled with crushed mussel shell, distilled water and twenty 4-6 mm steel ball bearings. This was then set to a 15-minute spin, 15-minute rest, then 15-minute reverse cycle to mill the shell. Once milling was completed, the shell slurry was removed from the steel cylinder and dried in an oven at 100°C for a minimum of 48 hours.

By-product characterisation

The characteristics of both the shell and processed powder could be assessed by many methods including Thermal gravimetric analysis (TGA) and microscopy. TGA was important as it showed the change in mass as a material reached thermal degradation. The use of optical microscopy and scanning electron microscopy (SEM) allows for an in-depth analysis of the materials structure. These methods are important as it shows characteristics of materials below macroscopic level. The ability to understand and visualise characteristics of a material is essential when producing a composite plastic as the properties of the by-product play an important role in the overall properties of the composite material. Although X-ray diffraction (XRD) is a common characterisation technique it was not used in this experimental due to the composition and phase of mussel shell already being well documented in literature.

Optical microscopy

An Olympus BX60 optical microscope was used to observe macroscopic features and fracture surfaces of the shell under a 5-20 times magnification. Imaging of the shell and powder used reflected light on the brightfield mode.

Scanning electron microscopy

SEM achieved the ability to visualise grain boundaries and structure down to one nanometre (Stokes, 2008). Samples were dried overnight at 100℃ to remove moisture. Samples were coated in platinum to improve conductivity when under the electron beam to show highly detailed images. A Regulus 8230 Scanning Electron Microscope was used to take images of mussel shell and mussel shell powder on a low energy beam setting (3kV).

Thermal gravimetric analysis

The PerkinElmer STA8000 machine can perform Simultaneous Thermal Analysis (STA) which is Differential Scanning Calorimetry (DSC) and Thermogravimetric Analysis (TGA) at the same time. For each sample a program was run to hold at 30ºC for 5 minutes, then increased to 800ºC at a rate of 10ºC/min followed by a 5-minute hold at 800ºC before finally cooling to room temperature. The furnace was filled with argon gas at a constant flow rate of 40mL/min. Under these conditions weight loss and both endothermic and exothermic heat flow data could be analysed.

Hydroscopic analysis

Initially 5 grams of mussel shell powder was weighed out into a beaker and left in the laboratory. Every hour the beaker was weighed, and the weight was recorded. The change in mass showed the moisture uptake of the mussel shell powder.

Particle size analysis

The Mastersizer 3000 was used to analyse particle sizes in a sample. Approximately, 2 grams of mussel shell powder was added to the wet dispersal unit with liquid Calgon to aid with the dispersal of particles. Particle sizes were determined due to light diffracting off the particles onto the detectors.

Experimental

For both the composites and foams, varying weight percentages (ranging between 0.5-30 wt%) of powdered mussel shell were introduced to polylactic acid and low-density polyethylene through a method of extrusion. For the experiments conducted in this study PLA 3052D and LD 2420D were used. Table 5 and 6 below defined the parameters that were tested in this section of the experiment. Figure 9 shows an experimental flowchart of the processes required to produce the initial materials into composites or foams and the testing completed.

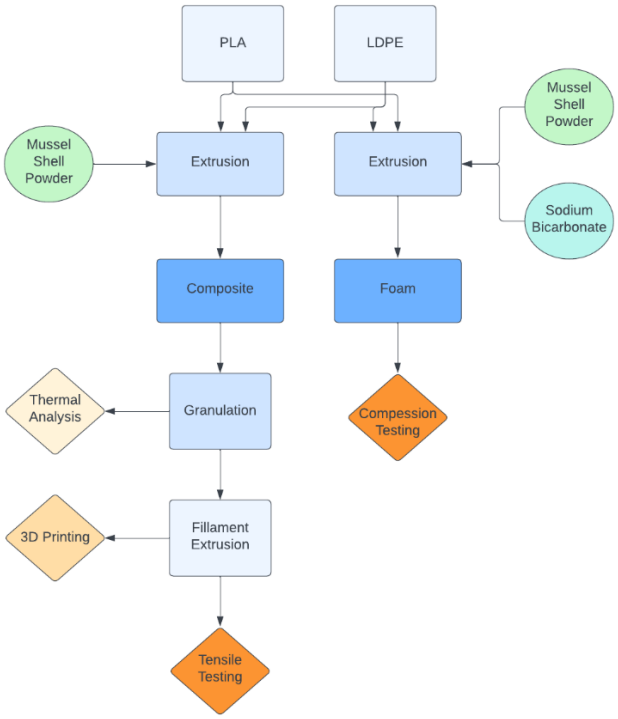

Figure 9: Experimental Flowchart.

Plastic grades

PLA 3052D

This grade of PLA was supplied by NatureWorks and is ideal for injection moulding to create applications such as packaging. It has a melting temperature of 153℃ with a glass transition temperature of 57.5℃ (Materials Data Center , n.d). This grade was chosen as it shows similar processing temperatures to the LDPE control. Properties for this material can be seen in appendix B.

LD 2420D

This grade of LDPE was supplied by InnoPlus and is used for film extrusion and blow moulding. It has great processability, high tensile strength, high elongation, and good toughness. This grade of LDPE has a melt temperature of 170-220°C (InnoPlus by PTT Global Chemicals, n.d). This grade of LDPE was chosen as it was the only grade available for purchase in small quantities. Properties for this material can be seen in appendix B.

Weight percentage

The amount of mussel shell powder used related to whether the composite sample was a nucleate or reinforcement. Low weight percentages (0-2%) of mussel shell were used to encourage nucleation in foams, where medium percentages (4-10) and high percentages (20-30wt%) of mussel shell were used to reinforce and increase the stiffness of the composites and foams.

Table 5: Powder for low weight percentages.

Plastic Type	**Mussel Shell Powder (wt%)**			
LD 2420D	0.5	1	1.5	2
PLA 3052D	0.5	1	1.5	2

Table 6: Powder for medium and high weight percentages.

Plastic Type	**Mussel Shell Powder (wt%)**					
LD 2420D	4	6	8	10	20	30
PLA 3052D	4	6	8	10	20	30

Sample preparation

Before any sample manufacture or testing, the neat polymers should be dried. Drying of these polymers removes any moisture that has accumulated. Polylactic acid is generally dried for 12 hours at 45ºC, this is to reduce moisture from causing hydrolysis during heating.

Although hydrolysis does not occur in LDPE, it is best practice to dry this polymer for 2 hours at 100ºC to reduce any possibility of moisture being present on the surface.

Extrusion

Using the Labtech LTE-20-44 twin screw extruder, the plastic and mussel shell powder were extruded into a mixed composite plastic. During the extrusion process, pellets are plastically deformed under heat and pressure through the barrel of the extruder. The temperature of the barrel varies, increasing as the material gets closer to the die. For both LDPE and PLA, the feed zone was set at a temperature of 160ºC and increased to 190ºC at the nozzle, respectively.

Table 7: Composite and foam extrusion processing profile.

Barrel Sections									
1	**2**	**3**	**4**	**5**	**6**	**7**	**8**	**9**	**10**
190ºC	185ºC	185ºC	180ºC	180ºC	170ºC	170ºC	165ºC	165ºC	160ºC

This shows the temperature settings at each point of the barrel used for the extruder. In this case section one was the nozzle and section ten was the feed zone.

Table 8: Plastic processing profile.

Plastic Type	**Melt Temp**	**Feed Temp**	**Nozzle Temp**	**Screw Speed**	**T_g Temp**
LD 2420D	170-220ºC	170ºC	190ºC	30rpm	-100ºC
PLA 3052D	200ºC	170ºC	190ºC	30rpm	57.5ºC

As the extruded plastic leaves the die, it is cut at approximate intervals of 15cm and left for five minutes to harden and dry.

For polymer foams, a chemical blowing agent (sodium bicarbonate) was introduced during the initial twin screw extrusion process. Approximately, 5% sodium bicarbonate is added to the mixture to produce an acceptable cell volume. The polymer foam was processed by the extruder into silicone moulds (80 x 30 x 25 mm) and left to harden and dry. These bars were cut into smaller cubes with a band saw and handsaw. The samples measured to 10mm x 10mm x 15mm (length, width, height).

To produce the 3D printed composite the polymer and mussel shell were blended (without the addition of a blowing agent), the blend was then granulated for further processing.

Granulation

The Moretto GR2020 granulator was used to reduce the size of the extruded plastic. Due to the ductile nature of LDPE, it was granulated using a 9 mm sieve to allow larger granules through the sieve. If a smaller sieve was used the material would conduct static electricity from the granulator and would attach to the side of the machine. This did not happen with PLA as it is a brittle material, and a 6 mm sieve was able to be used to make smaller granules.

Filament extrusion

The Filabot Filament Extruder single screw extruder was set to 180ºC with fans to cool the plastic as it left the extruder. The screw speed was adjusted accordingly to produce a strand of approximately 1.75 mm. The strand is pulled by a reel rotating at a similar speed to the screw speed. This produces a fine filament that can be rolled onto the reel and is suitable for 3D printing.

3D printing

A 3D printer was used to print PLA filament using a 0.75 mm diameter nozzle at 190℃. Samples were printed using a 100% infill typically uniaxial depending on purpose, with a print speed of 3600 mm/min. The printer bed was set to 60℃ with a thin layer of glue to aid with the initial layer sticking to the bed.

Sample characterisation and testing

Determining the tensile strength, ductile to brittle transition temperatures and thermal properties of a material is necessary to determine what conditions, environment, and applications that a material could be used for. Characterisation and Testing was conducted on the 3D printed filaments.

Optical microscopy

Similarly, to the mussel shell powder characterisation using optical and electron scanning microscopy could be used to visualise macroscopic and microscopic features of the composites, the fracture surfaces at break and microscopic pores in polymer foams. Imaging from an Olympus SZX7 stereo microscope was used to examine the fracture and/or deformation of the filaments. The microscope was set up to use refracted light through the sample on brightfield mode at 1x magnification setting. The actual magnification can be calculated by multiplying the eyepiece magnification (10x), built-in objective lens

magnification (1x) and auxiliary lens magnification (1.5x) together resulting in an overall image magnification of 15.

Scanning electron microscopy

SEM was used to get detailed images of fracture surfaces and morphology of both filament and foams after tensile and compression testing respectively. Firstly, the samples were dried overnight, at 45℃ for PLA samples and 100℃ for LDPE samples. The samples were cut to smaller sizes and prepped on black carbon tape. The samples were then coated in platinum to improve conductivity when under the electron beam. The Regulus 8230 Scanning Electron Microscope was used to take images of filament fracture surfaces and foam morphology on a low energy beam setting of 3 kV.

Thermal gravimetric analysis

The PerkinElmer STA8000 was again used for DSC and TGA on small pieces of granulated composite materials. The program was altered as plastic has a lower degradation temperature. In this case the only change was the maximum temperature which was decreased to 600ºC.

Tensile testing

The Instron 100 kN tester was used for filament tensile testing. Filament clamps were used to insert the samples into the machine clamps at approximately 30-40 mm in length. The samples were loaded to a starting force of 10 N, where the sample diameter and length could be recorded. The samples were tested at a rate of 5 mm/min until the material reached failure or appropriate data had been recorded. From this testing force, extension, Youngs' modulus, ultimate tensile stress, yield stress and strain could be determined.

Compression testing

The Instron 100 kN tester was used for compression testing of foam samples. Compression plates were used to test samples that were approximately 10 x 10 x 15 mm (length, width, height). Samples went through two different types of compression testing cyclic compression and compaction.

The samples were again loaded to a starting force of 10 N, where the samples where were compressed at 1 mm/min to 50% of the initial height or failure of the sample. This could determine compressive stress, compressive strain, and Youngs' modulus of the polymer foam.

Separate foam samples were loaded to a starting force of 10 N for cyclic compression, where the samples were compressed at 1 mm/min to 10% of the initial height of the sample and slowly released to test the elastic deformation and recovery of the foam.

Foam density and expansion

After volume and weight of the foam blocks were measured, density of a foam block could be calculated by dividing volume and weight. Density could be calculated using the equation below.

$$\rho_f = \frac{m}{V}$$

Expansion could then be simply calculated by dividing the density of a solid polymer block by the density of a foam block. Expansion ratio could be calculated using the following equation.

$$ER = \frac{\rho_s}{\rho_f}$$

Experimental plans

Chapter 3 - Characterisation outline

Thermal analysis of mussel shell and powder was conducted, which consisted of TGA and DSC testing. These tests showed the burning of residual organic matter, thermal degradation of calcium carbonate and weight loss of the materials during heating.

The hydroscopic behaviour of the mussel shell powder was conducted to determine moisture uptake.

Optical and scanning electron microscopy was used to image mussel shell and powder to show microscopic features that would not be noticeable to the naked eye.

Chapter 4 - Experiment one outline

The majority of testing for this thesis occurred in experiment one. Firstly, thermal analysis of granulated samples was conducted, which consisted of TGA and DSC testing. These tests showed melting points, thermal degradation, and weight loss during heating.

Next, tensile tests were conducted on filament samples, where the samples were put under tension until failure. This testing showed stress and strain of the material, other properties such as Youngs' modulus and ultimate tensile stress could be determined.

Lastly, optical and scanning electron microscopy was used to image the fracture surface of the filament samples, showing whether the material failed in a ductile or brittle manner.

Chapter 5 - Experiment two outline

Density and expansion ratios of the PLA and LDPE foams were firstly calculated.

This section involved two sets of compression tests cyclic compression and compaction. Cyclic compression tested 10% of the material and showed the recoverability of the polymer foam, compaction testing compressed 50% of the material resulting in greater plastic deformation and failure. Compaction testing showed properties such as compressive stress, compressive strain, and Youngs' modulus.

Optical and scanning electron microscopy was used to image the morphology of both PLA and LDPE foams. Images showed cell size, cell volume and wall thickness.

References

InnoPlus by PTT Global Chemicals. (n.d). *LD2420D.* https://www.indochempolymers.com/media/product/456066238_PTT2420D.pdf

Materials Data Center . (n.d). *Material Data Center Datasheet of Ingeo™ 3052D - PLA - NatureWorks LLC.* https://www.materialdatacenter.com/ms/en/tradenames/Ingeo/NatureWorks+LLC/Ingeo%E2%84%A2+3052D/1c1d8b83/5616

MatWeb: Material Property Data. (n.d.). *NatureWorks® Ingeo™ 4042D Film Grade PLA.* https://www.matweb.com/search/datasheettext.aspx?matguid=b0fb785721a145b28dbfced3a2dbf30b

NatureWorks. (n.d.). *Ingeo™ Biopolymer 2003D Technical Data Sheet For Fresh Food Packaging and Food Serviceware.* https://www.natureworksllc.com/~/media/Files/NatureWorks/Technical-Documents/Technical-Data-Sheets/TechnicalDataSheet_2003D_FFP-FSW_pdf.pdf?la=en

NatureWorks. (n.d.). *Ingeo™ Biopolymer 3001D Technical Data Sheet.* https://www.natureworksllc.com/~/media/Files/NatureWorks/Technical-Documents/Technical-Data-Sheets/TechnicalDataSheet_3001D_injection-molding_pdf.pdf?la=en

NatureWorks. (n.d.). *Ingeo™ Biopolymer 8052D Technical Data Sheet Foam Grade.* https://www.natureworksllc.com/~/media/Files/NatureWorks/Technical-Documents/Technical-Data-Sheets/TechnicalDataSheet_8052D_foam_pdf.pdf?la=en

Stokes, D. J. (2008). Principles and Practice of Variable Pressure Environmental Scanning Electron Microscope. https://books.google.co.nz/books?hl=en&lr=&id=TgYJv5BHIQ0C&oi=fnd&pg=PR7&dq=Principles+and+Practice+of+Variable+Pressure+Environmental+Scanning+Electron+Microscope&ots=G8qn_ThsO2&sig=RTkjLvdnt8oY7JWs_JVa-oP397E#v=onepage&q=Principles%20and%20Practice%20of

Chapter three: Characterisation

Objective: The characterisation of mussel shell waste through various methods such as Differential Scanning Calorimetry (DSC), Thermogravimetric Analysis (TGA), Hydroscopic behaviour, Particle size analysis Optical Microscopy and Scanning Electron Microscopy (SEM). The above characterisation techniques were used to determine heat transfer, mass loss, moisture uptake, particle size and microscopic features. Another common characterisation technique is X-ray diffraction (XRD) which was not studied in this experiment due to the composition and phase of mussel shell already being well documented in literature.

Mussel waste characterisation

The composition of mussel shells equates to more than 70% of the mollusc, with over 90% of the shell consisting of calcium carbonate ($CaCO_3$) the remainder being protein (Hamester, Balzer, & Becker, 2012). Due to the filter feeding nature of mussels the other components of the shell are related to what the shellfish has absorbed. It has been noted that in poor and polluted water conditions that the composition of the mussel shells was found to contain traces of heavy metals such as mercury (Hg), lead (Pb) and in some cases copious quantities of iron oxide (Fe_2O_3) (Hamester, Balzer, & Becker, 2012).

Shell characterisation

The images below show the half mussel shells before (left of each image) and after (right of each image) cleaning. It was important to remove all byssus and foreign objects from the shells before a powder could be made. Having miscellaneous material in the mussel shell powder can cause further problems during the processing of the composite plastics. Furthermore, this research studies the addition of calcium carbonate fillers, the addition of byssus strands would act as fibre reinforcement which is not a focus in this study.

a) b)

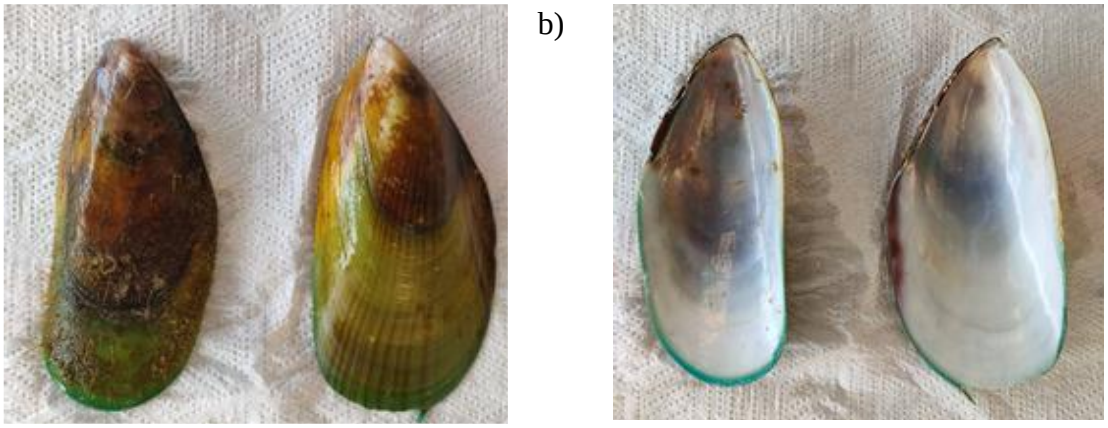

Figure 10: Half mussel shells a) outside and b) inside.

SEM and optical microscopy

Microscopy was used to determine the unique features of the shell and the shell powder. This is important because the characteristics for large pieces of shell and fine powder will vary. When processing the mussel shell powder, a microscope was used to determine the visual effects that machinery such as the ball mill has on the material. This could further determine the size of the particles within the bulk powder.

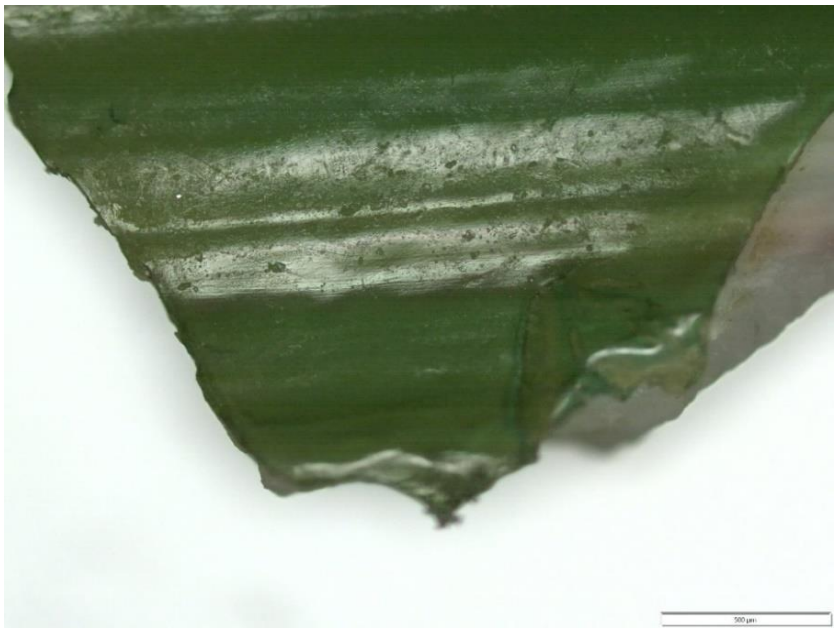

Figure 11: Mussel shell x5 magnification.

Figure 11 shows the macroscopic surface of the mussel shell using reflective light microscopy. While the shell was wet the white and green sections acted as if it was one material, but it is notable that once the shell was dried there was a visible difference between the white calcium carbonate and the outer green film of the shell. The outer film of the shell was called the periostracum (Bamigboye, et al., 2021). The periostracum is composed of organic material and fibrous protein called conchiolin which was seen in various other molluscs (Liu, 2001).

a) 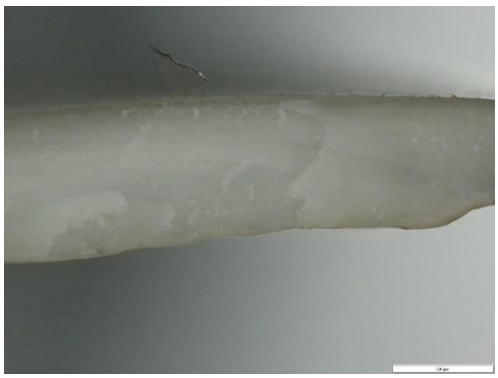 b) 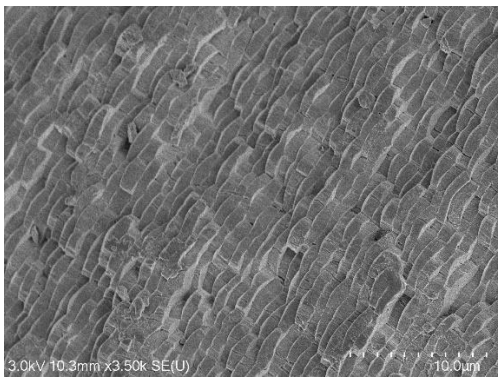

Figure 12: a) Mussel shell fracture surface x5 magnification, b) Mussel shell fracture SEM.

Figure 12 shows the fracture surface of the mussel shell which was made up of calcium carbonate. The shell exhibited brittle properties, shown by the flat style of fracture. The section of the mussel shell was made up of crystalline calcium carbonate in the form of calcite and a smaller proportion of aragonite. The shell structure consisted of overlapping platelets (Liu, 2001), which are visible through SEM. Under SEM the shell had large plate-like shapes with diverse spacing between each particle. The particles within the mussel shell appeared course, showing irregular shape (Sari & Yusuf, 2018).

a)  b) 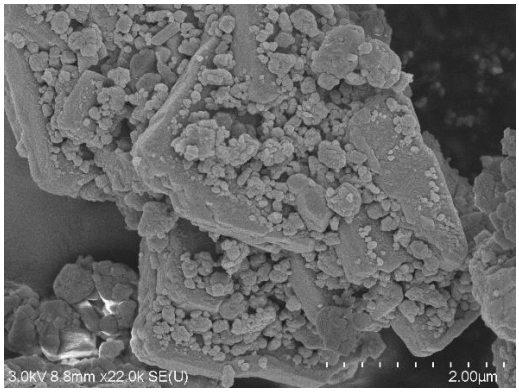

Figure 13: a) Calcium carbonate powder made from mussel shell x5 magnification, b) Calcium Carbonate powder made from mussel shell SEM.

Figure 13 shows a small amount of mussel shell powder at 5x magnification. The particulates are less than 500 µm in diameter, with the majority being less than 100 µm. It is notable that many small particles clustered together to form large groups of particles. These larger clusters could be separated with minimal force required. Therefore, during extrusion the clusters will separate back into microscopic particulates with minimal force, which could be seen under high magnification such as SEM.

Particle analysis of mussel shell powder

Mussel shell particles were measured under 350 µm during particle analysis the median particle size was 8.68 µm, with the smallest size recorded at 0.490 µm.

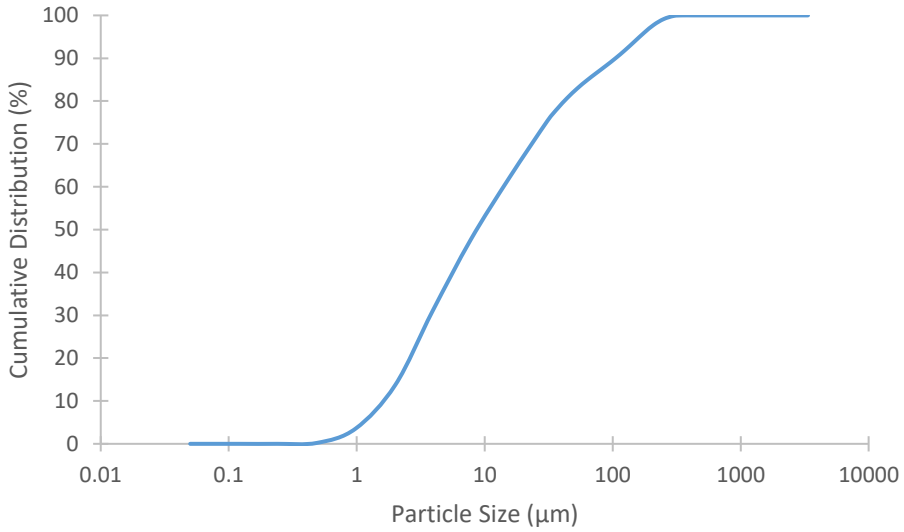

Figure 14: Cumulative distribution of mussel shell powder particle size.

The percentage of cumulative distribution relates to the particle size of mussel shell shown by the distribution curve in Figure 14. Particle size analysis was far more effective and accurate than the use of optical and scanning electron microscopy to determine the average size of mussel shell powder particulates. The results shown above determined that particle sizes were on average almost half the size estimated from SEM.

Hydroscopic behaviour of mussel shell powder

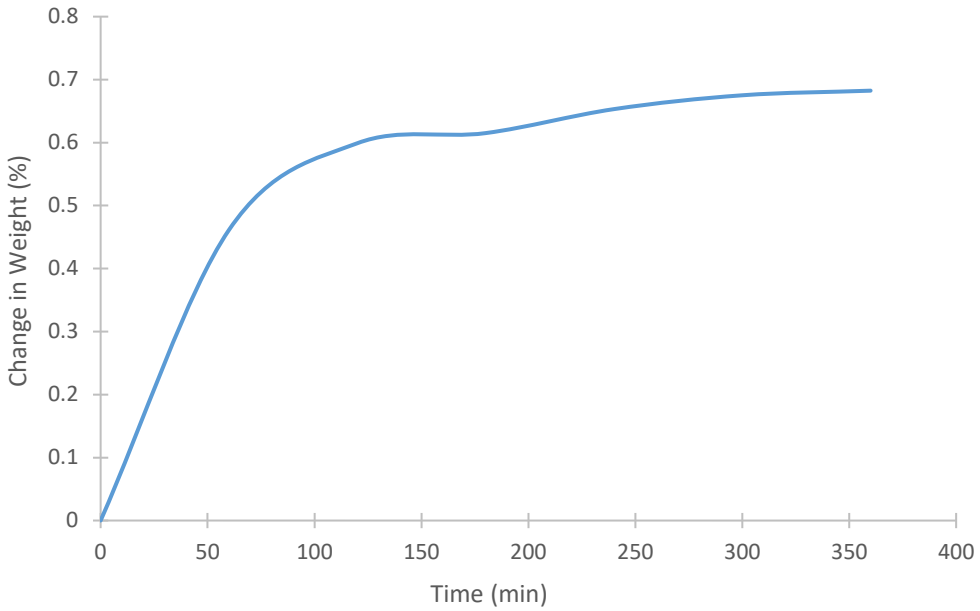

Figure 15: Hydroscopic behaviour of mussel shell powder.

The hydroscopic behaviour determines the amount of moisture uptake by the mussel shell powder. During processing with PLA, it is vital to reduce moisture as it can cause hydrolysis to occur. Over a six-hour period the mussel shell powder absorbed less than 1% of moisture in the air, with over half of that moisture obtained in the first two hours. With this known the mussel shell powder could be exposed to laboratory conditions while processing multiple batches without the risk of moisture being absorbed by the powder.

Simultaneous thermal analysis

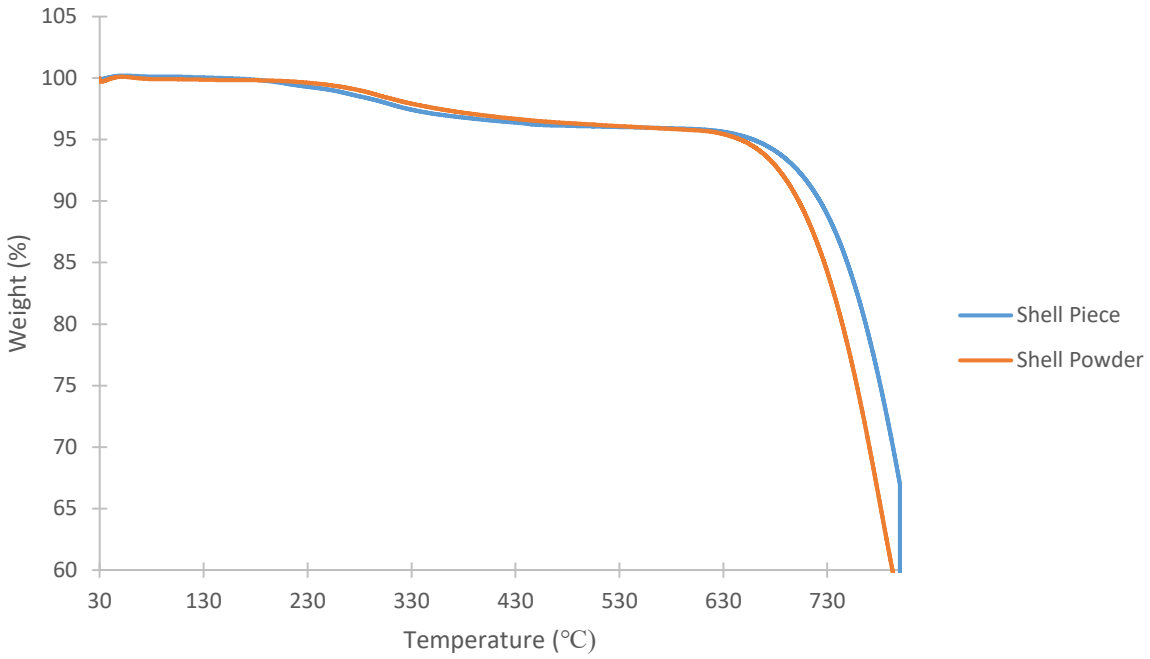

Figure 16: TGA for mussel shell.

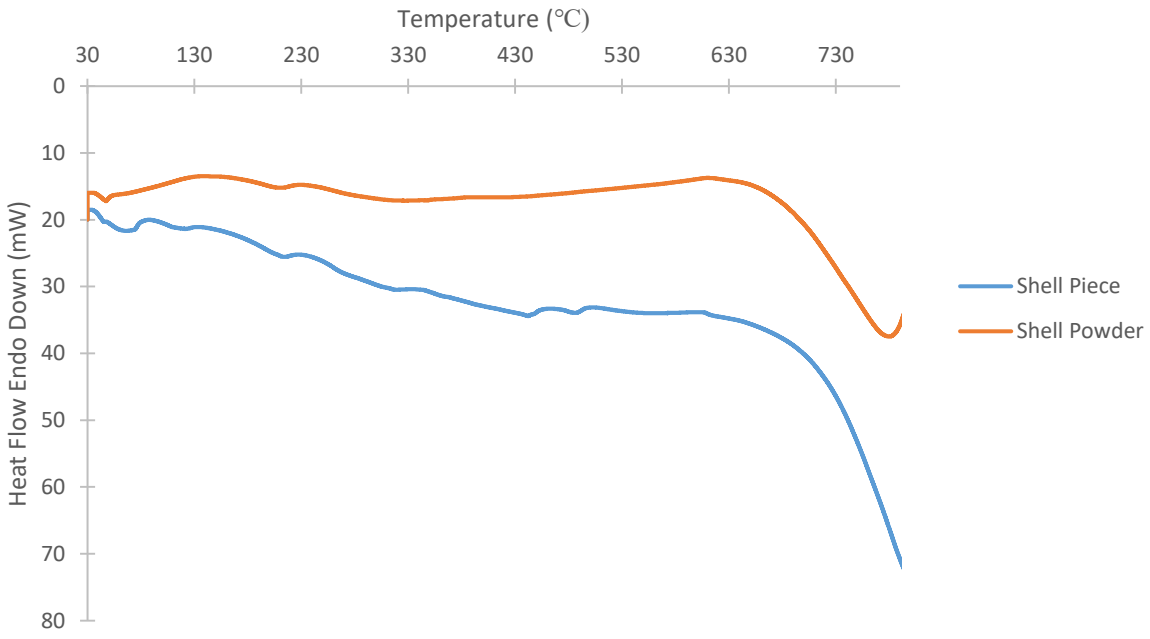

Figure 17: DSC for mussel shell.

Both mussel shell and mussel shell powder have a high degradation temperature of 650℃. It is notable that mussel shell powder has a greater surface area and therefore the material has a greater heat transfer and reaches degradation before a singular piece of mussel

shell. Figure 16 shows a slight decrease in weight percentage between 200℃ and 400℃. This weight decrease is due to the oxidation of the mussel shell, the removal of volatile matter and evaporation of residual moisture within the matrix of the mussel shell (Gigante, et al., 2020). Thermal decomposition of calcite occurs between 700°C to 800°C and tends to take place at a slow rate, followed by rapid decomposition when the temperature exceeds 750°C (Figure 17) (Karunadasa, Manoratne, Pitawala, & Rajapakse, 2019). During thermal decomposition calcium carbonate absorbs heat and shows a considerable weight loss due to the release of carbon dioxide (Karunadasa, Manoratne, Pitawala, & Rajapakse, 2019; Tian, Lin, Yan, & Zhao, 2022).

$$CaCO_{3\,(s)} \rightarrow CaO_{(s)} + CO_{2\,(g)}$$

With carbon dioxide released from calcium carbonate during thermal decomposition the remaining solid is calcium oxide as shown in the equation above.

This information is vital when producing plastics as it is important to reduce the number of gases being produced during extrusion and manufacturing of the composites. With the maximum processing temperature being 190°C it means there should not be any thermal decomposition of calcium carbonate during processing. Consequently, the mussel shell powder will be a composition of calcium carbonate and not calcium oxide from thermal decomposition.

References

Bamigboye, G. O., Nworgu, A. T., Odetoyan, A. O., Kareem, M., Enabulele, D. O., & Bassey, D. E. (2021). Sustainable use of seashells as binder in concrete production: Prospect and challenges. *Journal of Building Engineering,* 34. https://doi.org/10.1016/j.jobe.2020.101864

Gigante, V., Cinelli, P., Righetti, M. C., Sandroni, M., Tognotti, L., Seggiani, M., & Lazzeri, A. (2020, July 28). Evaluation of Mussel Shells Powder as. *International Journal of Molecular Sciences*, 21(15). https://doi.org/10.3390/ijms21155364

Hamester, M. R., Balzer, P. S., & Becker, D. (2012). Characterization of Calcium Carbonate Obtained from Oyster and Mussel Shells. *Materials Research*, 15(2), 204-208. 10.1590/S1516-14392012005000014

Karunadasa, K. S., Manoratne, C., Pitawala, H., & Rajapakse, R. (2019). Thermal decomposition of calcium carbonate (calcite polymorph) as examined by in-situ high-temperature X-ray powder diffraction. *Journal of Physics and Chemistry of Solids*, 134, 21-28. https://doi.org/10.1016/j.jpcs.2019.05.023

Liu, Y. (2001). Pearl. Encyclopedia of Materials: *Science and Technology (Second Edition)*, 6781-6783. https://doi.org/10.1016/B0-08-043152-6/01200-6

Sari, M., & Yusuf, Y. (2018). Synthesis and Characterization of Hydroxyapatite based on Green. *International Journal of Nanoelectronics and Materials,* 11(3), 357-370. http://dx.doi.org/10.1088/1757-899X/432/1/012046

Tian, X., Lin, S., Yan, J., & Zhao, C. (2022). Sintering mechanism of calcium oxide/calcium carbonate during thermochemical heat storage process. *Chemical Engineering Journal*, 428. https://doi.org/10.1016/j.cej.2021.131229

Valenti, W. C., Kimpara, J. M., & Preto, B. d. (2011). Measuring aquaculture sustainability. *World Aquaculture*, 43(3), 26-30. https://www.caunesp.unesp.br/Home/publicacoes/fa_valenti_measuring-aquaculture.pdf

Chapter four: Experiment one

Objective: Chapter four covers the creation, characterisation, and testing of the filament composites. Characterisation in this section includes thermal gravimetric analysis (TGA) and differential scanning calorimetry (DSC) to determine thermal stability such as weight loss and heat transfer. The samples were classified as either: low weight percent (0-2wt%), medium weight percent (4-10wt%) or high weight percent (20-30wt%) filaments. These samples were tensile tested before 3D printing. From this it is possible to determine whether processing had caused a loss in mechanical performance by the force required to break the filament sample, the Youngs' modulus, and general behaviour of the stress and strain curve. Scanning electron microscopy (SEM) and optical microscopy (OM) were used to visualise the fracture surface after tensile testing.

Filament composites

It was imperative that the composite filaments had a diameter close to 1.75 mm as that measurement was acceptable for 3D printing. Filament for 3D printing was a crucial factor as it was a versatile method of manufacturing products. Filaments with diameters lower than 1.60 mm were found to be difficult to tensile test as samples began to slip in the clamps.

Overall, PLA filaments showed good extrusion capabilities, with little hydrolysis present in samples from 0-10wt% of mussel shell powder. The filament demonstrated good processability due to the rapid cooling speed, specifically when the cooling fan was used (Figure 18a). The extruded PLA sample's diameters measured close to 1.75 mm although this value fluctuated by ± 0.10 mm. PLA samples showed somewhat brittle properties when on the spool, but also a degree of flexibility.

When the PLA filament was extruded at weight percentages that exceeded 10wt%, strands became increasingly difficult to extrude. Filaments at these greater percentages exhibited decreased viscosity and extruded with more liquid characteristics, with a higher probability for bubbles to have occurred. Liquid melt was more difficult for a strand of filament to be held and typically broke due as it took longer to cool and didn't solidify

a)

b)

c)

Figure 18: Filament process, a) Filament cooling fans, b) Filament measurement system, c) Filament spool collection.

LDPE composites were successfully filament extruded to a weight percentage of 30wt% of mussel shell powder. Low weight percent filaments were more difficult to extrude but could be produced with consistent adjustments. The diameter of LDPE filaments was larger than PLA due to thermal expansion of the polymer after extrusion which became difficult to control and predict. The successful creation of both PLA and LDPE filaments shows that not only can the composite be made but it can be re-extruded at least once.

Figure 19: LDPE + 30wt% filament during tensile testing.

Tensile testing

In this section the results of the low, medium, and high weight percentage filament samples made with PLA and LDPE will be discussed. Samples were tensile tested to determine properties such as Youngs' modulus, ultimate tensile stress, yield stress, and strain.

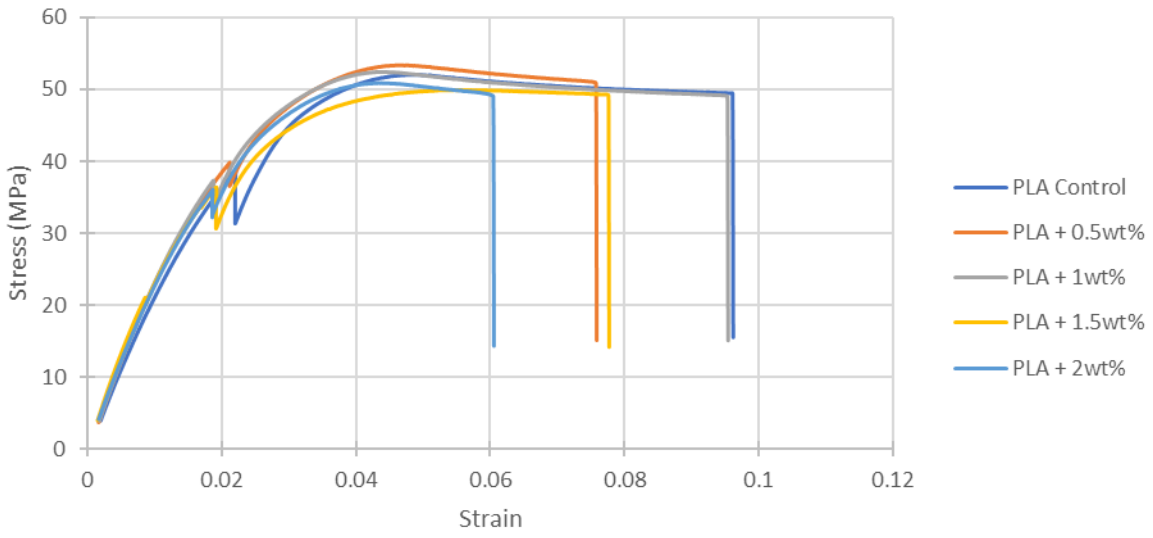

Figure 20: Tensile results for PLA 0-2wt% samples.

The tensile stress from low weight percentage samples remained consistent between each sample. The majority of yield stress results occurred at 53 MPa, with all samples ranging between 50 MPa and 55 MPa. The most notable difference between the control sample and the 2wt% sample is the reduction in elongation to break. Between these two samples the strain reduced by 0.04, although this is only a minor change it was notable to point out that as the weight percentage of mussel shell increased the strain tended to decrease as well. Strain decreases as the composites developed more brittle properties with larger amounts of mussel shell, which becomes more noticeable in the following graphs.

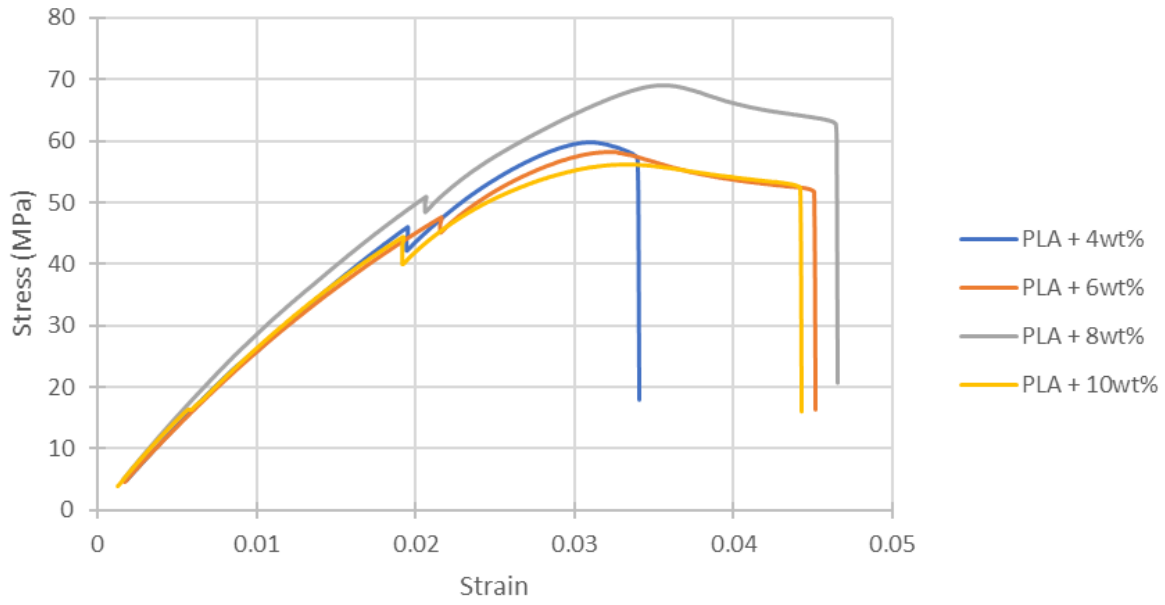

Figure 21: Tensile results for PLA 4-10wt% samples.

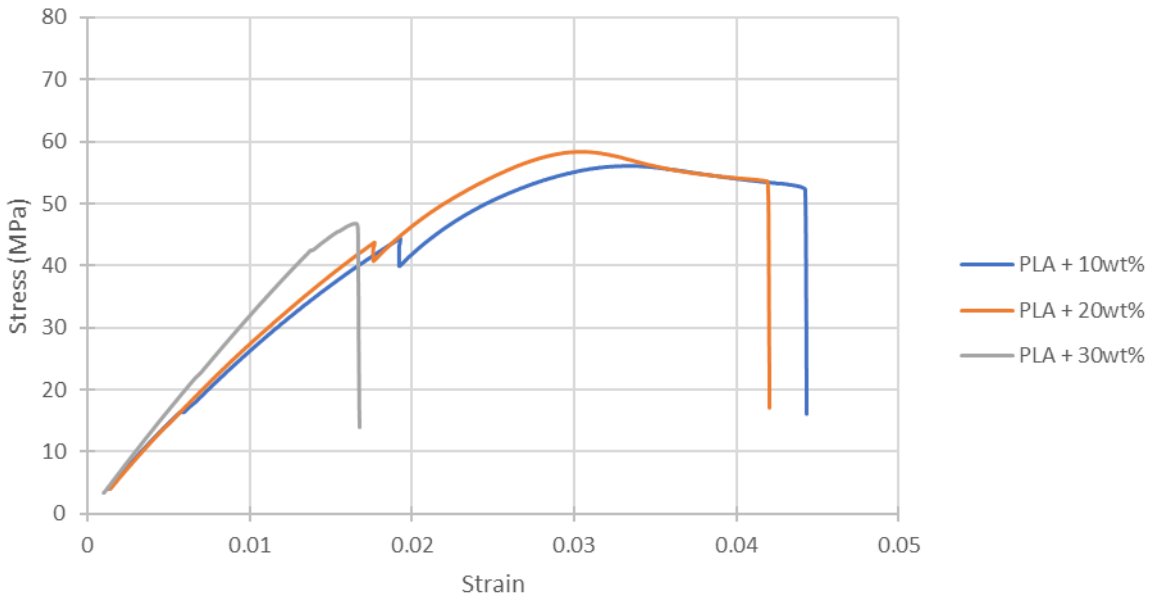

Figure 22: Tensile results for PLA 10-30wt% samples.

As the composites reached higher percentages of mussel shell two things were happening:

1. During processing an acid-base reaction between PLA and $CaCO_3$ was occurring, which resulted in the production of H_2O. Water produced from this reaction caused hydrolysis of the PLA, which effectively reduced the structural properties of the polymer and weakened the molecular bonds, by making the polymer chains shorter.

2. A substantial increase of particulates in the composite were acting as stress concentrators within the filament.

Once 30wt% of the mussel shell powder was reached it had detrimental effects on the stability of PLA, which resulted in the material becoming extremely brittle and reaching failure almost instantly. It could be determined that previous academic research did not display results with 30wt% due to the poor tensile properties and results shown in Figure 22.

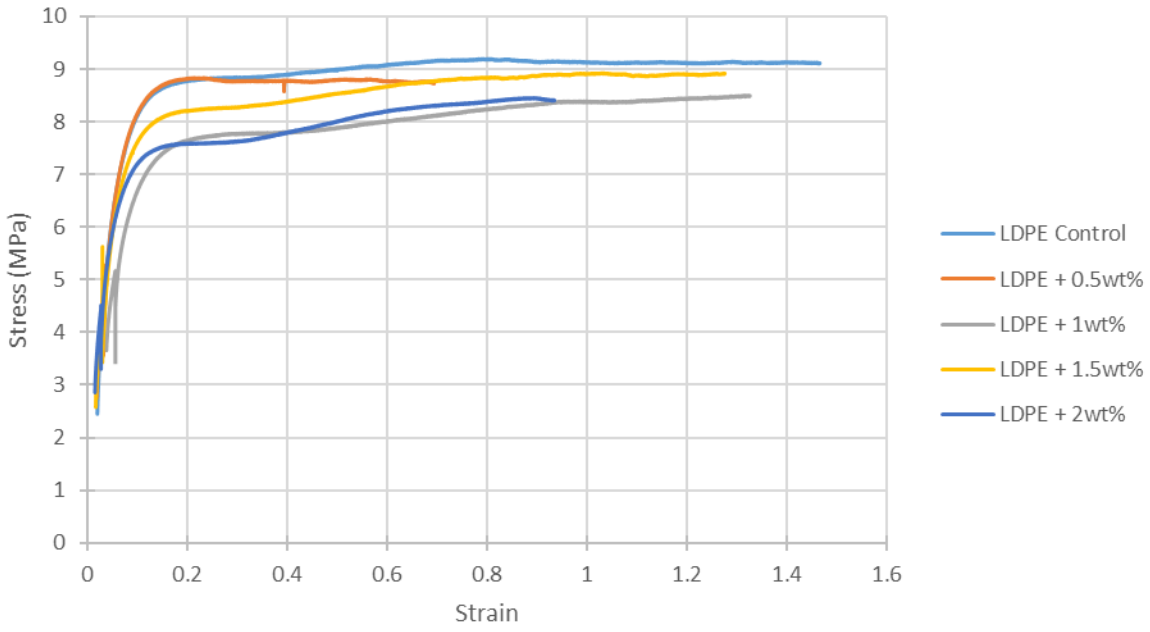

Figure 23: Tensile results for LDPE 0-2wt% samples.

LDPE samples showed much lower tensile strength, Youngs' modulus, and ultimate tensile strength than the PLA samples. Although these properties in LDPE were much lower, LDPE samples show exceptional elongation and plastic deformation properties. LDPE showed decreasing tensile strength as the weight percentage of LDPE was increased, reducing 1.5 MPa from the LDPE control to 2wt% sample. The low weight percent LDPE samples all ranged between 7-9 MPa for tensile strength at yield.

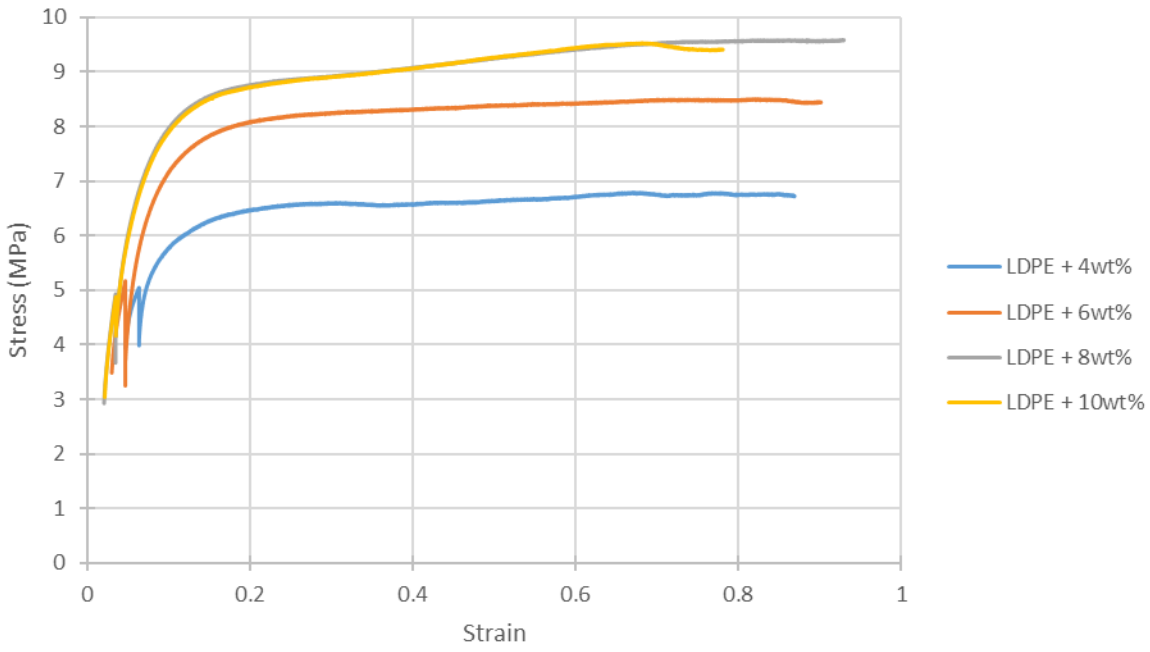

Figure 24: Tensile results for LDPE 4-10wt% samples.

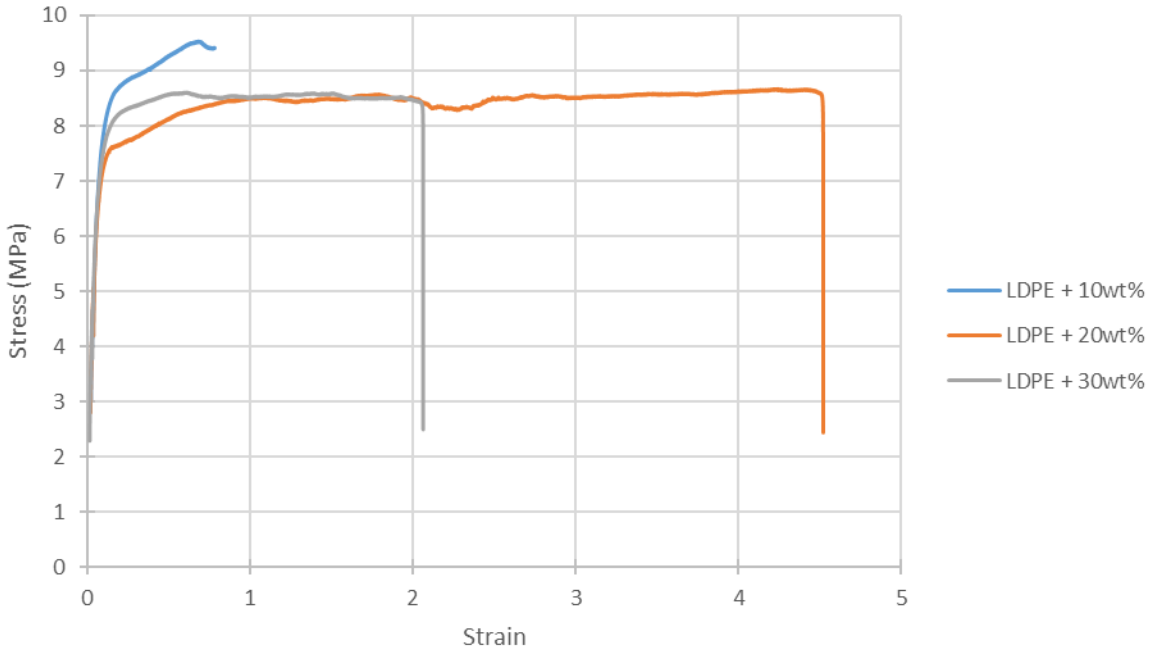

Figure 25: Tensile results for LDPE 10-30wt% samples.

The medium weight percent LDPE samples showed comparable results to the low percent samples, ranging between 7-8 MPa for tensile strength at yield. LDPE 4-10wt% showed lower results than studies conducted by Zapata, et al. (2019), although 3wt% and 5wt% of calcium carbonate were used as a filler, the results for yield stress were 9 MPa for both samples.

The 4wt% sample showed exceptionally low tensile results, which seemed inconsistent in comparison to other LDPE results in this experiment. Although 5-8 samples were tested these results could be due to defects in the filament, such as large particulates or a cluster of particulates acting as a stress concentrator, reducing the overall tensile strength. Defects in filament could implicate 3D printing materials by blocking the extruder nozzle. Another, implication that could occur would be a decrease structural integrity in application.

LDPE 20wt% and LDPE 30wt% showed less ductility with a higher percentage of mussel shell powder. This was noticeably due to the failure of the material at decreasing strains of 2.06 and 4.5, with strain decreasing by 2.5 between the two samples. Both LDPE 20wt% and LDPE 30wt% showed similar UTS values of 8.5 MPa, although LDPE had a lower tensile yield strength. LDPE 10wt% showed greater properties than LDPE 20wt% and LDPE 30wt% as shown above. A study by Prabhu, Mendonca, Darren, Gladson, & Bhat, (2016) examined LDPE with 20wt% calcium carbonate. This study showed slightly higher tensile results of 10 MPa than was was observed in this study.

Overall LDPE samples in this thesis tend to have showed less superior results than what was covered in literature. This could be related to the grade of LDPE used which was tailored to towards film extrusion rather than conventional extrusion.

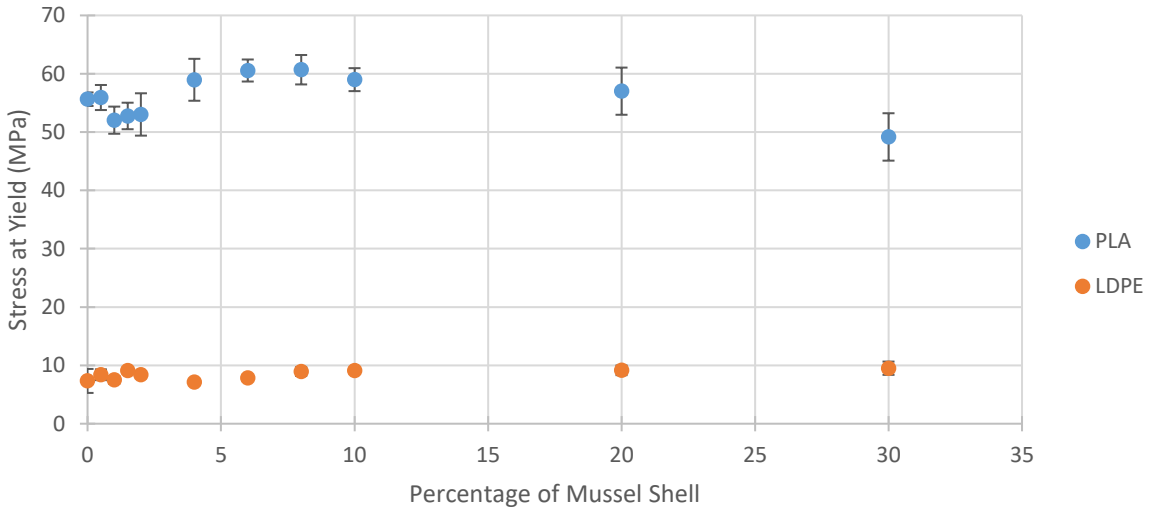

Figure 26: Yield stress of PLA and LDPE composites in relation to weight percentage of filler.

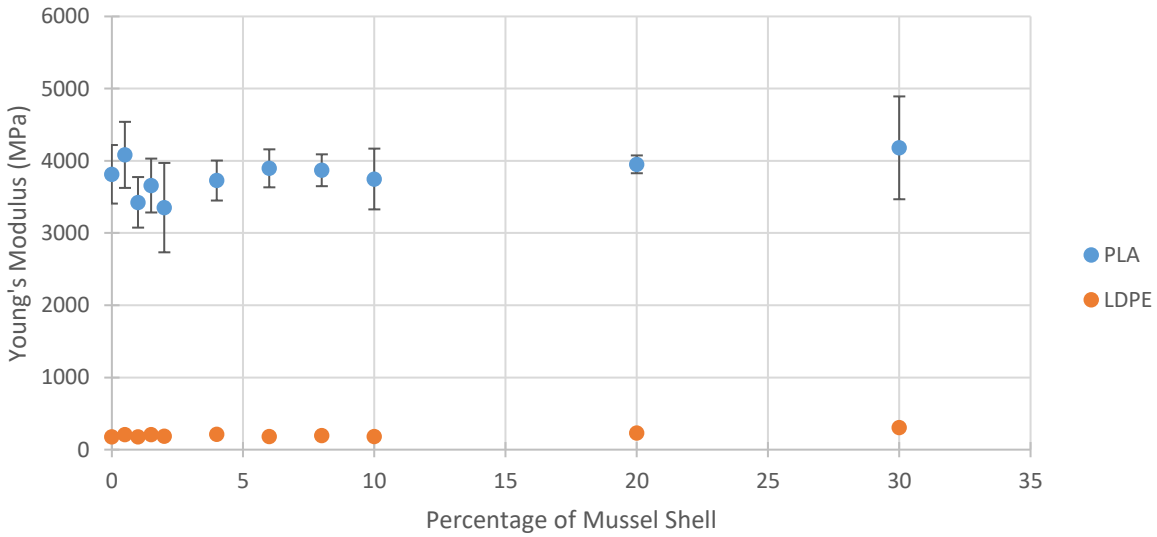

Figure 27: Youngs' modulus of PLA and LDPE composites in relation to weight percentage of filler.

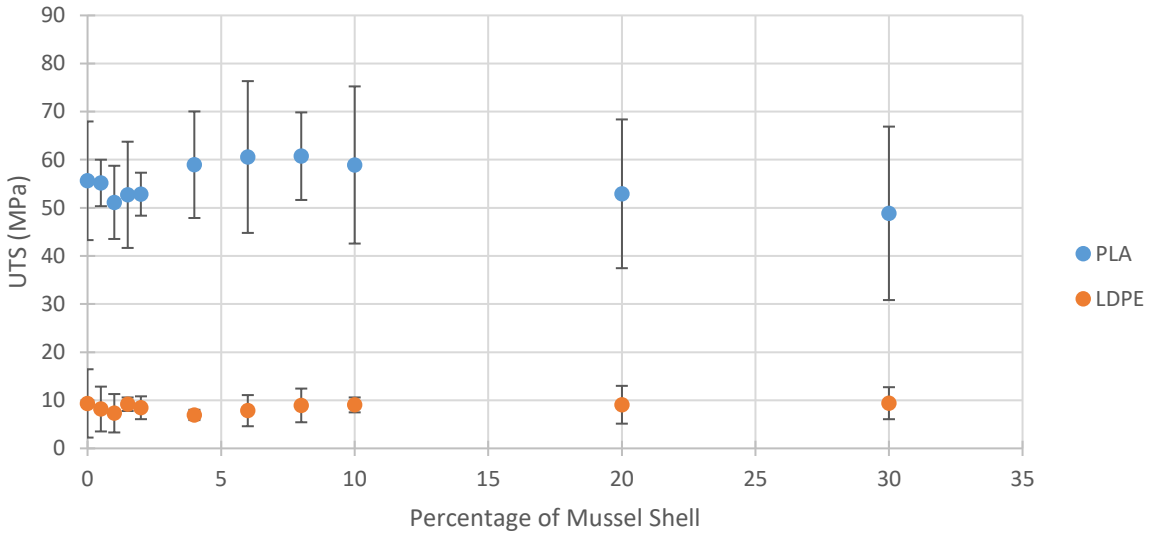

Figure 28: Ultimate tensile stress of PLA and LDPE composites in relation to weight percentage of filler.

Average stress, Youngs' modulus and UTS was plotted for each percentage of mussel shell. The uncertainty was calculated through the standard deviation of each sample. The standard deviation shows the accuracy of each result and where the results would lie if the test were repeated multiple times.

Tensile stress at yield showed an average of 4% variation between most samples. The 30wt% samples showed the greatest variation of 8%, which is expected as the samples became more unreliable during processing. Youngs' modulus had varying slope between samples showing approximately 10% variation. The 30wt% sample showed the greatest variation of 17% due the inconsistent failure of the samples.

Microscopy/SEM

PLA samples failed in a brittle manner during tensile testing which resulted in a flat fracture surface. The flat or smooth surfaces shown at the bottom of each image in Figure 29 relates to the highly stiff properties in PLA. During tensile testing brittle failure occurs as a single defect/crack propagates throughout the sample, creating a fracture point and the immediate failure of the sample (Obi, 2018). This fracture surface was expected to remain consistent between all PLA samples.

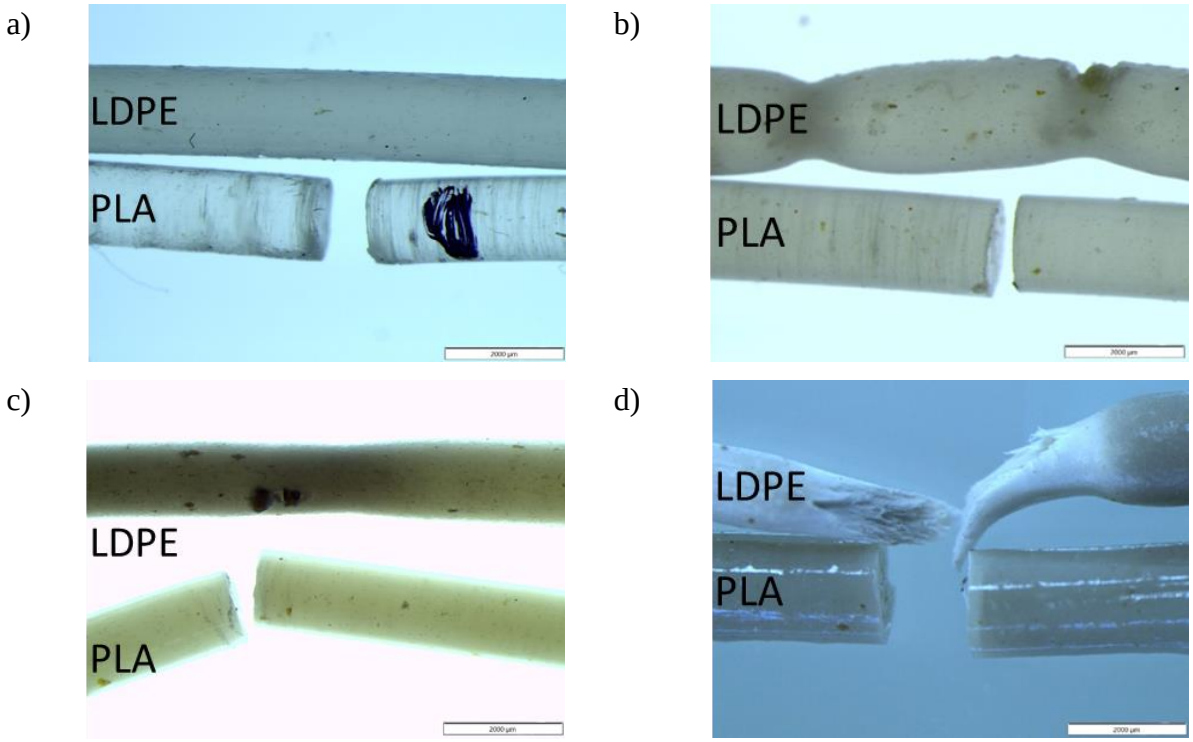

Figure 29: Tensile images a) control b) 2wt% c) 10wt% d) 30wt%. [note: the top sample in each image is LDPE and the bottom sample in each image is PLA].

LDPE samples began to show deformation and necking when larger particulates acted as a stress concentrator within the filaments, which can be seen occurring in the top sample of Figure 29b. Increasing the amount of mussel shell in LDPE reduced ductility of the filaments resulting in more rapid failure.

SEM images showed the PLA control had a smooth fracture surface with little features, with the addition of 10wt% mussel shell it is notable to see mussel shell particulates imbedded in the fracture surface. Particulates in the PLA were smaller than 50 µm and showed defined shell structures as seen in Chapter 3 SEM images.

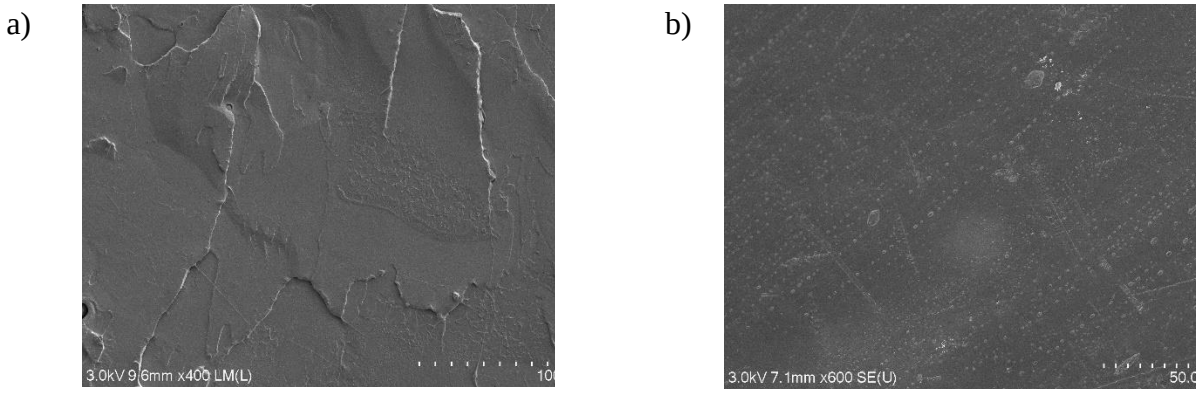

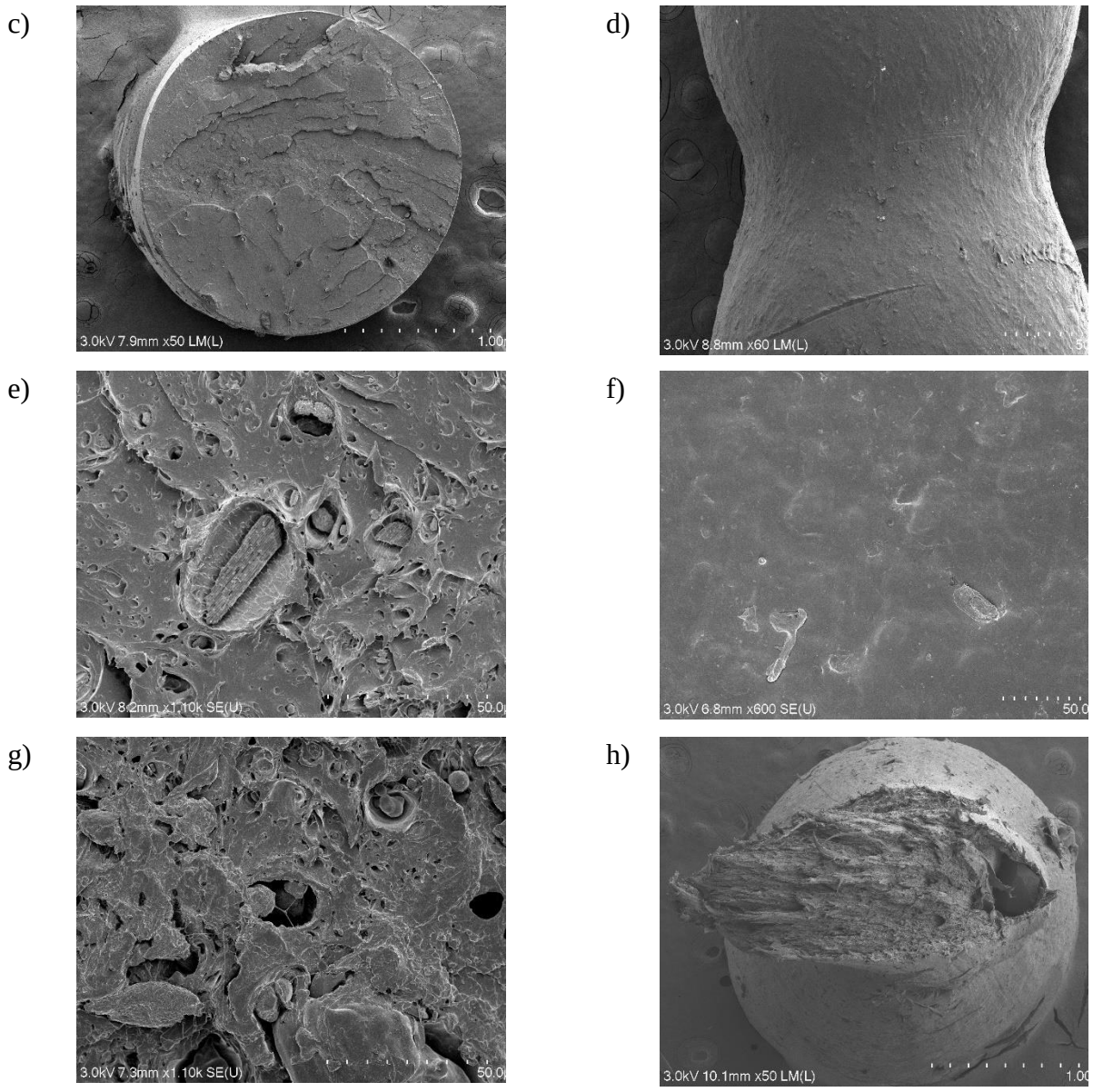

Figure 30: SEM tensile images a) PLA control, b) LDPE control, c) PLA 2wt%, d) LDPE 2wt%, e) PLA 10wt%, f) LDPE 10wt%, g) PLA 30wt%, h) LDPE 30wt%.

LDPE samples showed ductile fracture at 30wt%, with the SEM images showing large mussel shell particles acted as a stress concentrator within the filament. Images b), d) and f) in Figure 30 showed side profile on the filament due to the material taking a long time to reach failure. It is notable that d) shows necking and plastic deformation during tensile testing.

Thermal analysis

This section presents the thermal properties of the composite materials (PLA and LDPE) to determine the thermal capabilities that these materials could withstand. The information provided by thermal analysis could show melting points, glass transition temperatures and thermal degradation.

The ***melting point*** of a material occurs when a solid material transitions from a solid state to a liquid state (Qiu, 2018)

Glass transition temperature occurs during heating or cooling of an amorphous material as a specific temperature. During cooling the material becomes brittle whereas during heating the material becomes soft (Dastidar & Chakrabarti, 2019).

The ***degradation temperature*** in thermoplastic polymers occurs when $T \geq T_m$, this typically involves the depolymerization of the plastic. Thermal degradation is the limit of heat a material can withstand before the polymer degrades and begins to transfer into a gaseous state, which results in the release of gases such as carbon monoxide and carbon dioxide and a substantial amount of mass of the material is lost (Niaounakis, 2015; Süli, 2019).

The properties of these composites were studied at various temperatures spanning from 30-600℃ covering the processing temperatures that the materials are likely to reach during peak temperatures of extrusion. Processing temperatures during extrusion ranged between 160-190℃, therefore thermal analysis could determine whether degradation is occurring during this stage.

Thermogravimetric analysis

TGA studies the mass transfer of a material as it is heated. Polymers are heated to temperatures of thermal degradation, where most of the composites thermally combust resulting in dramatic weight loss. This technique allows for the uppermost thermal limits of a material to be exposed. Knowing the degradation temperature is important as it indicates the maximum temperature a material could withstand. Firstly, this section presents TGA data on PLA samples ranging from 0-30wt% followed by LDPE samples in the same range.

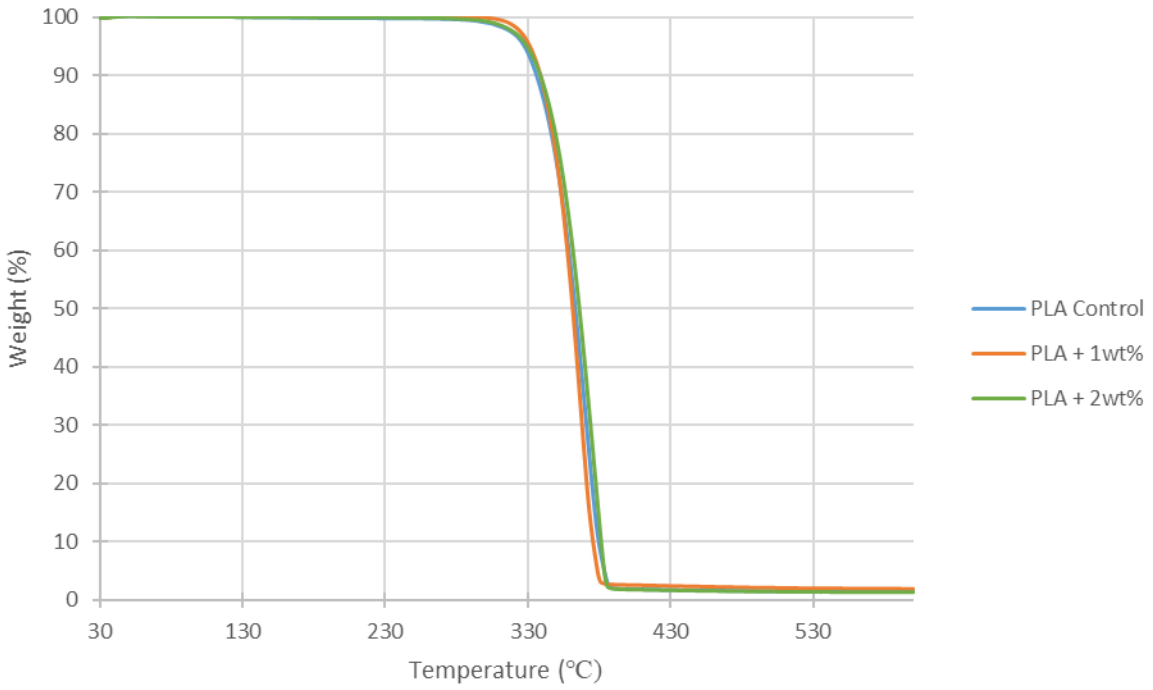

Figure 31: TGA of PLA 0-2wt% samples showing thermal degradation.

As the weight percentage of mussel shell was increased there was a slight increase in residual weight due to the $CaCO_3$ that did not degrade during heating. This is due to the far greater thermal degradation temperature of $CaCO_3$ as shown in Chapter 3. Although there was an increase in mussel shell powder there was only slight change to be noted for the TGA curves. This shows at low concentrations there is no positive or negative effects to the degradation temperature by adding mussel shell powder to the polymer at these percentages.

The temperature remained the same throughout the PLA 0-2wt% samples at approximately 340°C. PLA composites were processed at 190°C which was much lower than the thermal degradation. Therefore, the temperature at which the composites were processed will not be affected by any sort of thermal degradation.

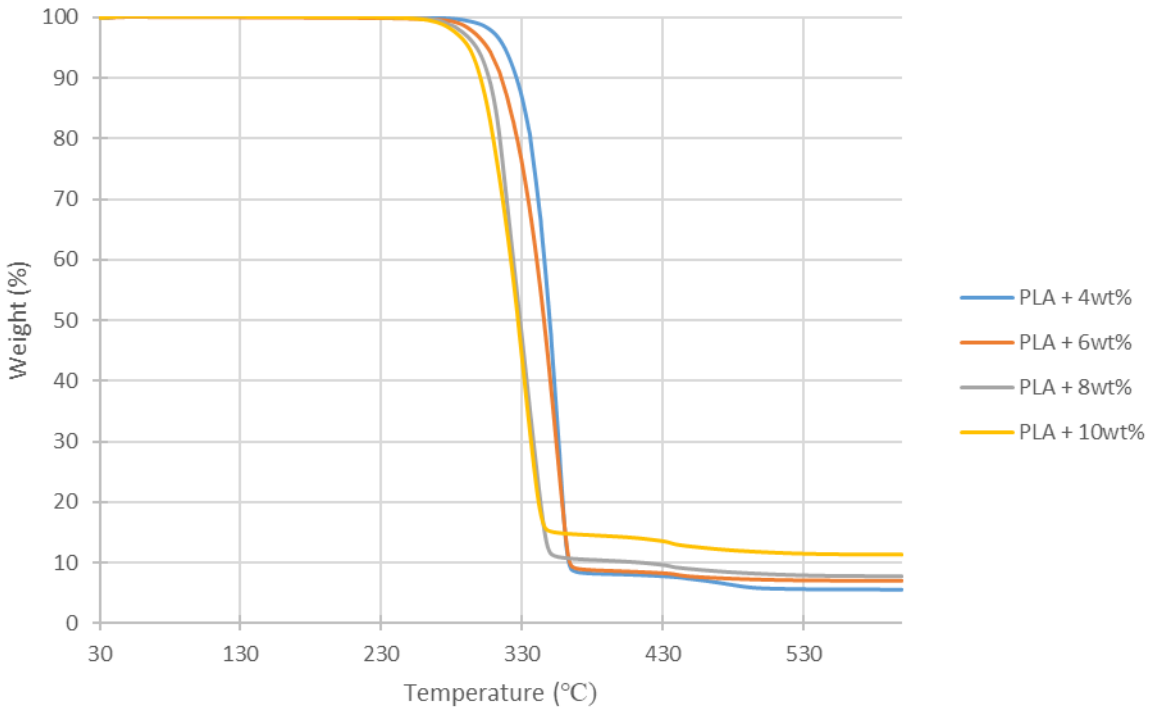

Figure 32: TGA of PLA 4-10wt% samples showing thermal degradation.

PLA thermal degradation occurred at lower temperatures as the weight percentage of mussel shell was increased. These results were unexpected, as degradation of mussel shell occurs at higher temperatures and in this case the degradation of PLA was decreasing.

The lower thermal degradation temperature of PLA compared to other thermoplastics was caused by the aliphatic ester structure of the polymer. This resulted in random chain scission or specific chain-end scission, when combined with hydrolysis it breaks down the ester structure effortlessly (Li, Qiang, Chen, & Ren, 2019). During extrusion hydrolysis could occur with the introduction of moisture in the barrel, causing a potential decrease in thermal degradation. Degradation through heat or moisture breaks down the PLA chains into shorter chains with lower molecular weight, shorter PLA chains had the ability to biodegrade or in this case with constant heat the polymer degrades further, producing methane and carbon dioxide which allows for PLA to be composted in similar environments (Kost, et al., 2022). Although chain-end scission could occur in PLA, it is unlikely to happen during this process of thermal analysis due to the machine being continuously purged with argon gas. It is notable to mention as it could occur in the extrusion process due to the variability of heat and moisture in the extruder barrel. Hydrolysis could be seen to occur when >4% of mussel shell was added, notably, due to the decrease in onset of thermal degradation between PLA + 4wt% and PLA + 10wt%, which could be seen in Figure 32.

Onset occurred at 320°C for PLA + 4wt% and 290°C for PLA + 10wt%, showing a 10°C change between the two samples. PLA + 6wt% showed a similar onset temperature as PLA + 10wt% although showed a final weight percentage similar to that of PLA + 8wt% (as shown in Figure 32). This could show a slight inconsistency with how the extruder mixed the polymer and mussel shell powder, resulting in some granules with lower percentages and lower than expected final weigh percentages. With higher volumes of mussel shell there was more material left over as calcium carbonate has a much higher degradation temperature. The remaining weight percentage showed a 5% increase between the PLA + 4wt% sample and PLA + 10wt% sample.

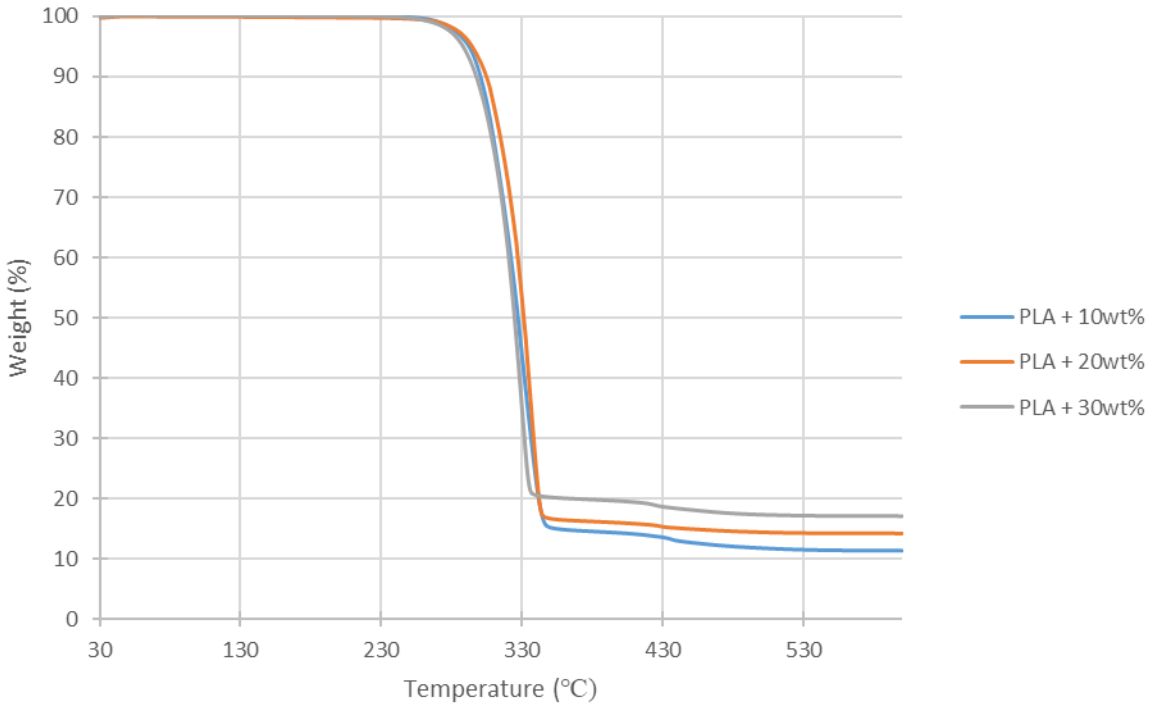

Figure 33: TGA of PLA 10-30wt% samples showing thermal degradation.

Thermal degradation of PLA 10-30wt% is shown in Figure 33 and remained remarkably similar between each sample, only decreasing by a total of 3°C (~1.5°C per sample). As mentioned above PLA + 10wt% showed a thermal degradation temperature of 290°C, with PLA + 20wt% at 288.5°C and PLA + 30wt% at 287°C. Degradation remains constant as there is far more mussel shell powder in the samples. PLA + 20wt% and PLA + 30wt% showed final weight percentages that were lower than expected, this could be due to the volatile organic matter in the mussel shell powder burning off as it reached higher temperatures.

Thermal degradation reduced from 340°C to 287°C between the PLA control and PLA + 30wt%, showing an overall decrease of 50°C. A study by Nekhamanurak, Patanathabutr & Hongsriphan (2014) showed similar decreases in thermal degradation temperatures using PLA and three different grades of $CaCO_3$. One grade of $CaCO_3$ consisted of micro-particles at 1600 µm, the other two grades consisted of nano-particles at 40 µm and 40-60 µm. Samples consisted of PLA and 0-20wt% of $CaCO_3$ resulting in thermal degradation tempurature ranging from 340°C at 0wt% to 280°C at 20wt% for the two grades of nano-$CaCO_3$. Both these grades of $CaCO_3$ remain consistent with the data collected in Figure 31, Figure 32 and Figure 33. The micro- $CaCO_3$ samples showed a lower decrease in the thermal degradation temperature. Thermal degradation ranged from 340°C at 0wt% to 300°C in these samples, which showed greater thermal properties (Nekhamanurak, Patanathabutr, & Hongsriphan, 2014).

Nekhamanurak, Patanathabutr & Hongsriphan (2014) states further that the addition of fatty acids added to some grades of $CaCO_3$ result in a negative effect and a chemical reaction between the ester linkage in PLA promoting chain scission and a further reduction of the thermal degradation of the composite.

According to Miller, Pearce, & Bettjeman (2014) Greenshell™ mussels consist of omega-3 and polyunsaturated fatty acids between calcium carbonate layers. Traces of fatty acids in the mussel shell itself could affect the thermal decomposition of PLA composites showing a direct correlation between data produced from Nekhamanurak, Patanathabutr, & Hongsriphan (2014) and data recorded in Figure 31, Figure 32 and Figure 33.

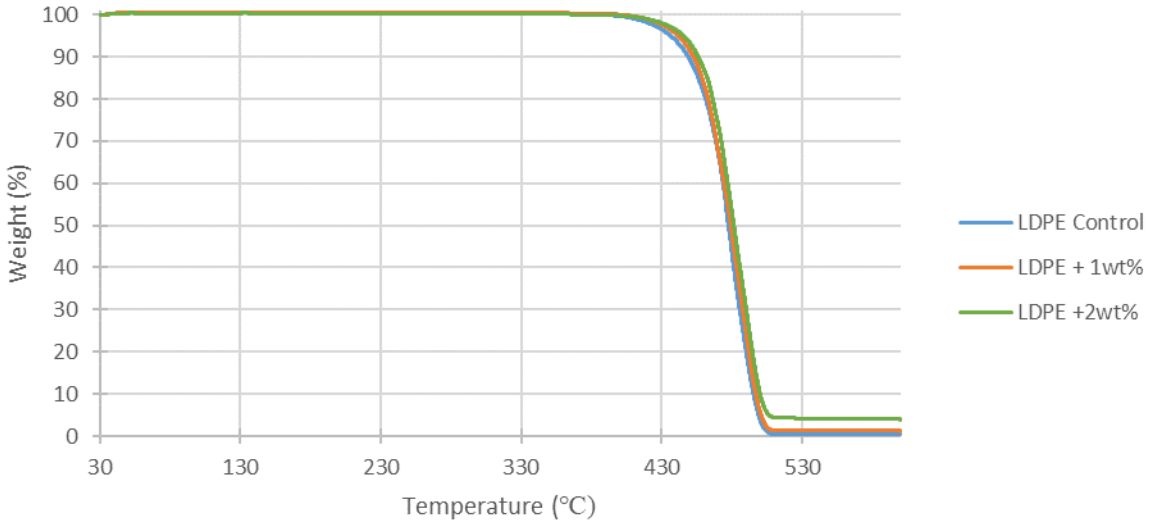

Figure 34: TGA of LDPE 0-2wt% samples showing thermal degradation.

LDPE samples containing 0-2wt% mussel shell showed a loss in weight that tends to occur at similar temperatures approximately 440℃. Notably, as the weight percentage is increased by 1% the onset temperature of degradation increases by 2℃ for the samples in Figure 34. Onset occurs at 442℃ for neat LDPE, 445℃ for LDPE + 1wt% and 447℃ for LDPE + 2wt% (Figure 34). In comparison to the PLA 0-2 wt% samples in Figure 31, the LDPE samples have a much higher thermal degradation temperature. Thermal degradation on LDPE occurs 100℃ higher than that of similar PLA samples due to the different chemical structures of the polymers.

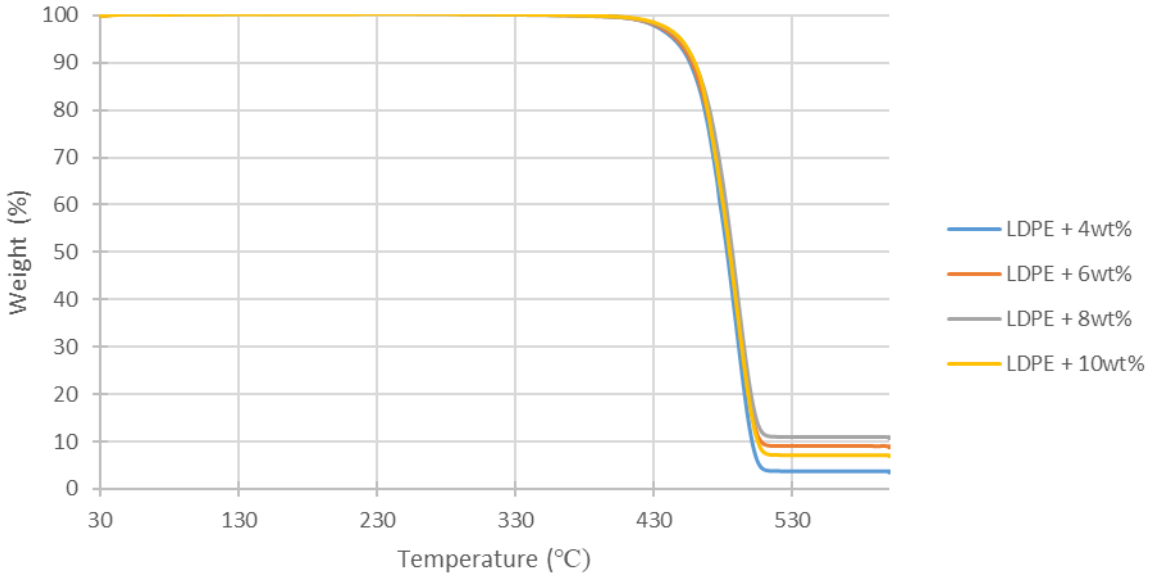

Figure 35: TGA of LDPE 4-10wt% samples showing thermal degradation.

Similar to Figure 34 there is little change between the onset of degradation between samples in Figure 35. Thermal degradation temperatures occurred at 454℃ (LDPE + 4wt%), 456℃ (LDPE + 6wt%), 459℃ (LDPE + 8wt%) and 462℃ (LDPE + 10wt%). This showed a 6℃ increase between LDPE + 4wt% and LDPE + 10wt%, which is approximately a 2℃ change between each sample in Figure 35.

Interestingly, LDPE + 10wt% showed low residual weight, which was lower than LDPE + 6wt% and LDPE + 8wt%. This could be due to composite containing lower percentages of mussel shell powder based on each granule or the mussel shell powder itself contained high quantities of residual organic matter, proteins, or fatty acids.

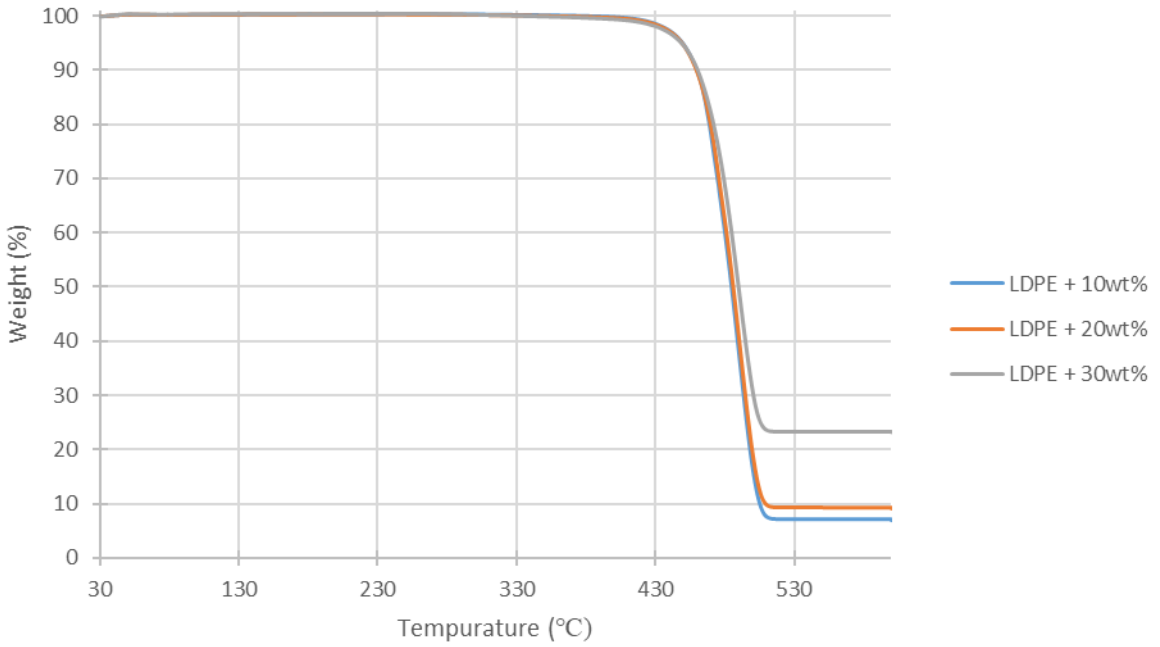

Figure 36: TGA of LDPE 10-30wt% samples showing thermal degradation.

The samples in Figure 36 showed no change in thermal degradation temperature at 462°C showing a limit to thermal degradation. Thermal degradation increases 22°C between LDPE control and LDPE + 30wt%. The degradation increase of LDPE is much different to PLA as the degradation temperature for PLA samples decreased as mussel shell powder was increased.

Notably, LDPE + 30wt% showed a large quantity of residual weight which was expected due to the high percentage of mussel shell in the sample.

Figure 37 clearly shows the change in thermal degradation temperatures for both PLA and LDPE in relation to the percentage of mussel shell powder in the composite. As mentioned earlier PLA composites showed a decrease in onset of thermal degradation where LDPE composites showed an increase. This was related to how the mussel shell powder behaved with the type of polymer. In this case, PLA experienced a decrease due to hydrolysis and a reaction between the polymer and filler, where LDPE showed an increase because of the high percentage of ceramic material (mussel shell) and no cause of reaction.

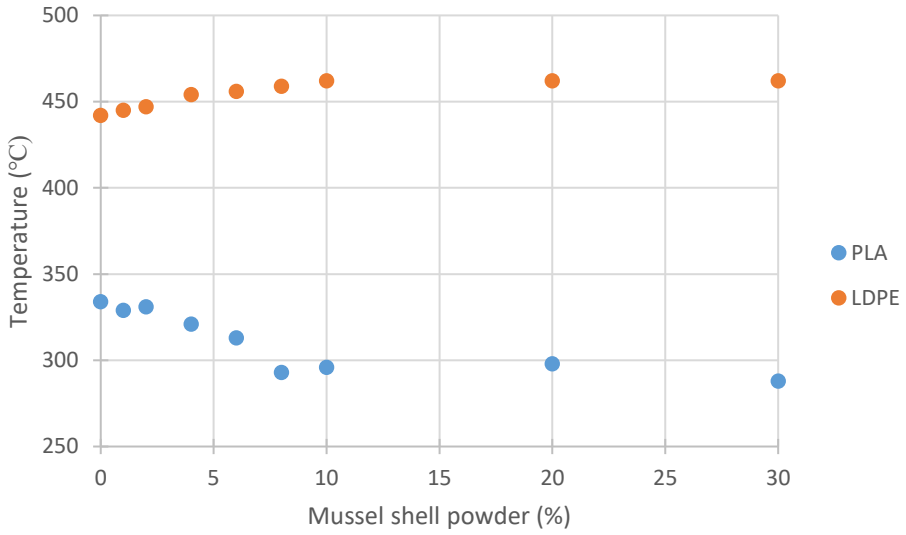

Figure 37: Thermal degradation temperatures of PLA and LDPE composites in relation to weight percentage of filler.

Differential scanning calorimetry

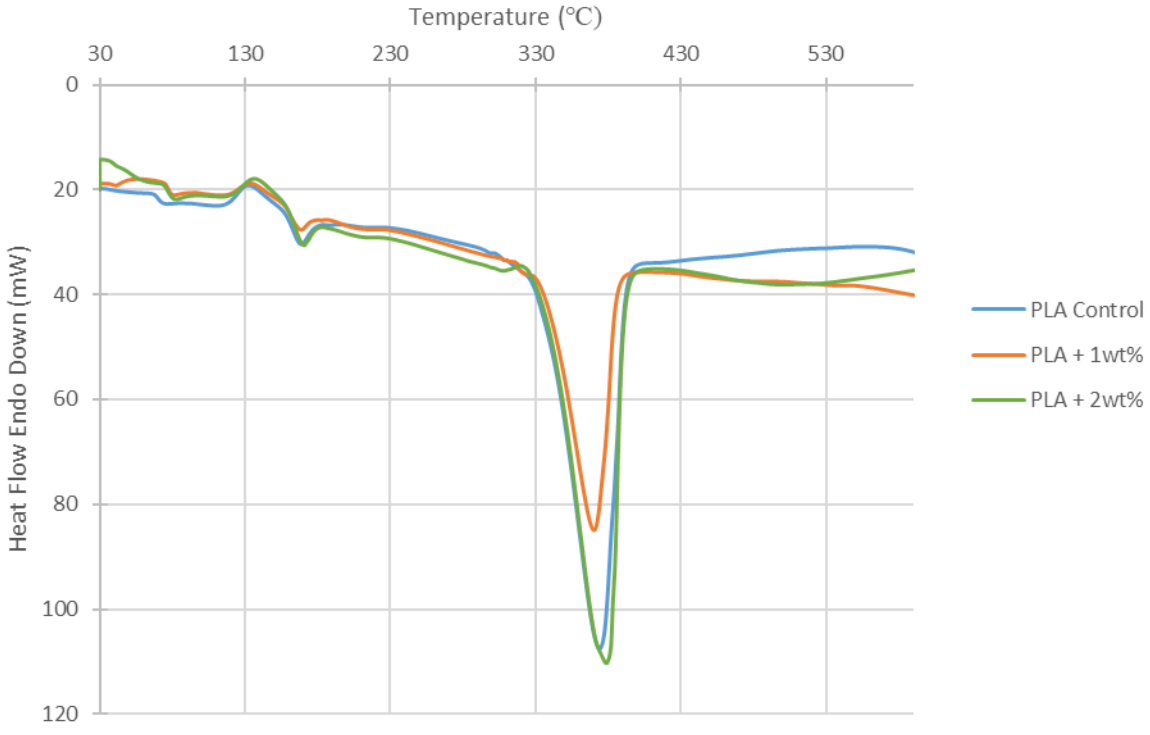

Figure 38: DSC of PLA 0-2wt% samples showing thermal peaks.

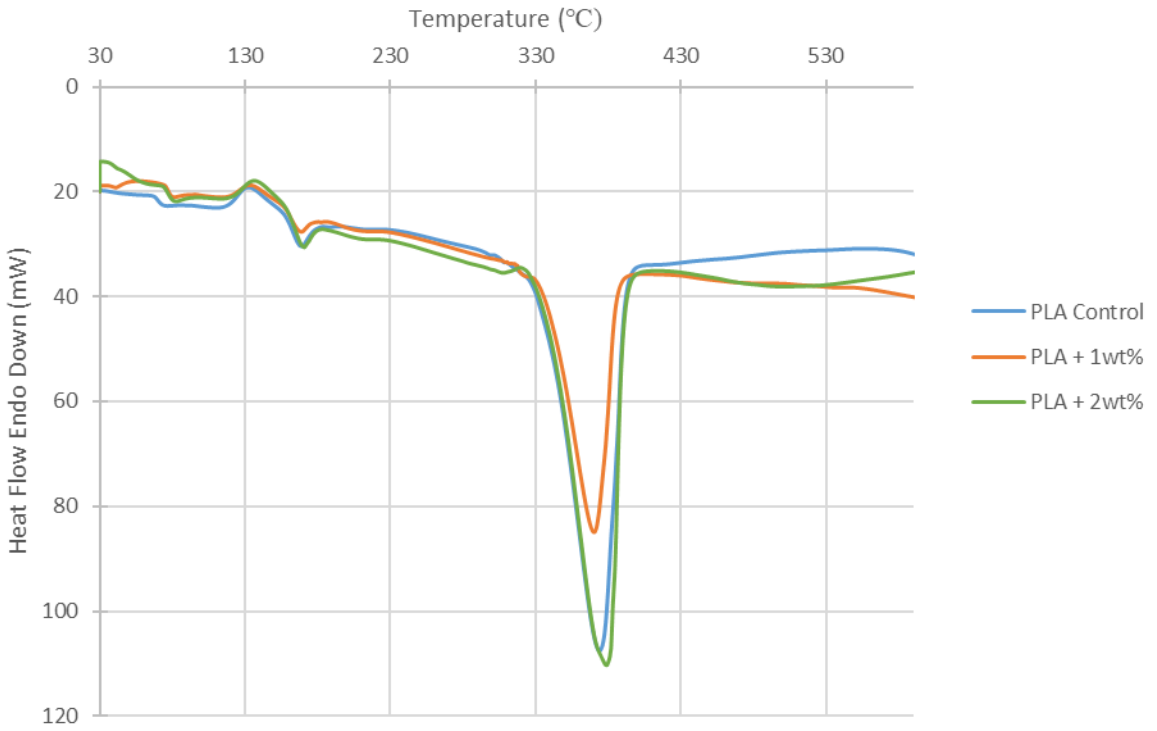

Figure 38 shows the endothermic peaks on the DSC graph at various points that are notable in the heating of PLA samples. Firstly, there is a small but notable peak at 60°C that occurs with the 1wt% and 2wt%, which shows the glass transition of the sample. The addition of calcium carbonate fillers did not affect the glass transition temperature of PLA at low weight percentages of mussel shell powder but resulted in an intensified cold crystallization (Piekarska, Piorkowska, & Bojda, 2017; Piekarska, Piorkowska, & Bojda, 2017)

At 146°C an exothermic peak occurs which releases heat and shows the cold crystallisation of PLA. Cold crystallisation occurs between glass transition and the melting point (Yu, Liu, Dean, & Chen, 2008) which could be seen in the data above. Cold crystallisation was caused by the increased mobility of polymer chains as a polymer is heated It was found in a study conducted by Tarani, et al. (2021) that cold crystallisation of PLA is affected by increased heating rates, resulting in a thermal delay of the polymer. Athough, heating rates remained constant during thermal analysis techniques, Tarani, et al. (2021) continues to mention that the cold crystallisation temperature could be shown to decrease in the presence of fillers. PLA composites that have consisted of Ag and TiO_2 have demonstrated to be nucleation sites for cold crystallisation. In this work a mixture of heating rates and $CaCO_3$ fillers could be related to the increased amplitude of the cold crystallisation peak and slight decrease in the crystallisation temperature in Figure 39 and Figure 40.

The peak occurring at 170℃ shows the melting point of PLA, at this point the material is beginning to soften and transition into a liquid state. X. Cao, et al (2003) states that DSC graphs of neat PLA consist of a glass transition peak at 61.8℃, crystallization exotherm peak at 127℃ and melting endotherm peak at 157℃, which roughly coincides with the data collected in this report (Cao, Mohamed, Gordon, Willett, & Sessa, 2003).

Melting of polymers is endothermic due to the material absorbing heat as it transitions from solid state to liquid state. The final notable peak occurs at approximately 370℃. This is where the plastic meets its thermal capacity and begins to rapidly degrade due to the extreme temperatures. At this point, the material beings to reduce in mass, which could also be clearly seen in Figure 38.

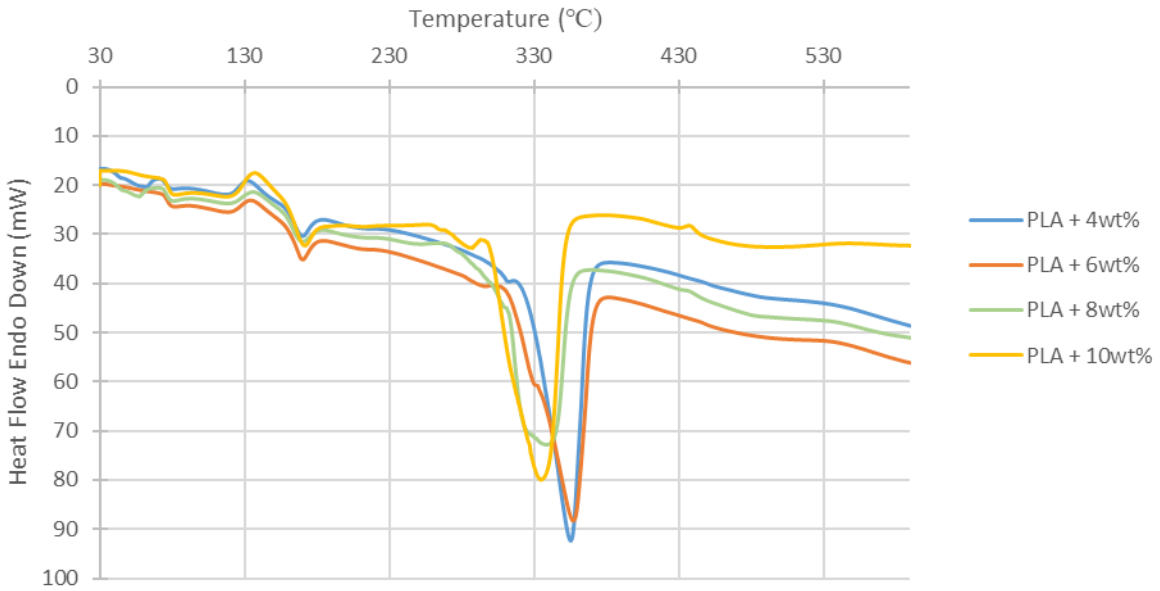

Figure 39: DSC of PLA 4-10wt% samples showing thermal peaks.

As the weight percentage of mussel shell was increased it is notable that thermal degradation temperature has decreased. The amplitude of exothermic and endothermic peaks at 130℃ and 160℃ have shown an overall increase.

The thermal degradation peak on the DSC curve relates to the TGA degradation curve in Figure 32. Similar to TGA the dgradation peak of PLA decreases as the weight percentage on mussel shell is increased.

Data from thermal analysis shows that PLA samples would be best suited in applications below 60℃ and more specifically room temperature where the material is brittle

and not transitioning into a ductile thermoplastic. With such a high glass transition temperature compared to other thermoplastics PLA applications where the polymer has variable temperatures must not exceed the glass transition temperature or the material may fail as the polymer softens.

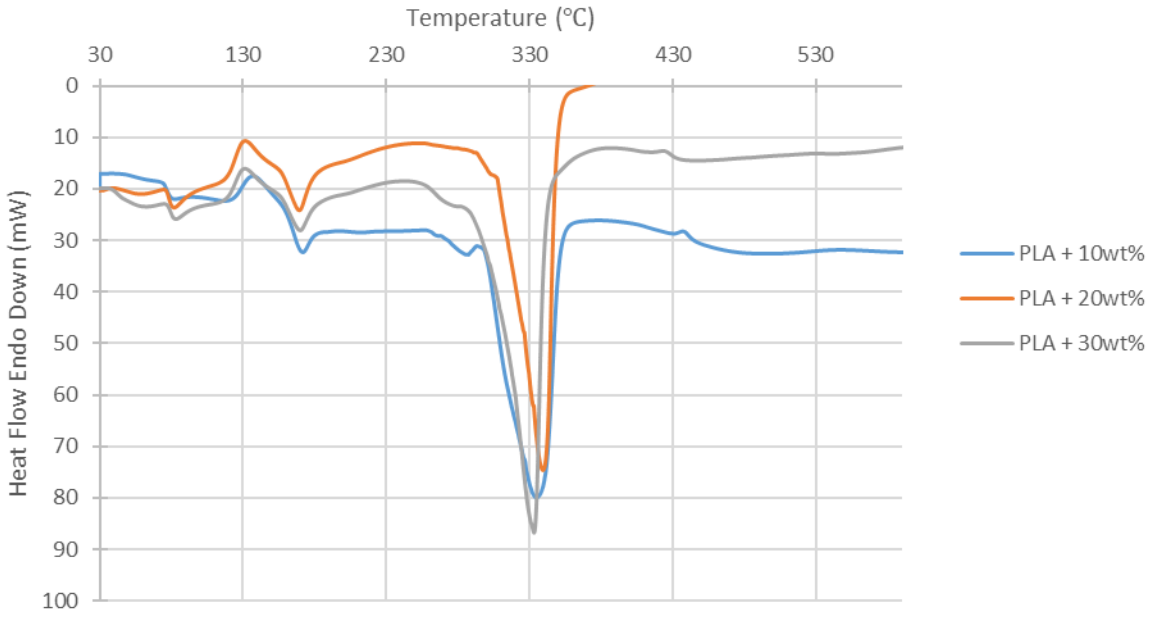

Figure 40: DSC of PLA 10-30wt% samples showing thermal peaks.

To summarise the amplitude of the DSC peaks continued to increase as the weight percentage of mussel shell was increased from 10wt% to 30wt%. Notably, the thermal degradation peaks decreased in accordance with the TGA curve in Figure 36. Melting temperatures remained at approximately 170°C between 0wt% and 30wt% samples, varying by only 2°C. Cold crystallisation temperature decreased from 132°C to 129°C between 0wt% and 30wt% showing similar changes to the melting temperature. Glass transition temperature showed an increase of 13°C between 0wt% and 30wt%, resulting in a more brittle material at higher temperatures.

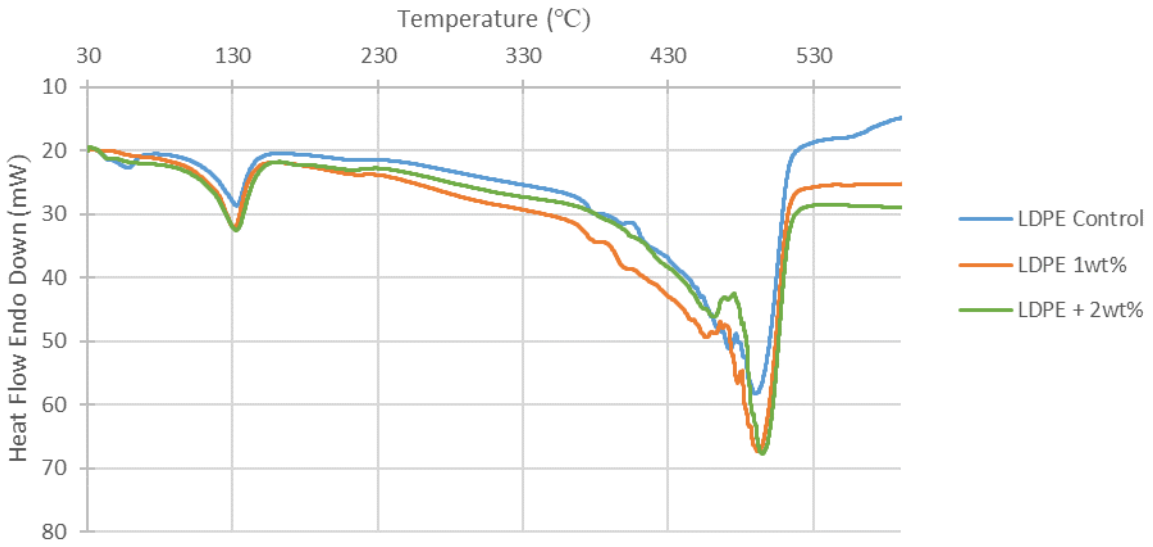

Figure 41: DSC of LDPE 0-2wt% samples showing thermal peaks.

LDPE samples showed degradation that occurred over a much greater temperature range compared to PLA. Figure 41 LDPE 0-2wt% samples show a gradual endothermic heat flow peak that occurs over the range of 200°C, followed by a sudden peak after exceeding 400°C. Depending on the density of neat LDPE the melting temperature is defined by a peak in a lower range of 106°C to 112°C or a higher range of 120°C to 134°C (Prasad, 2004). In the results for 0-2wt% samples the melting point occurred in the higher range at 130°C. Unlike PLA, LDPE samples do not show a glass transition temperature on these DSC graphs. This is due to the glass transition temperature occurring below the temperature range conducted in these experiments. The typical glass transition temperature of LDPE occurs at -100°C, showing the material is ductile until low temperatures.

The melting point of LDPE occurs at the same temperature as the cold crystallisation temperature as PLA, with LDPE showing a far higher thermal degradation temperature.

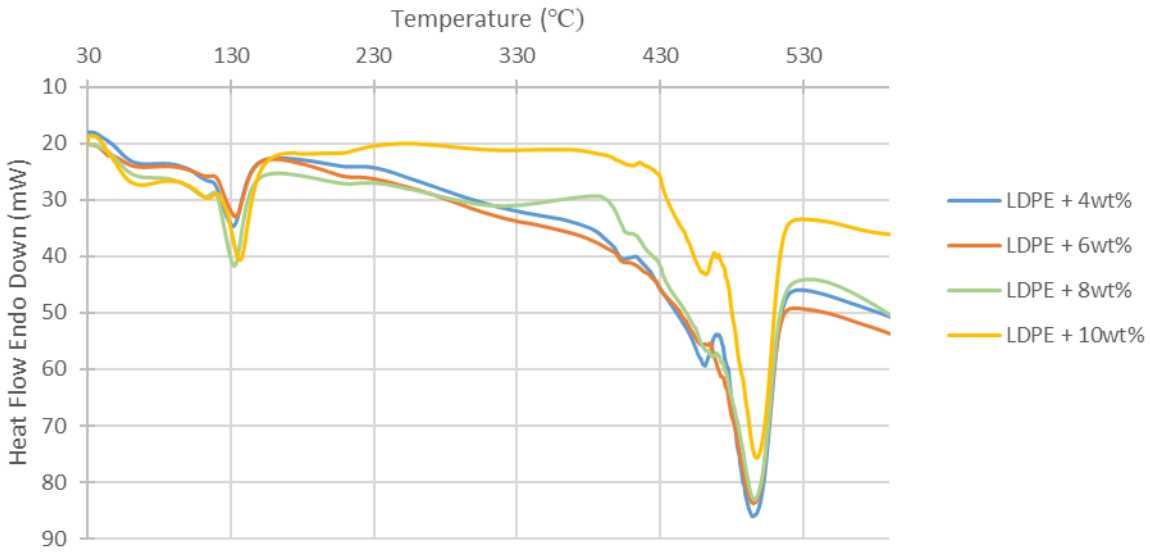

Figure 42: DSC of LDPE 4-10wt% samples showing thermal peaks.

Melting temperature of the 4-10wt% composites remained similar with little to no change. Similarly, thermal degradation showed only a modest increase which was mentioned in TGA.

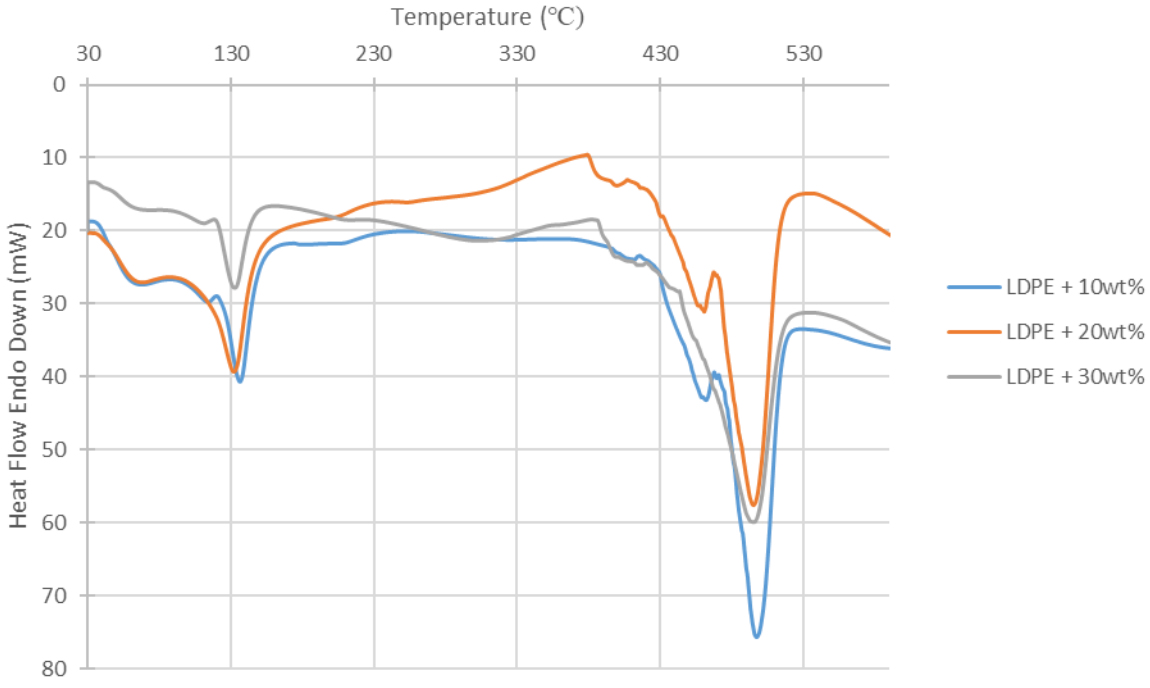

Figure 43: DSC of LDPE 10-30 wt% samples showing thermal peaks.

Once again there is a slight change to the DSC data with increased percentage of mussel shell. Both melting and thermal degradation temperatures remain the same. The amplitude of the peaks showed increases similar to the PLA 10-30wt% samples.

3D printing

It was found that PLA samples could be 3D printed into tensile bars from 0wt% to 8wt%. Reaching weight percentages above 10wt% showed poor prints as the filament showed high viscosity and hydrolysis. This resulted in bubbling as the molten plastic left the extruder nozzle of the 3D printer. Low weight percent composites showed good prints with less risk of hydrolysis. One problem that occurred was varying filament diameters that tend to disrupt flow through the 3D printer and tend to leave slight gaps in prints that did affect the print quality.

a)

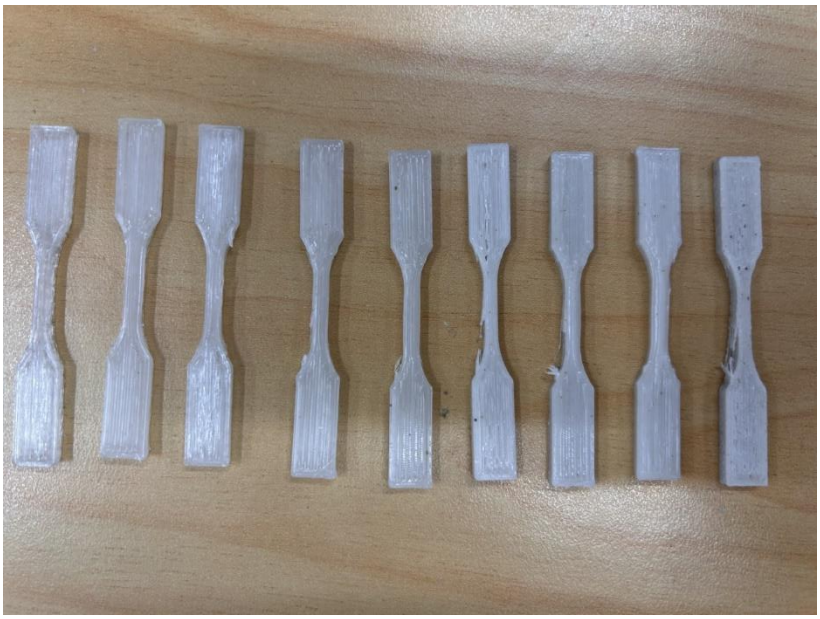

b)

Figure 44: PLA tensile bars a) 0-10wt% bars, b) close view of tensile bars.

Further research needs to be conducted on 3D printing LDPE filaments as the material was too ductile to print even at 30wt%. LDPE has been 3D printed in the past, but it is not a desirable material to work with.

Throughout this experiment it is notable that filament samples tend to be difficult to produce. Firstly, hydrolysis was introduced into PLA filament during extrusion after 30wt% was added, resulting in a low viscosity polymer that was found to be exceedingly difficult to hold a strand without breaking before being cooled. Secondly, LDPE at any wt% was unable to maintain a constant filament diameter due to the ductile properties of the material and extended cooling times. It was found that once LDPE filament had left the extruder that polymer would expand upon heating and cool to different diameters.

Overall testing of PLA and LDPE resulted in valuable data that tested the limits of the composites produced in this chapter. Tensile and thermal analysis showed similar trends throughout both polymers and matched with similar academic research. It was possible to produce both materials although 3D printing was not the most desirable application.

References

Cao, X., Mohamed, A., Gordon, S., Willett, J., & Sessa, D. (2003). DSC study of biodegradable poly(lactic acid) and poly(hydroxy ester ether) blends. *Thermochimica Acta*, 406(1-2), 115-127. https://doi.org/10.1016/S0040-6031(03)00252-1

Dastidar, D. G., & Chakrabarti, G. (2019). Chapter 6 - Thermoresponsive Drug Delivery Systems, Characterization and Application. *Applications of Targeted Nano Drugs and Delivery Systems,* 133-155. https://doi.org/10.1016/B978-0-12-814029-1.00006-5

Hamester, M. R., Balzer, P. S., & Becker, D. (2012). Characterization of Calcium Carbonate Obtained from Oyster and Mussel Shells. *Materials Research*, 15(2), 204-208. 10.1590/S1516-14392012005000014

Kost, B., Basko, M., Bednarek, M., Socka, M., Kopka, B., Łapienis, G., . . . Brzezinski, M. (2022). The influence of the functional end groups on the properties of polylactide-based materials. *Progress in Polymer Science*, 130. https://doi.org/10.1016/j.progpolymsci.2022.101556

Li, Y., Qiang, Z., Chen, X., & Ren, J. (2019). Understanding thermal decomposition kinetics of flame-retardant thermoset polylactic acid. *RSC Advances* (9), 3128-3139. https://doi.org/10.1039/C8RA08770A

Miller, M. R., Pearce, L., & Bettjeman, B. I. (2014). Detailed Distribution of Lipids in Greenshell™ Mussel (Perna canaliculus). *Nutrients,* 6, 1454-1474. https://doi.org/10.3390/nu6041454

Nekhamanurak, B., Patanathabutr, P., & Hongsriphan, N. (2014). The influence of micro-/nano-CaCO3 on thermal stability and. *Energy Procedia*, 56, 118-128. https://doi.org/10.1016/j.egypro.2014.07.139

Niaounakis, M. (2015). Chapter 2 - Properties. *Biopolymers: Processing and Products*, 79-116. https://doi.org/10.1016/B978-0-323-26698-7.00002-7

Obi, B. E. (2018). 7 - Structure–Property Relationships of Polymeric Foams. *Polymeric Foams Structure-Property-Performance.* https://doi.org/10.1016/B978-1-4557-7755-6.00007-0

Piekarska, K., Piorkowska, E., & Bojda, J. (2017). The influence of matrix crystallinity, filler grain size and modification on properties of PLA/calcium carbonate composites. *Polymer Testing*, 62, 203-209. https://doi.org/10.1016/j.polymertesting.2017.06.025

Prabhu, R., Mendonca, S., Darren, Gladson, & Bhat, T. (2016). Mechanical and Tribological Properties of Injection Moulded Modified CaCO3/PP, LDPE Composites. *American Journal of Materials Science*, 6(4A), 61-66. 10.5923/c.materials.201601.12

Prasad, A. (2004). A quantitative analysis of low-density polyethylene and linear low density polyethylene blends by differential scanning calorimetery and fourier transform infrared spectroscopy methods. *Polymers Engineering and Science*, 38(10), 1716-1728. https://doi.org/10.1002/pen.10342

Qiu, F. (2018). Chapter 4 - Practical Considerations. *Accelerated Predictive Stability*, 75-103. https://doi.org/10.1016/B978-0-12-802786-8.00004-8

Süli, F. (2019). 10 - Environmental considerations. *In Electronic Enclosures, Housings and Packages* (pp. 415-497). Woodhead Publishing. https://doi.org/10.1016/B978-0-08-102391-4.00010-1

Tarani, E., Crešnar, K. P., Zemlji, L. F., Chrissafis, K., Papageorgiou, G. Z., Lambropoulou, D., . . . Terzopoulou, Z. (2021). Cold Crystallization Kinetics and Thermal Degradation of PLA Composites with Metal Oxide Nanofillers. *Applied Science*, 11(3004). https://doi.org/10.3390/app11073004

Yu, L., Liu, H., Dean, K., & Chen, L. (2008). Cold crystallization and postmelting crystallization of PLA plasticized by compressed carbon dioxide. *Polymer Physics*, 46(23), 2630-2636. https://doi.org/10.1002/polb.21599

Zapata, P. A., H. P., Díaz, B., Armijo, A., Sepúlveda, F., Ortiz, J. A., . . . Oyarzún, C. (2019). Effect of CaCO3 Nanoparticles on the Mechanical and. *Molecules*, 24(126). https://doi.org/10.3390%2Fmolecules24010126

Chapter five: Experiment two

This chapter presents the results of PLA and LDPE foams nucleated with mussel shell powder. It provides an overview of sample manufacture, expansion ratio, cellular structure as observed using microscopy (cell size and wall thickness), and compressive performance. Cyclic compression tests were also conducted to determine foam recovery.

Cell nucleation and cell growth was controlled by pressure, temperature and thermodynamic instability produced from the sodium bicarbonate blowing agent. The foams produced were predominantly closed cell. During foaming, the polymer matrix interacts with CO_2 produced during the decomposition of sodium bicarbonate resulting in the increase of intermolecular distance causing expansion or swelling (Nofar & Park, 2014). Polymer chains become more tightly aligned together as cell walls decrease in thickness, which results in a limited amount of available space for cells to grow (Chen, Das, & Battley, 2015). This typically happens in closed cell foams where gas is trapped within the foam itself. These foams are excellent for thermal insulation (Gibson, 2003).

Foam samples were produced via extrusion into moulds using 5% sodium bicarbonate as the blowing agent. PLA and LDPE foam samples consisted of two sections 0-2wt% which were trialled as nucleating samples and 4-10wt% that were trialled as reinforcing samples. After the samples were removed from the moulds, regular blocks of 10 x 10 x 15mm were cut as seen in Figure 45 for compression testing. Foams that consisted of 20-30wt% were not tested in this section due to hydrolysis that occurred with the filaments in Chapter 4. This would make foaming at those weight percentages extremely difficult.

a)  b) 

c) 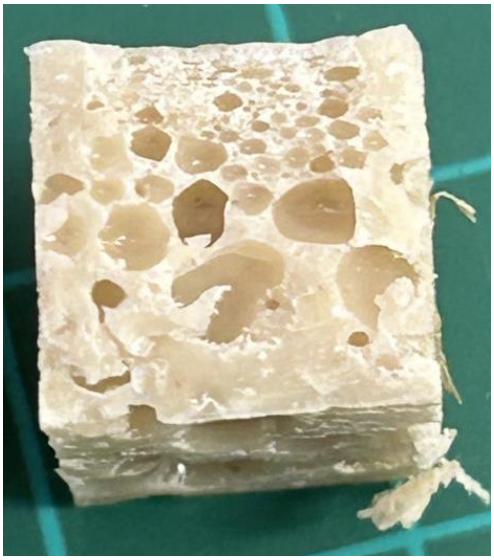

d) 

Figure 45: PLA foam compression blocks (0.5wt%), b) LDPE foam compression blocks (0.5wt%), c) PLA foam compression blocks (8wt%), d) LDPE foam compression blocks (8wt%).

Density and Expansion Ratios

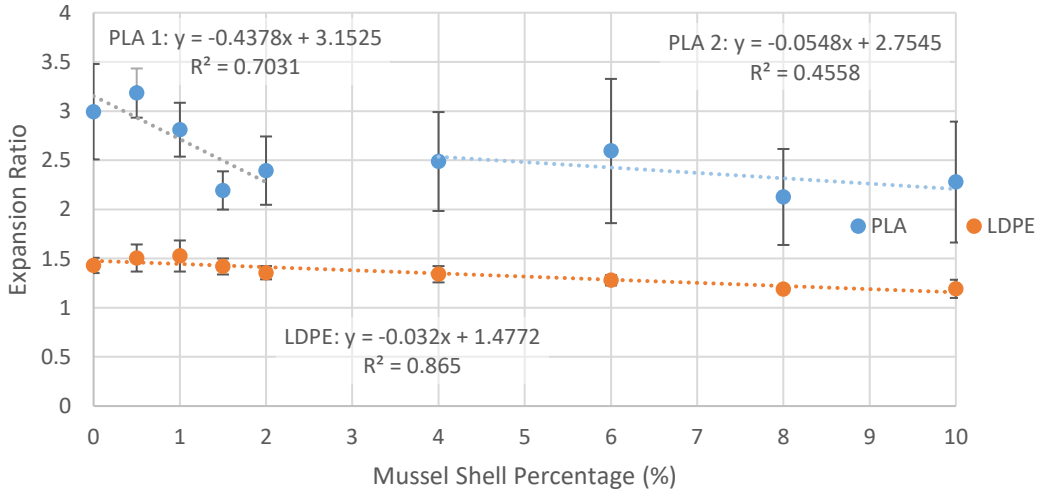

Figure 46: Expansion ratio of PLA and LDPE with increasing nucleating agent.

Nucleating samples were hypothesized to occurred between 0.5wt% and 2wt% of mussel shell powder. Figure 46 showed a linear decrease from 0.5wt% to 2wt% for PLA samples, resulting in 0.5wt% producing a desirable nucleating effect. LDPE samples in the same range showed no change, resulting in little to no benefit of adding mussel shell powder to aid foaming.

Reinforcing of the polymer is believed to have occurred at levels above 2wt% (4 – 10wt%). Notably, both PLA and LDPE samples showed no increase in expansion and remained relatively similar throughout the results. Reinforcing samples showed an overall decrease in expansion from the nucleating samples and typically showed more variation with the PLA samples.

Trendlines for PLA were split into two sections based upon the natural division in the data with the 0-2wt% samples showing a R^2 value of 0.7031 that was close to one. Trendline two for PLA shows an R^2 value of 0.4558 which shows a drastic decrease from trendline one. The trendline for LDPE remains constant with an R^2 value of 0.865. The R^2 value determines how accurate the data points are in a series, corresponding to the trendline, with the most accurate data equalling a value of 1.

PLA samples show a higher expansion ratio compared to LDPE samples. PLA samples typically have a greater margin of error due to the variation of cells in the foam. The expansion ratio of samples decreased as the percentage of mussel shell increased, beginning to act as a reinforcing agent rather than a nucleating agent. Although PLA samples showed a decrease in expansion ratios above 8wt% compared to the 0.5wt% samples, the expansion ratio of all ten samples tested was still relatively high compared to the overall LDPE samples.

It was found that foam morphology is dependent on nucleation, growth, and stabilisation of cells within the polymer. This tends to affect viscosity and glass transition as CO_2 produced by a chemical blowing agent was noted to decrease the glass transition of PLA which showed a decrease from 60 to 20℃ with a CO_2 concentration of 5wt% (Parker, Garancher, Shah, & Fernyhough, 2011). In this thesis CO_2 produced from sodium bicarbonate was less than 5wt% but, exceeding this could result in a blowing agent that plasticised the polymer, lowering the viscosity and therefore affecting the thermodynamics of foaming. According to Parker, Garancher, Shah, & Fernyhough (2011) less thermodynamically stable polymers show a lower Gibb's free energy and voids in the polymer matrix become less stable affecting nucleation.

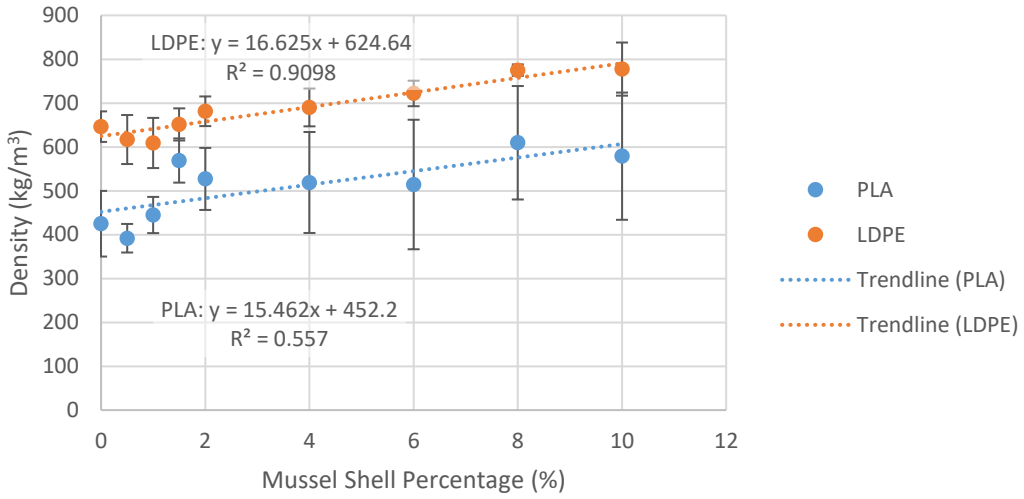

Figure 47: Density of PLA and LDPE with increasing nucleating agent.

Both PLA and LDPE samples showed increases in density as the percentage of nucleating agent was increased, showing a positive link between expansion ratio and density. Due to the larger cells in PLA the density is lower than LDPE samples. It was expected that the density of foam would increase as the mussel shell started acting as a reinforcing agent rather than a nucleating agent. With the mussel shell acting as a nucleating agent there is likely to be more cells per volume, resulting in lower densities due to the considerable number of air gas pockets in the foam blocks. This relates to the expansion ratios in Figure 46.

PLA shows a low R^2 value of 0.557, where LDPE shows an ideal value of 0.9098 for density. This value represents the variation of the points potted on the graph in comparison to the trendline. In this case data plotted for LDPE samples were very close to the trendline on the graph.

The density of un-foamed PLA was 1240 kg/m^3 which is approximately three times the density of foamed PLA, showing high expansion ratios. The density of LDPE before being foamed was 922 kg/m^3.

Conventional polymer foams such as polystyrene have a density of 960 kg/m^3 which is much higher than PLA (1240 kg/m^3), yet PLA foams show much higher compressive properties than polystyrene. Typically foams with higher densities have lower stiffness values, but this is not the case with PLA as the material is a rigid foam. With PLA foams maintaining a rigid structure at lower densities the result is the foam can withstand more compressive stress than ductile materials at higher densities. Although PLA can withstand higher compressive stress it is prone to failure as the overall material is brittle.

SEM/microscopy

PLA samples showed varying cell structure throughout the mould blocks with tight packed cells close to the edge and larger cells in the centre, so that it appeared functionally graded. It was notable that the inconsistent morphology of the PLA foam resulted in different failure types. This was directly connected to the number of cells, size of the cells and size of the cell walls in the foam. PLA samples consisting of thicker cell walls experienced sections of the foam cracking and breaking off under compression. PLA samples with much thinner cell walls with high cell volumes resulted in crumbling under compression. Further testing resulted in samples with sides in direct contact with the mould bowing under compression.

LDPE foam samples have been noted to have an extremely high density due to the microscopic cells within the ductile polymer. Although the cells appeared uniform under the microscope, it was noted that larger cell or deformities were introduced due to the moulding of the foam. LDPE foams left the extruder far more solidified than PLA foams which resulted in the material having difficulties forming within the mould.

a) 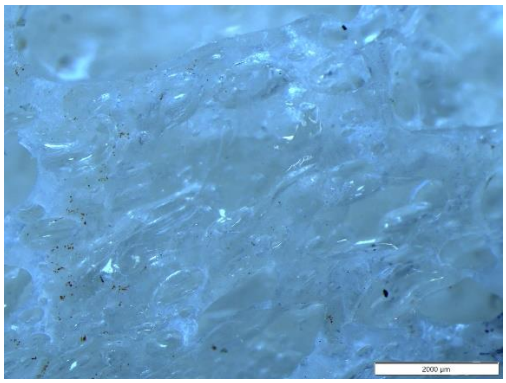

b) 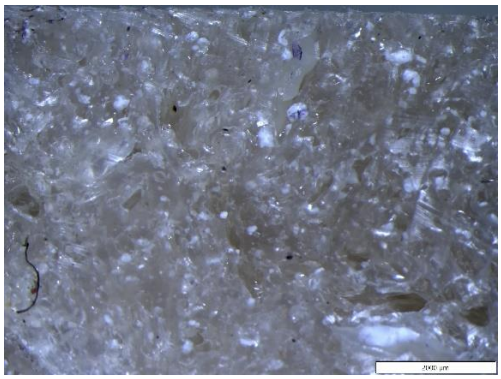

c) 

d) 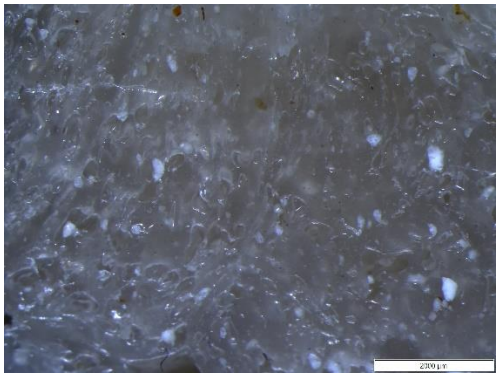

e) 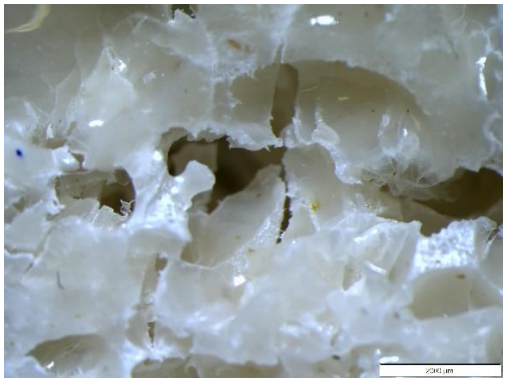 f) 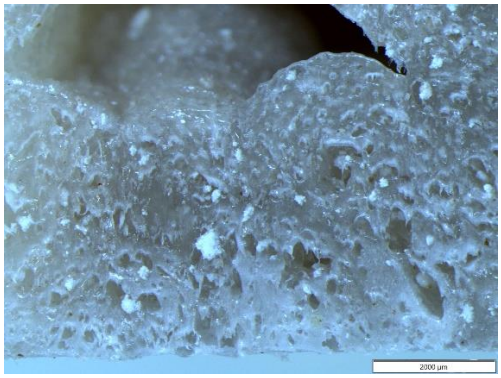

Figure 48: Foam images at 1x stereo microscope: a) PLA control, b) LDPE control, c) PLA + 2wt%, d) LDPE + 2wt%, e) PLA + 10wt%, f) LDPE +10wt%.

PLA samples showed a change in cell morphology as the percentage of mussel shell increased. Notably, the size of the cells increased with a corresponding change in the cell wall size. Cell sizes in the PLA control and PLA + 2wt% samples ranged from 500 – 2000 µm in diameter (Figure 48a and b). Cell sizes for PLA + 10wt% showed larger cell sizes reaching over 2000 µm in diameter and in some cases merging of cell sizes became notable when reaching higher weight percentages in PLA samples. Merging cells showed rigid and non-uniform cell walls, which is a direct result of a combination of multiple cells, showing the polymer did not solidify in time after extrusion.

During PLA foaming there is acid – base reactions that occurs between the polylactic acid and calcium carbonate and/or sodium bicarbonate. Acid – base reactions have a H_2O by-product that contributes to hydrolysis of PLA during extrusion. The effect of hydrolysis shortens the PLA chains and lowers viscosity. With a lowered viscosity there is less constraints for cell formation and larger bubble growth occurs.

The combination of cells is often undesirable (Figure 48c) and can occur during extrusion where nucleation was promoted earlier on in the barrel of the extruder or in the mould during cooling. The cell size from this research tends to be larger than research conducted by other academics such as Osman, Virgilio, Rouabhia, & Mighri, (2022) where the cell size could be controlled during cooling. It was found with correct cooling cells would not rupture as PLA would have a higher viscosity. Cell sizes were averaged at 300 µm. Standau, Zhao, Castellón, Bonten, & Altstädt, (2019) states cell sizes can range from 10-800 µm. Simply put if PLA foam cooling was controlled in this research a desireable cell size could be produced. Neat PLA foams produced from Mort, Peters, Curtzwiler, Jiang, & Vorst, (2022) showed average cell diameters of 400 - 500 µm

LDPE samples showed far smaller cell sizes than PLA at approximately 50-100 µm in diameter. Cells in LDPE foams showed slight variation in size, showing an almost uniform morphology. The cells shown in SEM imaging are far smaller than what was seen under the stereo microscope in Figure 48 due to the ability to reach much greater magnifications with much higher resolution, resulting in more in-depth images.

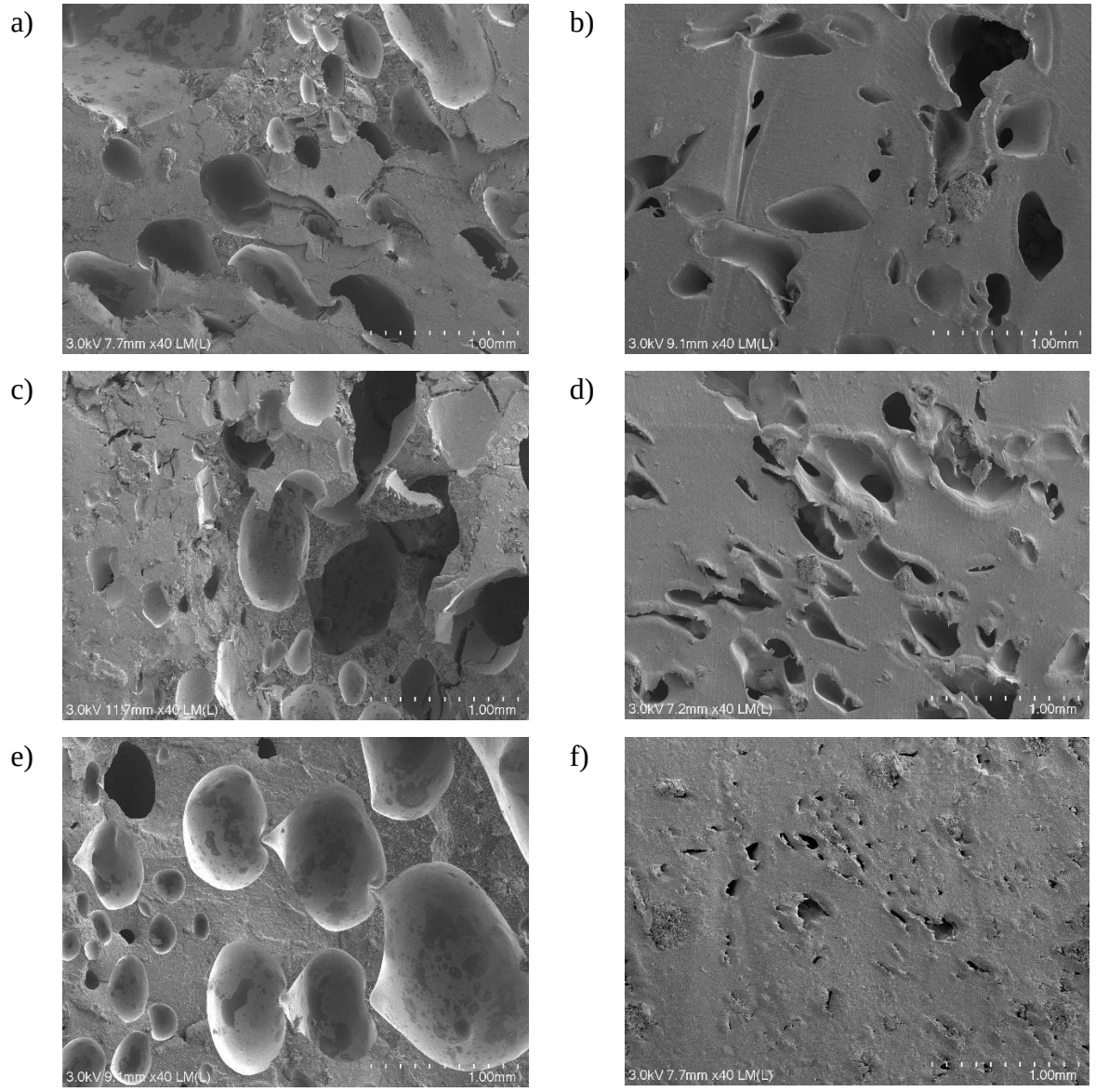

Figure 49: SEM images of foam a) PLA control, b) LDPE control, c) PLA + 2wt%, d) LDPE + 2wt%, e) PLA + 10wt%, f) LDPE +10wt%.

Notably, SEM imaging showed cell sizes for both PLA and LDPE reduced as the weight percentage of mussel shell increased. This relates to the density results shown in Figure 47. The relationship between the density (Figure 47) and cell morphology (Figure 49) shows as the

density of the foam is increased, the cell sizes appear to decrease showing larger cell walls and a greater volume of polymer. In this case cell growth could be resisted by particle movement.

Compression

In this section the results of the low (0-2wt%) and medium (4-10wt%) weight percentage filament samples made with PLA and LDPE were discussed. Samples were tested to determine properties such as compressive stress, compressive strain, and Youngs' modulus.

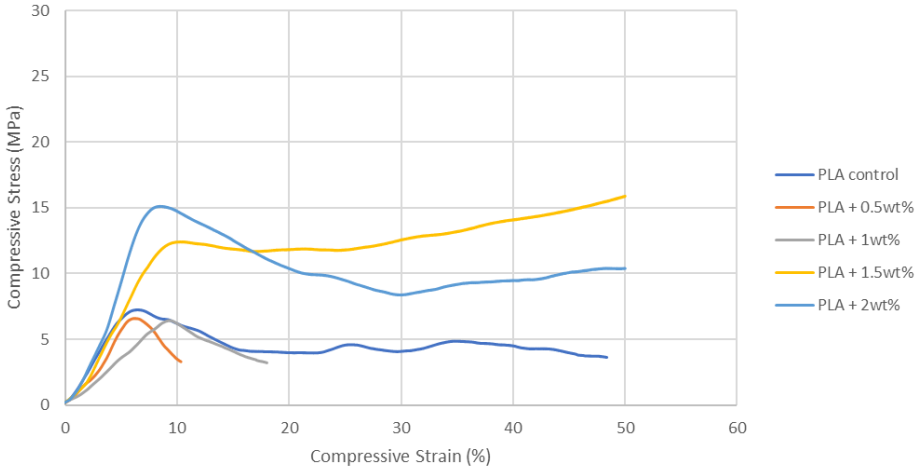

Figure 50: PLA foam compression 0-2wt% (low weight percentage).

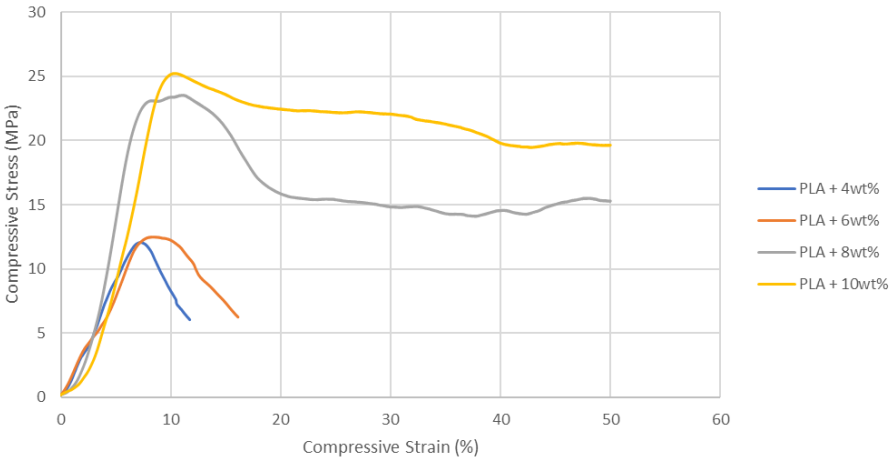

Figure 51: PLA foam compression 4-10wt% (medium weight percentage).

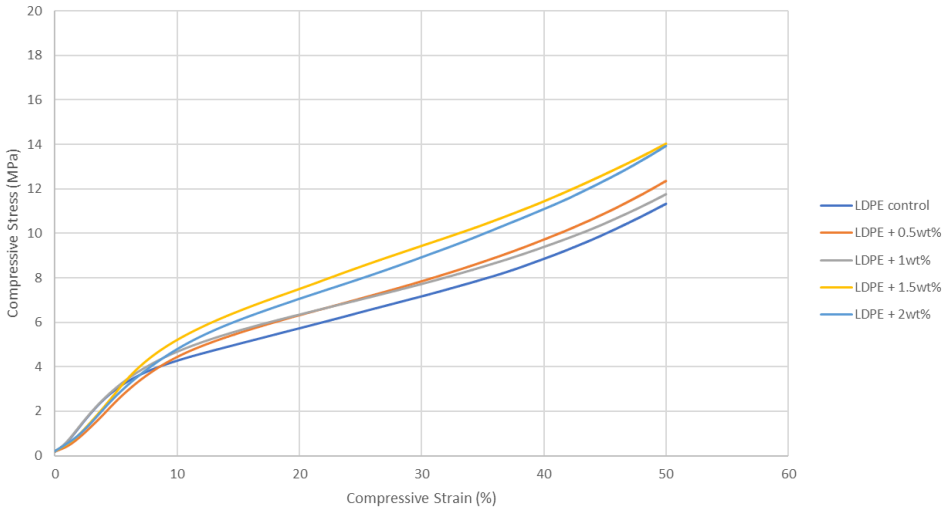

Figure 52: LDPE foam compression 0-2wt% (low weight percentage).

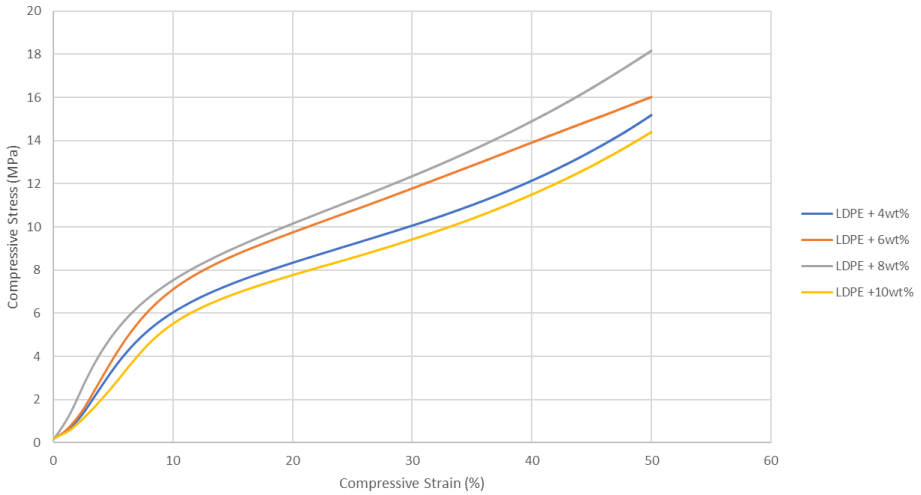

Figure 53: LDPE foam compression 4-10wt% (medium weight percentage).

PLA and LDPE samples showed vastly different compressive graphs to each other. Based on data from Mei, Yin, Zhang, & Zhao, (2018) the PLA graphs are only showing the opening portion of the compression graph, because the foam samples in Figure 50 have not reached the densification stage. PLA graphs showed a high yield strength, followed by a declining tail then failure. LDPE samples showed a low Youngs' modulus, followed by further increasing compressive stress. With PLA being a rigid foam and LDPE being ductile, it is likely to see a much higher Youngs' modulus on the PLA graphs, reaching values of 75 MPa for pure un-foamed PLA (Mei, Yin, Zhang, & Zhao, 2018). Maximum compressive stress reached 25 MPa for PLA + 10wt% whereas LDPE + 8wt% reached a max of 18 MPa.

Although the graphs are variable the maximum compressive stress increased as the percentage of mussel shell increased, showing reinforcement of the foams. PLA + 10wt% resulted in the highest compressive stress of 25 MPa where LDPE + 10wt% only reached 14 MPa.

Research by Mort, Peters, Curtzwiler, Jiang, & Vorst, (2022) showed neat PLA foams tend to show a compressive stress value of approximately 7 MPa at 4% strain. These results are very similar to the results gathered in this experiment of 6-8 MPa at double the strain (8%). This showed that the compressive strain of the grade of PLA used in this thesis showed superior compression properties.

The compressive stress of LDPE increased as the material plastically deforms and becomes compact, showing densification. As the compressive stress was applied to PLA the material reaches a maximum stress then began to show brittle failure resulting in a decreasing stress value as seen in Figure 50.

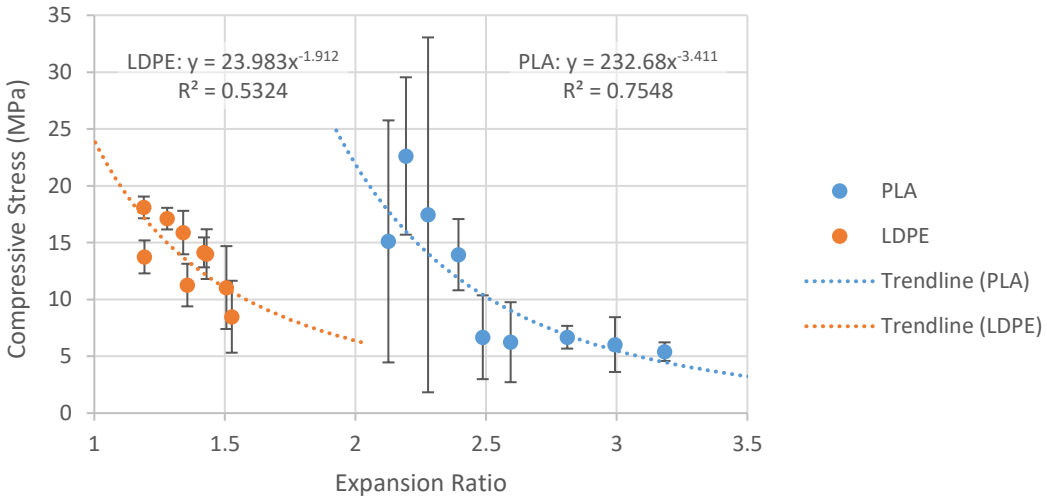

Figure 54: Compressive stress of PLA and LDPE with various expansion ratios.

When plotting the expansion ratio against compressive stress it was notable that there was an inconsistent morphology and cell distribution within the specimens. PLA samples with higher percentage of filler or lower expansion ratios showed the greatest variation in compressive stress.

LDPE samples showed lower compressive stress of 10-15 MPa as these samples tended to reach 50% compression of the sample. PLA + 1.5wt% reached 50% compression and showed compressive stress values around 20 MPa. PLA + 8wt% and PLA + 10wt% both

had lower compressive strain values, reaching failure at 11.7% and 23.1% but showed high compressive stress values of 20-22 MPa. This was due to the impact of reinforcement from the high weight percentage of mussel shell. PLA samples could be ideal in higher stress environments where support and high stress of a rigid foam may be required. On the other hand, LDPE showed substantial amounts of plastic deformation which could be suitable in situations where deformation could allow for protection.

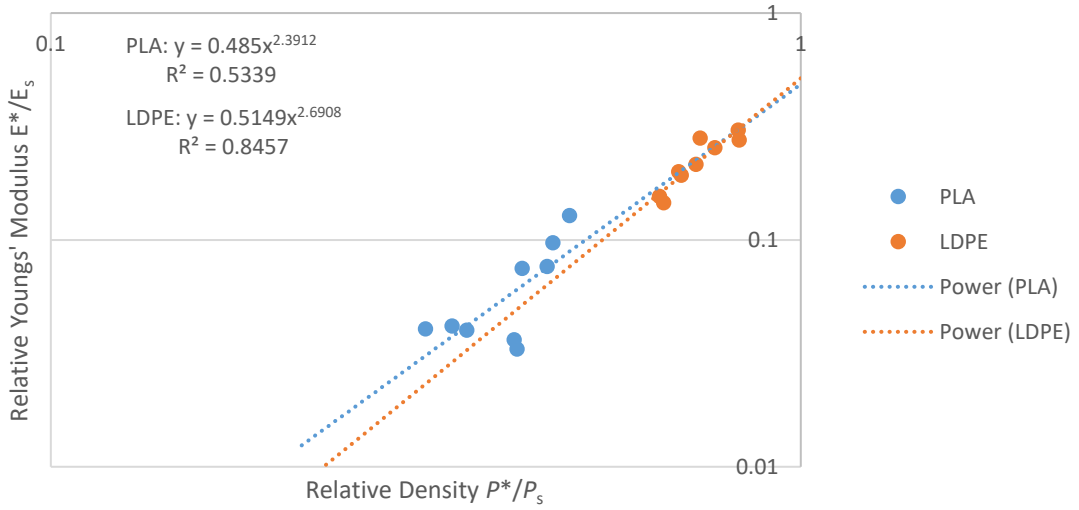

Figure 55: Relative stiffness of PLA and LDPE for relative density.

The Gibson-Ashby model plots relative Youngs' modulus against relative material density. This model has been used to previously represent open and closed cell foam theory. This model shows trendlines for both open and closed cells and could be compared to results in this experiment. Closed-cell foams from this experiment coincided with similar trendlines with modelled data. The change in stiffness is noted to be similar to the closed cell model between the range of 0.6 and 0.8. LDPE foams followed similarly to what was suggested by the Gibson-Ashby model between, 0.8 closed cell model and the open cell model (Gibson & Ashby, 1999).

Cyclic compression

In this section the results of the low (0-2wt%) and medium (4-10wt%) weight percentage filament samples made with PLA and LDPE were discussed.

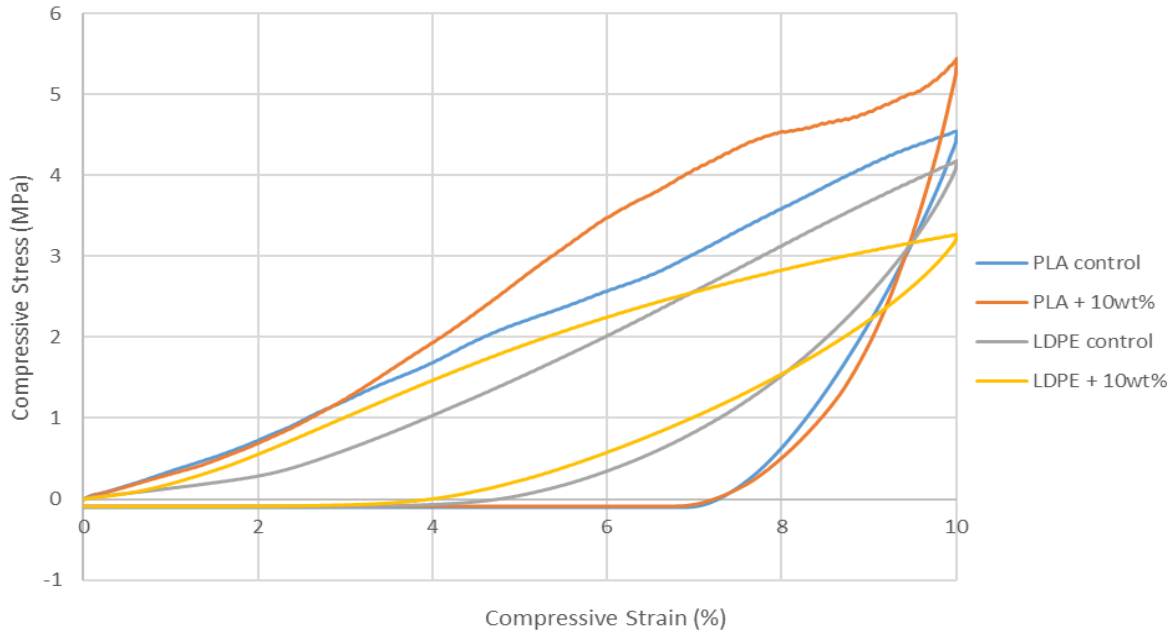

Figure 56: Cyclic compression of PLA and LDPE.

Compressive recovery was shown by the following graph (Figure 56). The foam sample was compressed to 10% of the initial height and released to determine the elastic potential of the foam. Notably, PLA and LDPE had very different recovery which was expected due the properties of each material. PLA samples showed between 30-40% recovery where LDPE samples were closer to 70%.

Compression summary

This section illustrated the compression and cyclic compression of PLA and LDPE foams. It showed results of low (0-2wt%) and medium (4-10wt%) samples, displaying properties such as compressive stress, compressive strain, Youngs' modulus, and foam recovery.

Table 9: PLA foam properties.

Material	***Compressive Stress (MPa)***	***Compressive Strain (%)***	***Young' Modulus (MPa)***	***Recovery (%)***
PLA Control	6.41 ± 2.6	7.7 ± 1.6	129.0 ± 68	40 ± 0.7
PLA+0.5wt%	5.41 ± 0.8	8.5 ± 3.7	125.6 ± 126	24 ± 1.7
PLA+1wt%	6.68 ± 1.0	14.9 ± 11.7	123.7 ± 27	30 ± 0.6
PLA+1.5wt%	22.62 ± 6.9	50.0 ± 0.01	236.5 ± 40	38 ± 1.6
PLA+2wt%	13.94 ± 3.1	11.2 ± 3.8	231.6 ± 123	36 ± 0.5
PLA+4wt%	6.67 ± 3.7	10.2 ± 2.8	102.1 ± 82	30 ± 0.7
PLA+6wt%	6.24 ± 3.5	8.6 ± 1.3	112.3 ± 68	38 ± 0.4
PLA+8wt%	22.64 ± 3.7	11.7 ± 1.4	396.8 ± 121	30 ± 0.8
PLA+10wt%	20.73 ± 15.9	23.1 ± 18.1	301.0 ± 193	30 ± 0.6

Table 9 shows the properties of PLA foams as the weight percentage of mussel shell was increased. PLA samples showed good compressive stress properties but lacked the ability to deform under extreme amounts of stress, typically only reaching 10-15% in compressive strain at max/break. Although PLA foams had low resistance to deformation, the foams had an exceptional Young' modulus compared to LDPE samples and a somewhat good percentage of recovery considering the brittle properties. During cyclic compression tests samples that had larger cell volumes with thin cell walls showed more elastic deformation and recovery. Samples with larger cell walls typically showed a greater Youngs' modulus and a higher maximum compressive force being applied to the samples. PLA foams could be beneficial in applications such as sandwich structure composites as the foam produced shows low weight

and high stiffness properties. This could result in a great stiffness to weight ratio in this application.

Table 10: LDPE foam properties.

Material	***Compressive Stress (MPa)***	***Compressive Strain (%)***	***Young' Modulus (MPa)***	***Recovery (%)***
LDPE Control	13.99 ± 2.2	50.0 ± 0	59.9 ± 10	74 ± 0.5
LDPE+0.5wt%	11.05 ± 3.6	49.9 ± 0.01	43.7 ± 7	72 ± 0.4
LDPE+1wt%	8.48 ± 3.2	49.9 ± 0.01	46.6 ± 16	76 ± 0.6
LDPE+1.5wt%	14.14 ± 1.3	49.9 ± 0.01	57.7 ± 10	76 ± 0.5
LDPE+2wt%	11.26 ± 1.9	49.1 ± 2.02	64.4 ± 23	76 ± 0.5
LDPE+4wt%	15.88± 1.9	49.9 ± 0.01	84.2 ± 15	72 ± 0.4
LDPE+6wt%	17.11 ± 0.9	50.0 ± 0	76.5 ± 18	76 ± 0.5
LDPE+8wt%	18.09 ± 0.9	49.9± 0.02	91.2 ± 16	68 ± 0.4
LDPE+10wt%	13.74 ± 1.4	49.9 ± 0.02	82.6 ± 18	64 ± 0.3

Table 10 shows the properties of LDPE foams as the weight percentage of mussel shell was increased. All LDPE foam samples reached 50% strain resulting in high compressive stress values. Compressive stress values reached a maximum of 18 MPa for LDPE + 8wt%. It is notable that the Youngs' modulus for LDPE is much lower than PLA, with PLA samples having double the stiffness of LDPE foams. Due to LDPE being ductile it was expected that the samples would have a lower Youngs' modulus than PLA. Samples such as LDPE + 6wt% and LDPE + 8wt% showed an increase in compressive stress reaching values of 17 MPa and 18 MPa, with a far higher Youngs' modulus than lower percent samples. This shows the addition of mussel shell powder has increased the stiffness of the foam, while still providing

ductile properties. LDPE samples showed excellent recovery due to the ductile nature of the material, reaching an average of 72% across all samples. As the weight percentage of mussel was increased the recovery of the LDPE foams decreased as the material started displaying less ductility due to the decrease in recovery at higher wt%. Recovery from cyclic compression testing due to the elastic properties of LDPE showed approximately 30% of the material plastically deforming under compression. This could be seen in Table 10 as the material did not recover to 100% showing some form of plastic deformation had occurred.

Due to the high recovery values, LDPE foam would be ideal for applications in packaging to support products from receiving damage. It would be advantageous in an aspect of a circular economy, with future research into the use of recycled LDPE as a more beneficial plastic in terms of having an impact on the environment. The use of calcium carbonate from mussel shells is a beneficial nucleating agent as it is a waste product of aquaculture that would typically be disposed of in landfills. Repurposing the waste from mussel shells contributes to a circular economy and reduces the overall amount of waste that would end up in landfills.

References

Chen, Y., Das, R., & Battley, M. (2015). Effects of cell size and cell walls thickness variations on the stiffness of closed-cell foams. *International Journal of Solids and Structures*, 52, 150-164. https://doi.org/10.1016/j.ijsolstr.2014.09.022Gibson, L. & Ashby, M. (1999). 5.3 Mechanical properties of foams: compression. *Cellular solids, structure, and properties- second edition*, 183-216.

Gibson, L. J. (2003). Cellular Solids. *MRS Bulletin*, 28(4), 270-274. doi:10.1557/mrs2003.79

Hamester, M. R., Balzer, P. S., & Becker, D. (2012). Characterization of Calcium Carbonate Obtained from Oyster and Mussel Shells. *Materials Research*, 15(2), 204-208. 10.1590/S1516-14392012005000014

Mei, H., Yin, X., Zhang, J., & Zhao, W. (2018). Compressive Properties of 3D Printed Polylactic Acid Matrix Composites Reinforced by Short Fibers and SiC Nanowires. *Advanced Engineering Materials*., 21.

Mort, R., Peters, E., Curtzwiler, G., Jiang, S., & Vorst, K. (2022). Biofillers Improved Compression Modulus of Extruded PLA Foams. *Sustainability*, 14(9). https://doi.org/10.3390/su14095521

Nofar, M., & Park, C. B. (2014). Poly (lactic acid) foaming. *Progress in Polymer Science*, 39(10), 1721-1741. https://doi.org/10.1016/j.progpolymsci.2014.04.001

Osman, M. A., Virgilio, N., Rouabhia, M., & Mighri, F. (2022). Polylactic Acid (PLA) Foaming: Design of Experiments for Cell Size Control. *Materials Sciences and Applications*, 13(2), 63-77. https://doi.org/10.4236/msa.2022.132005

Parker, K., Garancher, J.-P., Shah, S., & Fernyhough, A. (2011). Expanded polylactic acid - an eco-friendly alternative to polystyrene foam. *Journal of Cellular Plastics*, 47(3). https://doi.org/10.1177/0021955X11404833

Standau, T., Zhao, C., Castellón, S. M., Bonten, C., & Altstädt, V. (2019). Chemical Modification and Foam Processing of Polylactide (PLA). *Polymers*, 11(2), 306. https://doi.org/10.3390/polym11020306

Chapter six: Applications

This chapter discusses potential projects, products and applications that could arise from the composites and foams developed in this research. The PLA and LDPE composites/foams showed very different structures (cell size and morphology), and performance (tensile and compression). Therefore, this section outlines applications which are suitable or advantageous for these composites and foams to be used in.

PLA composites

Data from thermal analysis (Chapter four: Figure 38, Figure 39 and Figure 40) shows that PLA samples would be best suited in applications below 60℃ and more specifically room temperature where the material is brittle and not transitioning into a ductile thermoplastic which may cause the material to fail as the polymer softens.

PLA composites showed a high tensile strength at yield of 55-60 MPa and a high Youngs' modulus of 3.5-4 GPa, which would be ideal for applications requiring polymers with high strength without exceeding failure. Chand & Fahim, (2021) states that sandwich composite panels have been used with natural fibres sheet materials and a corrugated core. This idea could be implemented into PLA sandwich composites. PLA laminates with mussel shell filler could be incorporated into a "cardboard style" plastic panel, which could potentially be used in packaging or construction applications.

With PLA having high viscosity during extrusion the polymer could be used as a coating to foams creating a structural composite. As the polymer hardens it will act as a strong layer with a high Youngs' modulus. This could promote a high stiffness to weight ratio, which is desirable in materials science and engineering. Surfboards use similar layered structures with foam core material and an outer resin. The addition of PLA composites and foams could provide a biodegradable aspect to surfboards and other sports applications that require similar properties and materials. The technical aspects of a surfboard are like traditional composite sandwich panels which commonly comprise of two materials, a soft foam core located between two stiff sheets of material serving as an outer face. These composite sandwich panels are highly sought after materials in aerospace due to the attractive properties, such as good acoustic damping properties, high-specific strength, and stiffness (Langdon, Guan, & Cantwell, 2018).

PLA + 8wt% mussel shell powder showed the best tensile results with a yield strength of 60 MPa and stiffness of 4 GPa while being able to be 3D printed without difficulty. This

polymer could be used to 3D print products such as plastic cups, or cutlery and specifically, designed, and complex shaped containers for transporting mussel products for consumption could contribute to a circular economy. Honeycomb structures could be 3D printed from PLA + 0-8wt% composites resulting in a stiff and light weight product that could be used in automotive and sports gear applications.

PLA composites have had a large background in biomedical applications by replacing conventional fossil-based plastics. It has been used in clinical applications because of the controllable degradation rates and ideal processing temperatures of the polymer. PLA has properties that resemble the human bone due to high stiffness and elastic modulus. With these properties applications for tissue engineering scaffolds, temporary and long-term implants, bone screws, anchors, spinal cages, prostheses, sutures, vascular grafts, drug encapsulation and delivery have been developed (Liu, et al., 2020). Implants consisting of 8wt% mussel shell would have a tensile strength of 60 MPa which is greater than PLA without mussel shell by close to 10%. This would result in stronger implants that can withstand higher stress. Beneficially, PLA implants could be permanent or temporary depending on the application. Permanent PLA implants would likely not be removed and must be able to withstand day to day stress. High tensile PLA with 8wt% mussel shell would likely increase the maximum stress of the material. Temporary implants could biodegrade as the new bone growth takes over the implant (Silva, et al., 2018) providing the bone with existing calcium carbonate which is a major ingredient of bone (Chaitow, Bradley, & Gilbert, 2002) from the PLA composites. Further research would be required in this field of study to determine whether this PLA composite is compatible with the human body.

PLA foams

PLA foams have been previously utilised in applications such as cushioning, packaging, heat insulation, noise reduction, filtration, absorption, and tissue engineering (Peng, et al., 2022). PLA foams have been studied for uses in aerospace due to mechanical properties such as high compressive strength and good impact toughness performance. PLA has been noted to have high absorbency, particularly for oils, and high absorption capacities which allows for applications in absorption and filtration. PLA foam has the potential to act as a biodegradable spill kit in the laboratory or could be used for bioremediation after an oil spill. Also, PLA shows great thermal conductivity which allows for heat preservation and insulation in packaging or construction (Peng, et al., 2022).

PLA foams could be beneficial in applications such as sandwich structure composites as the foam produced shows low weight and high stiffness properties. This could result in a great stiffness to weight ratio in this application. PLA foams would be ideal for a 'green', light-weight alternative to conventional foams such as polystyrene or polyurethane.

It was found in Chapter 5 that PLA + 0.5wt% increased nucleation of the foam resulting in a high expansion ratio and low density. This foam could be applied in situations where large cell sizes are preferred and a low density with a somewhat high stiffness is required. Foams with higher weight percentage of mussel shell (8wt%) show high tensile strength (22 MPa) and stiffness (0.396 GPa), with slightly lower expansion ratios. PLA + 8wt% and PLA + 10wt% would show to be beneficial where a greater tensile strength or stiffness is required, and foam expansion can be sacrificed. Foams with greater mechanical properties such as higher tensile strength, compressive strength or Youngs' modulus could be more suitable for applications in construction, where high strength is desirable.

LDPE composites

Low density polyethylene is conventionally used in plastic containers, bottles and food packaging and films (Dietrich, Sarmoria, Brandolin, & Asteasuain, 2018). These are a range of products that the LDPE composite have potential to be used in. The most common application that this composite can be used in is plastic boxes or containers which will include mussel shell powder to increase the polymer stiffness. Notably, ductility is reduced with the addition of mussel shell powder, but overall, the composite did not become brittle. LDPE + 10-30wt% has an increased stiffness of approximately 30 MPa compared to LDPE without mussel shell powder which would result in a material with a greater Youngs' modulus while still maintaining the ability resist plastic deformation. Repurposing mussel shell and adding it to a LDPE result in a circular economy where this composite could be used to replace conventional plastics used in tanks, nets, feed bags, liners, piping, polystyrene boxes, product transportation or chemical storage in the aquaculture industry (World Aquaculture Society, 2020).

LDPE has previously been applied to electrical cables and high-pressure water pipes due to the good physical and chemical properties (He, et al., 2022). Applications with the introduction of mussel shell powder could improve tensile strength while still maintaining the ductility needed to bend the pipe if required.

Similarly, to PLA, LDPE composite sheets or laminates could be incorporated into composite sandwiches with two flat sheets of LDPE and a corrugated core to create a material

with an increased strength to weight ratio. Additionally, LDPE and PLA laminates could be introduced into a multi polymer sandwich that takes advantage of properties from both polymers and takes further advantage of the mussel shell added to both composites.

LDPE foams

Due to the high recovery values, LDPE foam would be ideal for applications in packaging to support products from receiving damage. It would be advantageous in an aspect of a circular economy, with future research into the use of recycled LDPE as a more beneficial plastic in terms of having an impact on the environment. The use of calcium carbonate from mussel shells is a beneficial nucleating agent as it is a waste product of aquaculture that would typically be disposed of in landfills. Repurposing waste mussel shells contributes to a circular economy and reduces the overall amount of waste that would end up in landfills.

High density foam has been used as acoustic insulation, especially in noise and vibration. Acoustic foam materials have shown to be ideal in insulation properties in applications including automotive industries (Ahmed, Park, & Atalla, 2006), music production, and aerospace. With further research into LDPE and mussel shell foams, potential sound insulation could be developed. Ideally, this material would require high cell density to enhance the vibration damping properties. This polymer could be used in a vehicle's dash panels, door panels, floor panels, wheelhouses, cargo bays and roof panels to reduce external and engine noises (Ahmed, Park, & Atalla, 2006).

This chapter has identified that PLA and LDPE composite and foams could be used in a wide range of applications. The easiest of which to implement would be packaging followed by structural composites.

References

Abbasi, M., Khorasani, S. N., Bagheri, R., & Esfahani, J. M. (2011). Microcellular foaming of low-density polyethylene using nano-CaCo3 as a nucleating agent. *Polymer* Composites, 32(11), 1718-1725. https://doi.org/10.1002/pc.21188

Ahmed, M. S., Park, C., & Atalla, N. (2006). Control of the Structure and Morphology for Production of Novel LDPE Acoustical Foams. *Cellular Polymers*, 25(5), 277-292. https://journals.sagepub.com/doi/pdf/10.1177/026248930602500501

Chaitow, L., Bradley, D., & Gilbert, C. (2002). Chapter 9 - Other Breathing Issues. *Multidisciplinary Approaches to Breathing Pattern Disorders*, 223-240. https://doi.org/10.1016/B978-044307053-2.50013-7

Chand, N., & Fahim, M. (2021). 1 - Natural fibers and their composites. *Tribology of Natural Fiber Polymer Composites (Second Edition),* 1-59. https://doi.org/10.1016/B978-0-12-818983-2.00001-3

Dietrich, M. L., Sarmoria, C., Brandolin, A., & Asteasuain, M. (2018). High-Pressure Polymerization of Ethylene in Tubular Reactors: Prediction of the Bivariate Distributions of Molecular Weight-Branches with a Rigorous Reactor Model. *Computer Aided Chemical Engineering*, 44, 1447-1452. https://doi.org/10.1016/B978-0-444-64241-7.50236-6

He, L., Ye, Z., Zeng, J., Yang, X., Li, D., Yang, X., . . . Huang, Y. (2022). Enhancement in Electrical and Thermal Properties of LDPE with Al2O3 and h-BN as Nanofiller. *Materials (Basel),* 15(8). https://doi.org/10.3390%2Fma15082844

Langdon, G. S., Guan, Z., & Cantwell, W. J. (2018). 8.17 Blast Protection for Polymer Composite Materials in Structures Subjected to Air-Blast Loading. *Comprehensive Composite Materials II*, 8, 332-350. https://doi.org/10.1016/B978-0-12-803581-8.10067-0

Liu, S., Qin, S., He, M., Zhou, D., Qin, Q., & Wang, H. (2020). Current applications of poly(lactic acid) composites in tissue engineering and drug delivery. *Composites Part B: Engineering,* 199. https://doi.org/10.1016/j.compositesb.2020.108238

Peng, K., Mubarak, S., Diao, X., Cai, Z., Zhang, C., Wang, J., & Wu, L. (2022). Progress in the Preparation, Properties, and Applications of PLA and Its Composite Microporous

Materials by Supercritical CO2: A Review from 2020 to 2022. *Polymers*, 14(20), 4320. https://doi.org/10.3390/polym14204320

Silva, D. d., Kaduri, M., Poley, M., Adir, O., Krinsky, N., Shainsky-Roitman, J., & Schroeder, A. (2018). Biocompatibility, biodegradation, and excretion of polylactic acid (PLA) in medical implants and theranostic systems. https://doi.org/10.1016/j.cej.2018.01.010 340, 9-14.

World Aquaculture Society. (2020). *Plastics in Aquaculture – The WAS-IMarEST Roundtables.* https://www.was.org/articles/Plastics-in-Aquaculture-The-WAS-IMarEST-Roundtables.aspx#:~:text=Plastics%20are%20used%20at%20every,product%20transportation%20or%20chemical%20storage.

Chapter seven: Conclusion and recommendations

The development of new, sustainable materials is an important aspect of materials science and engineering. This master's thesis successfully developed bio-inspired composites and foams containing mussel shell powder, a form of aquaculture waste. Incorporating mussel shell waste from the growing aquaculture sector in New Zealand, which that cultivates green lipped mussels, was shown to improve tensile strength and stiffness of PLA and LDPE composites as 3D printed filaments, and foams when processed into a fine powder as hypothesised.

More specifically, this work achieves the objectives outlined at the beginning of this study. Below is the conclusion of the key findings of this work with the related objectives.

Composites:

PLA composites were able to be 3D printed from 0-10wt% while LDPE composites were far more difficult (Objective 1.4). PLA samples showed optimal tensile properties at 8wt% and were able to be 3D printed. Testing found that the PLA filament became complicated to extrude at 10wt% as the melt became increasingly viscous. This resulted in inconsistent melt and varying filament diameter. The inconsistent diameter and susceptibility to moisture resulted in poor print quality and a high quantity of misprints. LDPE filaments were far too ductile to print with the chosen 3D printer. The LDPE filament became jammed in the machine resulting in no plastic leaving the extruder barrel and the print not being complete.

It was determined through tensile experiments that PLA filaments showed increase tensile strength (55-60 MPa) increasing mussel shell powder to 8wt% (Objective 1.1). As hypothesised the tensile stress was expected to increase as the mussel shell powder was increased. In comparison to PLA, LDPE composites showed lower tensile results than PLA at 9 MPa, but notably increased tensile strength as mussel shell powder was added (Objective 1.2). It was also shown that elongation or strain at break of the LDPE samples were reduced with the addition of a more ceramic material. Hydrolysis occurred notably at 30wt% resulting in instant failure of the PLA filament. LDPE showed increased tensile properties from 0-30wt% with a decreasing strain value reaching 30wt%.

Thermal properties of PLA showed a decrease in thermal degradation temperature as the amount of mussel shell increased (340℃ to 287℃), due to the hydrophilic nature of the polymer (Objective 1.3). This showed the presence of moisture and hydrolysis at higher weight

percentages of mussel shell due to the acid – base reactions occurring between PLA and calcium carbonate. LDPE composites showed increase in thermal degradation due to the high volumes of mussel shell powder (440℃ to 462℃), in this case mussel shell has a far greater degradation temperature than both polymers and hydrolysis was not an issue with LDPE.

Based upon the thermal and tensile properties combined the optimal amount of additives was determined to be:

- 8wt% for PLA composites
- 10wt% for LDPE composites

Achieving objectives 1.1, 1.2 and 1.3.

Foams:

It was hypothesised that particulates would firstly act as a nucleating agent within the foam and then reinforce the material. However, it was also noted that these particles could function as

stress concentrators within the material at higher weight percentages leading to a decrease the compressive strength of the polymer foams. It was found that the compressive stress and Youngs' modulus continued to increase as mussel shell powder was increased to 8wt% for both PLA and LDPE, with PLA having the highest compressive stress.

PLA foams showed lower density (1240 kg/m^3) and higher expansion ratios, typically having larger cell sizes than LDPE foams (922 kg/m^3). PLA foams showed rigid and brittle properties, where LDPE foams remained very ductile even at high weight percentages. PLA foams showed good nucleation and expansion ratios with lower percentages of mussel shell < 2wt%, specifically at 0.5wt% which showed an average expansion ratio of 3.18 being the highest of all samples assessed (Objective 2.1). LDPE samples showed similar nucleation and expansion ratios to each other with only minor changes occurring between samples at 1.5. Although it was notable that compressive stress was seen to increase as mussel shell powder was added for both polymers (Objective 2.2). Foam recovery also showed slight decreases as percentage of mussel shell was increased showing added stiffness between both polymers but remained at approximately 30-40% for PLA and 65-75% for LDPE.

By analysing this behaviour, it was determined that the optimal weight percentage is:

- 0.5wt% for PLA (high expansion foam)
- 8wt% for PLA (high stiffness foam)
- 1-2wt% LDPE (high recovery foam)
- 10wt% LDPE (high stiffness foam)

Achieving objectives 2.1 and 2.2.

To conclude it could be determined by this research that PLA showed best reinforcement at 8wt%, best thermal properties between 0-2wt% and best foam nucleation results at 0.5wt%. LDPE samples showed comparable results with best reinforcement at 8wt%, best thermal properties between 20-30wt% and best foam nucleation results at 0.5-1wt%. Finally, PLA was able to be 3D printed but not LDPE.

Recommended areas of research to further this master's thesis would be:

- 3D printing PLA and LDPE foams,
- Use of recycled plastics in combination with mussel shell powder,
- Further thermal analysis on composites including Dynamic Mechanical Analysis.,
- Increase ductility in PLA composites and foams through additives,
- Quenching PLA to study uniform cell morphology,
- Production of PLA and LDPE laminates utilising these materials.
- PLA and LDPE foam acoustic and vibration testing.

This work has highlighted the ability for this waste stream to be turned into valuable materials with significant potential for application, and opened future avenues of research in aquaculture, bio-inspired plastics, and a circular economy. Further investigation and exploration are encouraged in this field of research to expand upon the objectives presented in this thesis. Notably, this study contributes to the overlapping fields of environmental protection, sustainable development and materials and process science and engineering.

Appendices

Appendix A: Brief history of fisheries

With the development of steam trawlers in 1880s there was an increased ability to fish at greater ranges from the previous nearshore fishing. The trawlers were able to extend range, duration and catch loads. The development of the gear used became larger and had the ability to reach fishes at much greater depths. With the increasing advancement in technology there was a notable decline in fish populations by approximately 90% from 1900 to 2003 (Thurstan et al., 2010). Capture fisheries harvest natural resource, using boats and low tide fishermen as the method of capturing wild shellfish (FOA, 2008; Goulletquer & Heral, 1997). Other methods for capturing fish include longline fishing from boats, with the use of a variety of circle hooks that are intended to catch a specific species (Andraka et al., 2013). However, this is not always the case, and these practises are unlike the agricultural techniques that take place in aquaculture farming, where there is a consistent addition to supply and therefore, a more sustainable aspect is reached (FOA, 2008). Statistically, farmed fish supplies have risen over 30% in the decade between 1986 and 1997 through aquaculture farming (Naylor et al., 2000). Aquatic farming is now being dominated by aquaculture, with respectively over 91% of worldwide aquaculture production being produced in Asia. Globally 53.4 million tonnes of fish were farmed in the aquaculture industry in 2017, showing an overall increase of close to 5% per year in 2000 (Tacon, 2020). Overall, both capture fisheries and aquaculture produced 167.2 million tonnes of fish in the year 2014, which has developed increased growth on waste management and environmental impacts (Pędziwiatr, Zawadzki, & Michalska, 2017).

Appendix B: Plastic processing profile

PLA 3052D properties (Materials Data Center , n.d).

Processing/Physical Characteristics	Value	Unit	Test Standard
ASTM Data			
Melt Flow Index, MFI	14	g/10min	ASTM D 1238
Temperature	210	°C	-
Load	2.16	kg	-

Mechanical properties	Value	Unit	Test Standard
ASTM Data			
Tensile Strength at Yield	62	MPa	ASTM D 638
Flexural Modulus	3600	MPa	ASTM D 790
Flexural Strength	108	MPa	ASTM D 790
Izod Impact notched, 1/8 in	16	J/m	ASTM D 256

Thermal properties	Value	Unit	Test Standard
ASTM Data			
Melting Temperature	153	°C	ASTM D 3418
Glass Transition Temperature	57.5	°C	ASTM E 1356

Other properties	Value	Unit	Test Standard
Density	1240	kg/m³	ASTM D 792

Processing Recommendation Injection Molding	Value	Unit	Test Standard
Processing humidity	≤0.025	%	-
Melt temperature	200	°C	-
Mold temperature	25	°C	-
Feed temperature	165	°C	-
Zone 1	195	°C	-
Zone 2	205	°C	-
Nozzle temperature	205	°C	-
Screw speed	100 - 175	rpm	-
Back pressure	0.345 - 0.689	MPa	-

LD2420D (LDPE) (InnoPlus by PTT Global Chemicals, n.d).

Properties	InnoPlus LD2420D	Units	Test Methods
Physical Properties (Based on pellets and press-molded sheet)			
Melt Flow Rate at 190 °C, 2.16 kg.	0.27	g/10 min	ISO 1133
Density	0.922	g/cm^3	ISO 1183
Melting Temperature	111	°C	ISO 11357
Vicat Softening Point	95	°C	ASTM D1525
Tensile strength at Yield	10	N/mm^2	ISO 527
Tensile Modulus	240	N/mm^2	ISO 527
Film Properties (Based on blown film)*			
Max. Tensile Strength (MD/TD)	24 / 18	MPa	ISO 527
Ultimate Elongation (MD/TD)	320 / 550	%	ISO 527
Dart Drop Impact	200	g	ASTM D1709
Haze	<15	%	ASTM D1003
Gloss (20°)	>20	-	ASTM D2457
** film properties obtained from 70 microns film which was blown film extruded at blow up ratio 2.5*			

Appendix C: Particle size analysis

Analysis - Under

Malvern Instruments

Malvern

Measurement Details	
Sample Name	MSP
SOP File Name	Calcium.msop
Lab Number	
Operator Name	rodgers

Measurement Details	
Analysis Date Time	30/05/2023 1:44:42 PM
Measurement Date Time	30/05/2023 1:44:42 PM
Result Source	Measurement

Analysis	
Particle Name	Calcium Carbonate CaCO3
Particle Refractive Index	1.580
Particle Absorption Index	0.020
Dispersant Name	Water
Dispersant Refractive Index	1.330
Scattering Model	Mie
Analysis Model	General Purpose
Weighted Residual	0.61 %
Laser Obscuration	15.34 %

Result	
Concentration	0.0081 %
Span	11.936
Uniformity	3.241
Specific Surface Area	1419 m^2/kg
D [3,2]	4.23 µm
D [4,3]	31.7 µm
Dv (10)	1.67 µm
Dv (50)	8.68 µm
Dv (90)	105 µm
Dv (95)	162 µm
Volume Below (31) µm	75.43 %

Frequency (compatible)

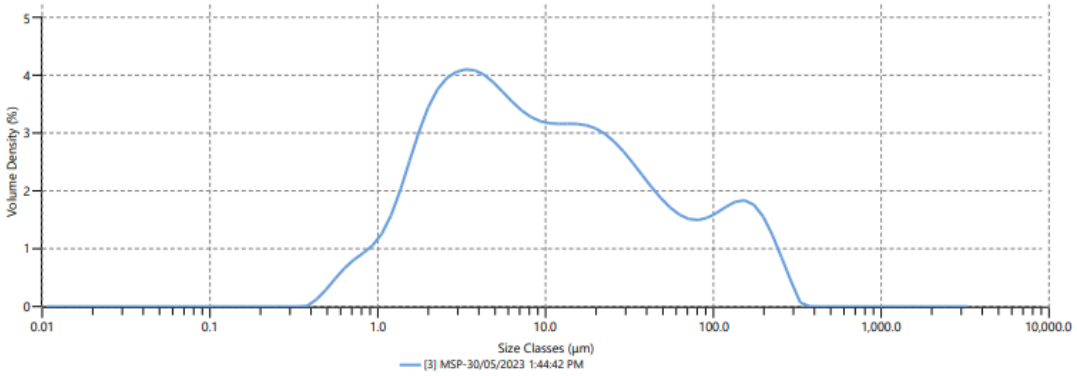

Result

Size (µm)	% Volume Under	Size (µm)	% Volume Under	Size (µm)	% Volume Under	Size (µm)	% Volume Under	Size (µm)	% Volume Under
0.0500	0.00	7.80	47.71	88.0	88.17	350	100.00	1410	100.00
0.0600	0.00	15.6	62.13	105	89.97	420	100.00	1680	100.00
0.120	0.00	31.0	75.43	125	91.89	500	100.00	2000	100.00
0.240	0.00	37.0	78.24	149	93.97	590	100.00	2380	100.00
0.490	0.22	44.0	80.68	177	96.01	710	100.00	2830	100.00
0.980	3.55	53.0	82.98	210	97.82	840	100.00	3360	100.00
2.00	13.72	63.0	84.86	250	99.14	1000	100.00		
3.90	30.90	74.0	86.47	300	99.88	1190	100.00		

Appendix D: Tensile graphs

PLA control.

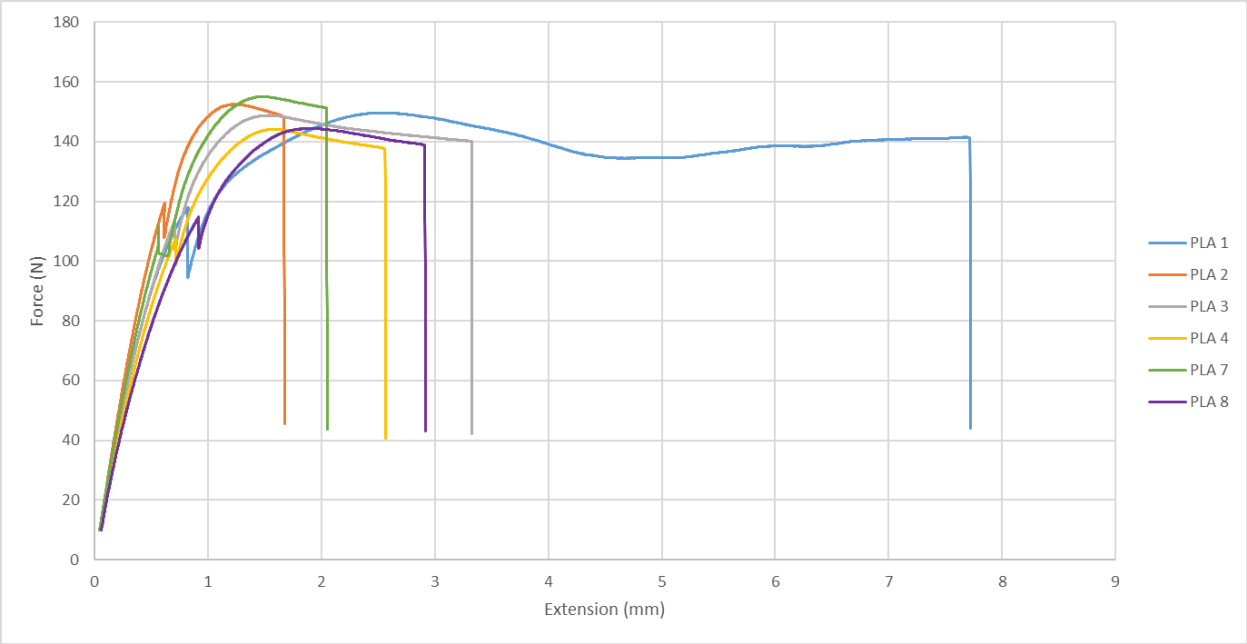

PLA + 0.5wt%.

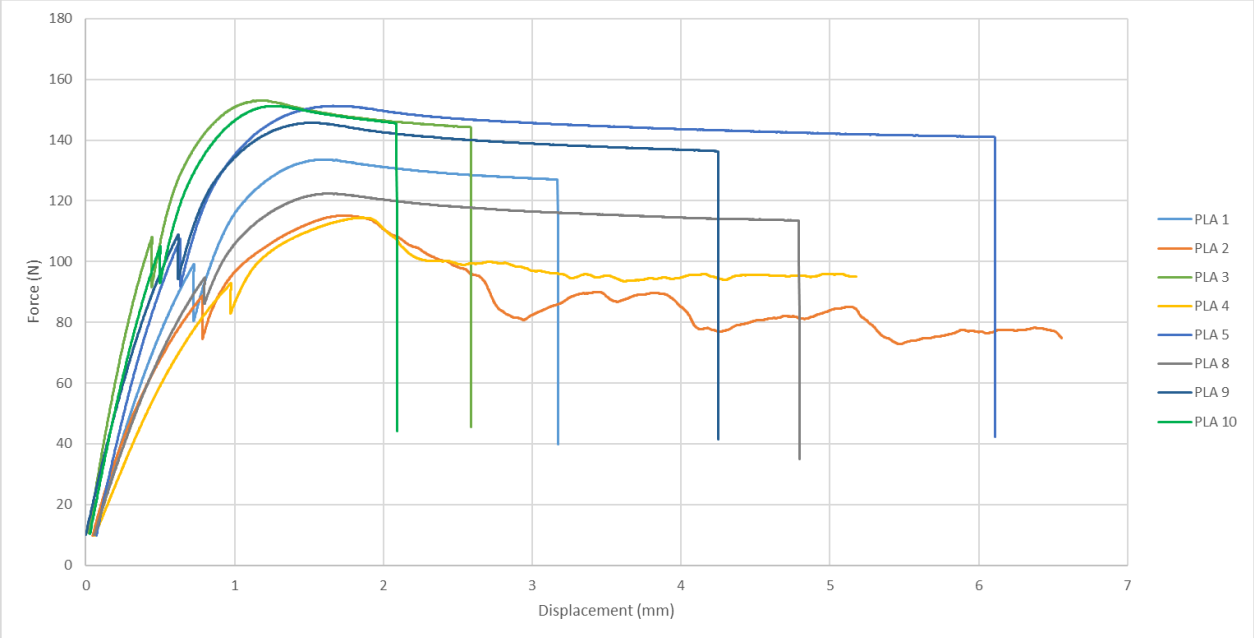

PLA + 1wt%.

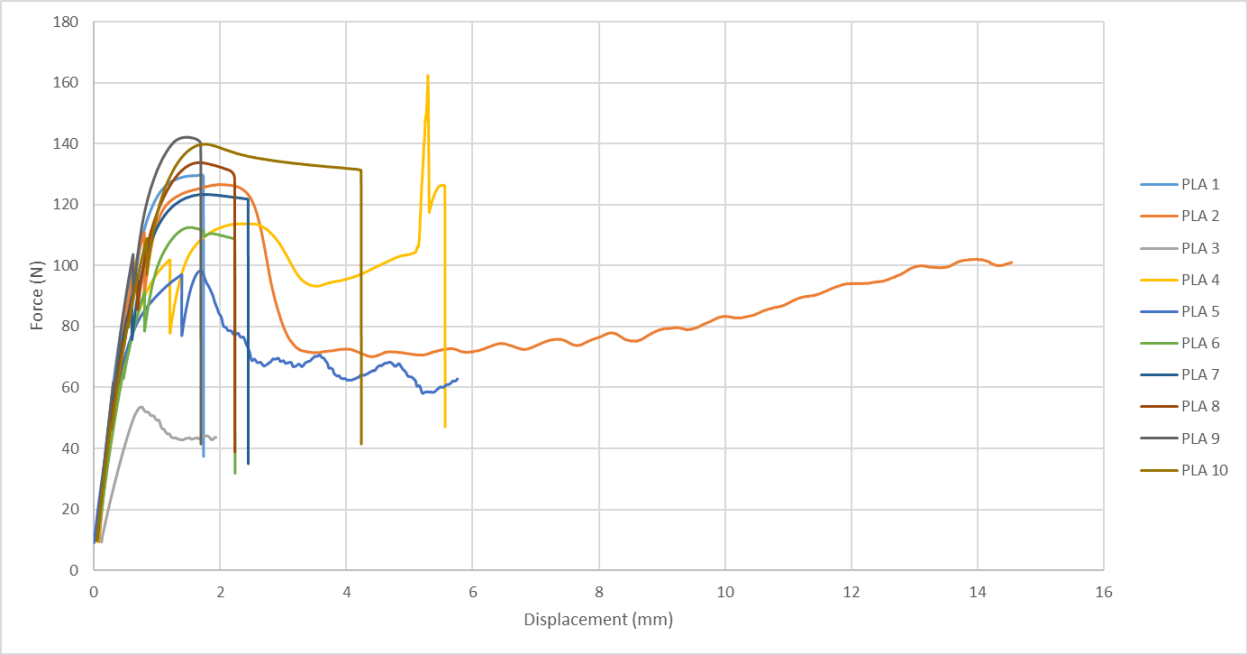

PLA + 1.5wt%.

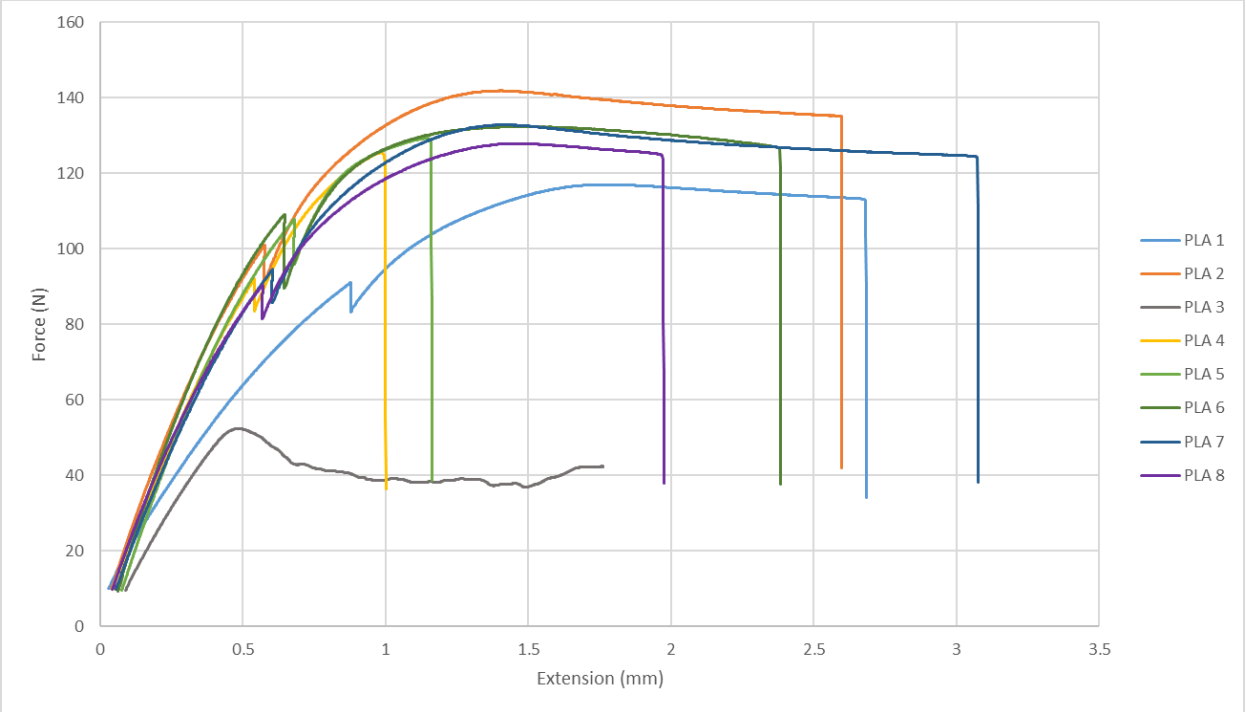

PLA + 2wt%.

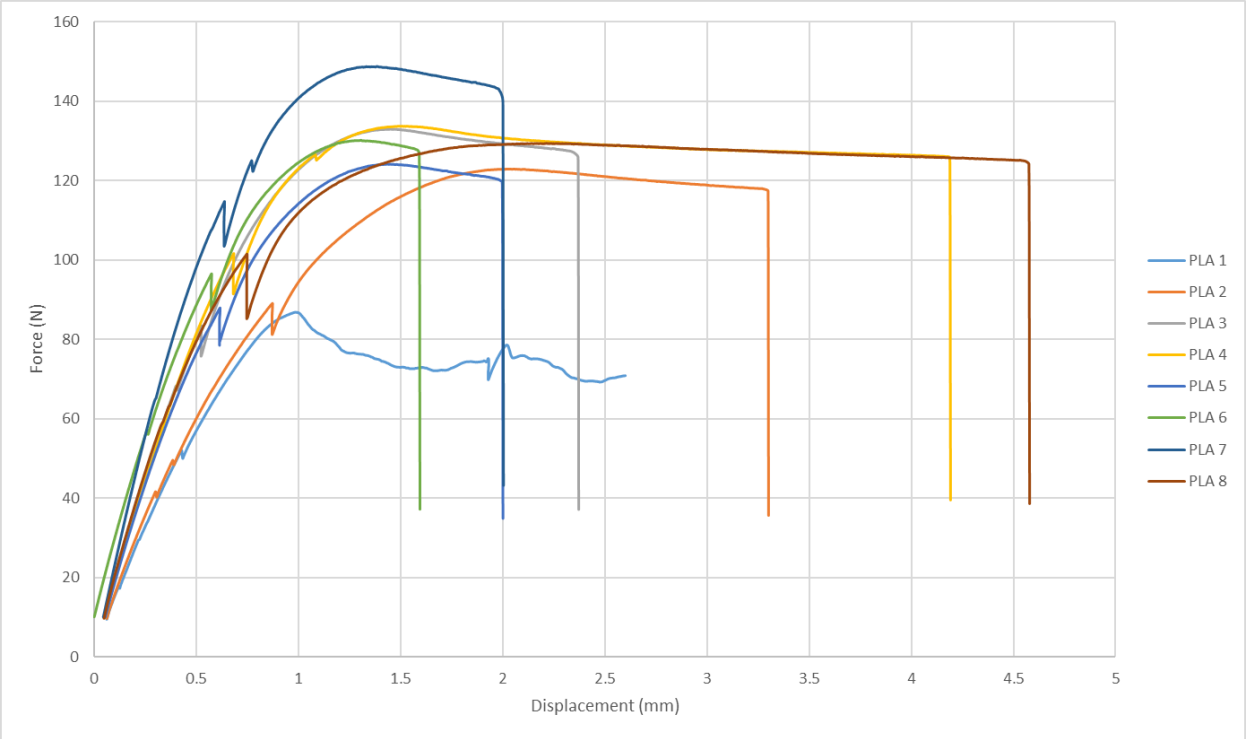

PLA + 4wt%.

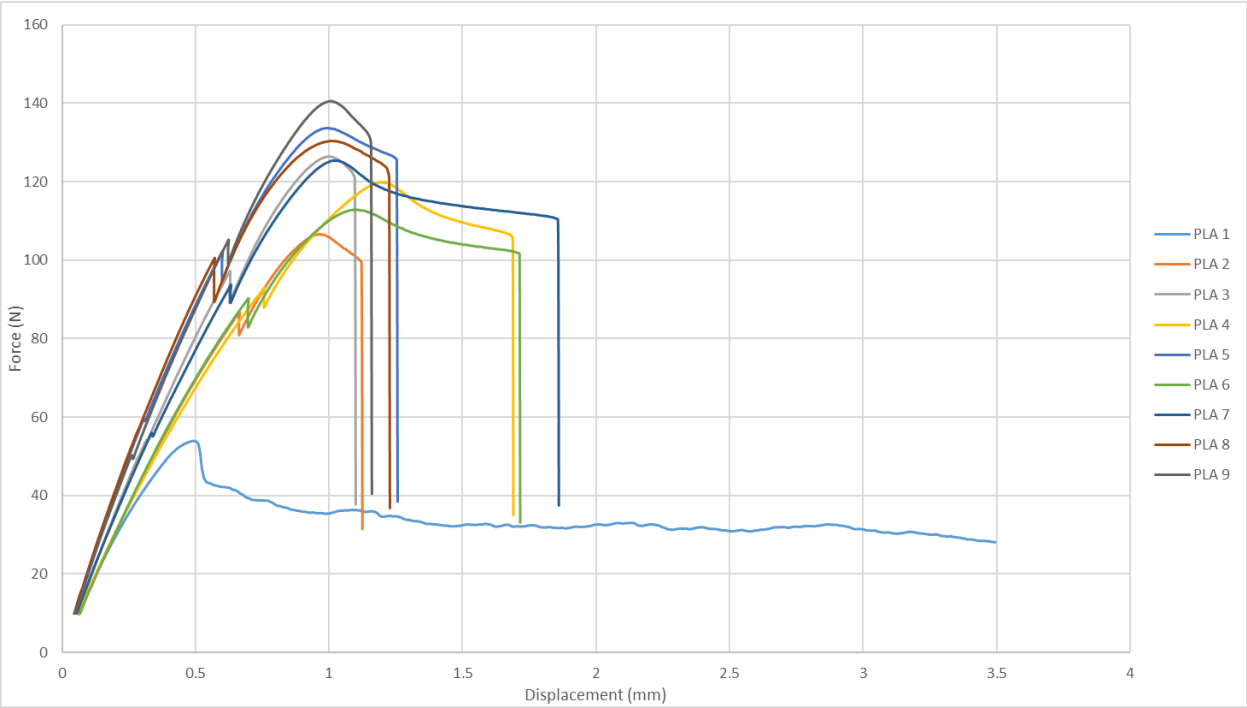

PLA + 6wt%.

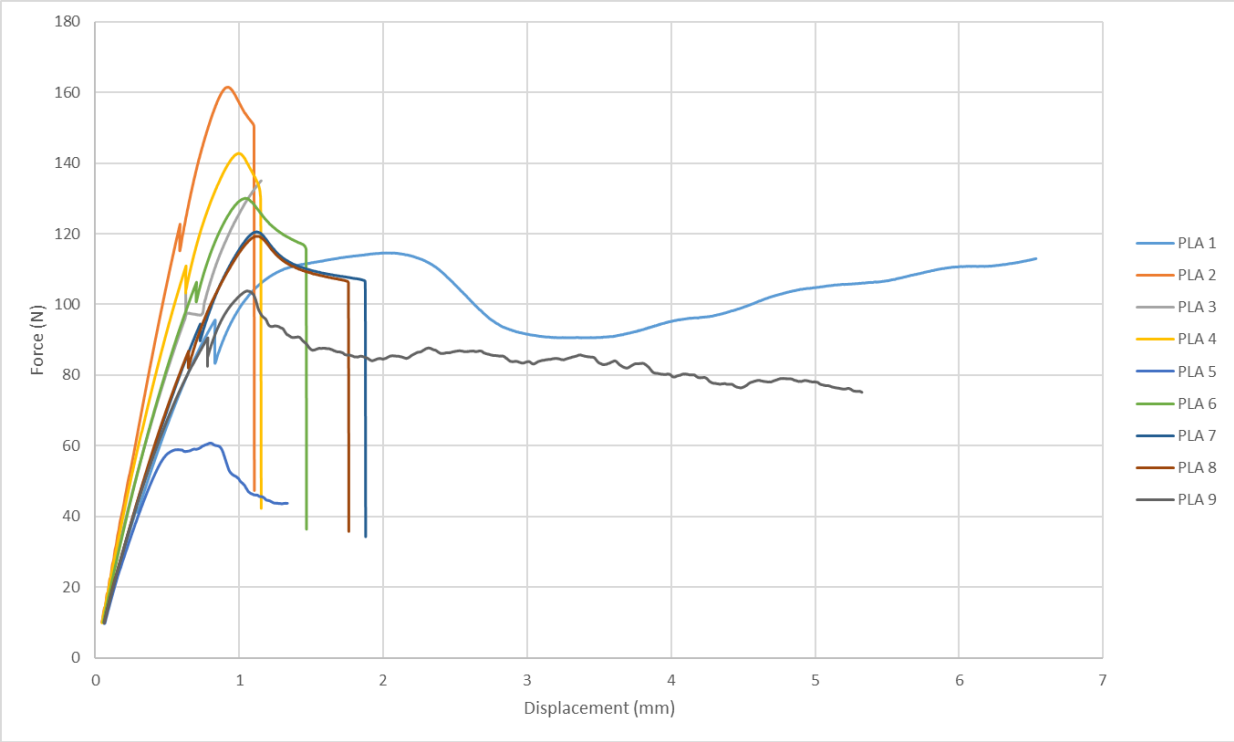

PLA + 8wt%.

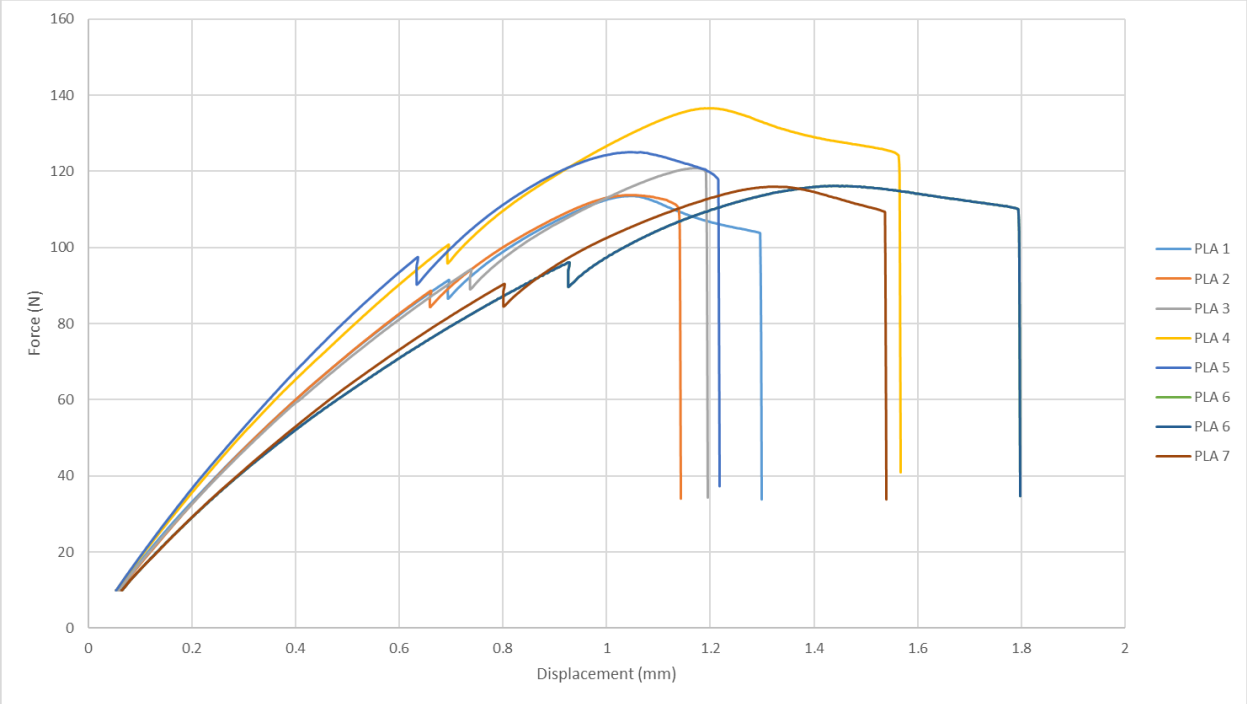

PLA + 10wt%.

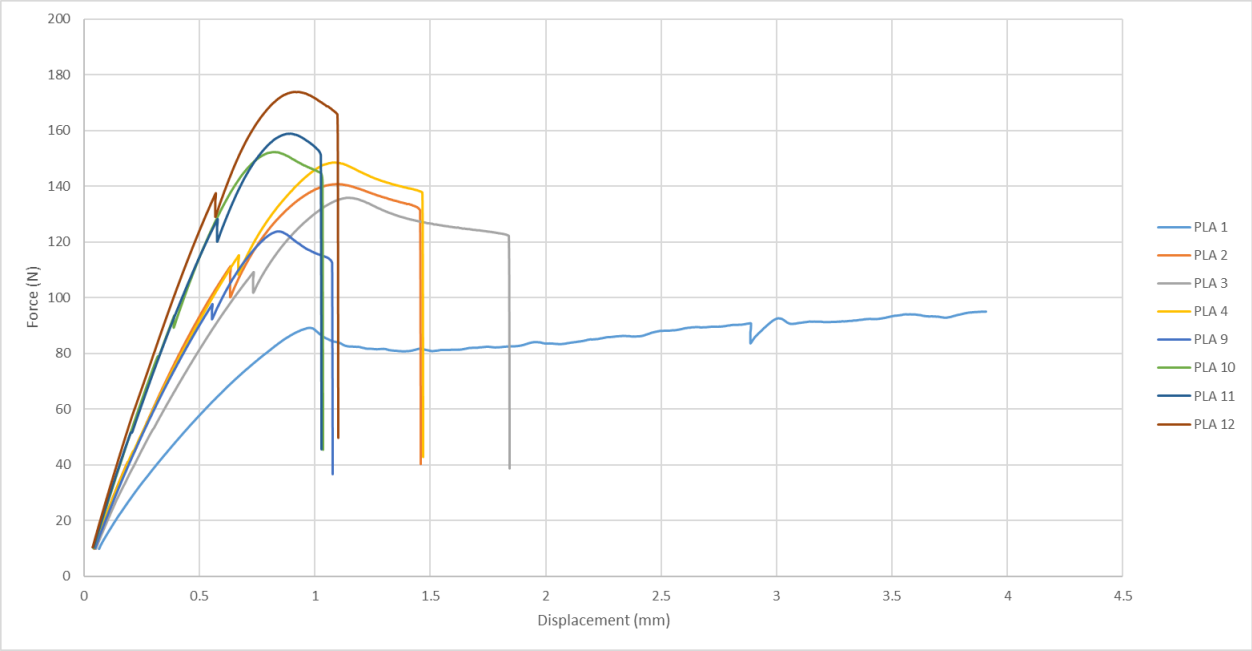

PLA + 20wt%.

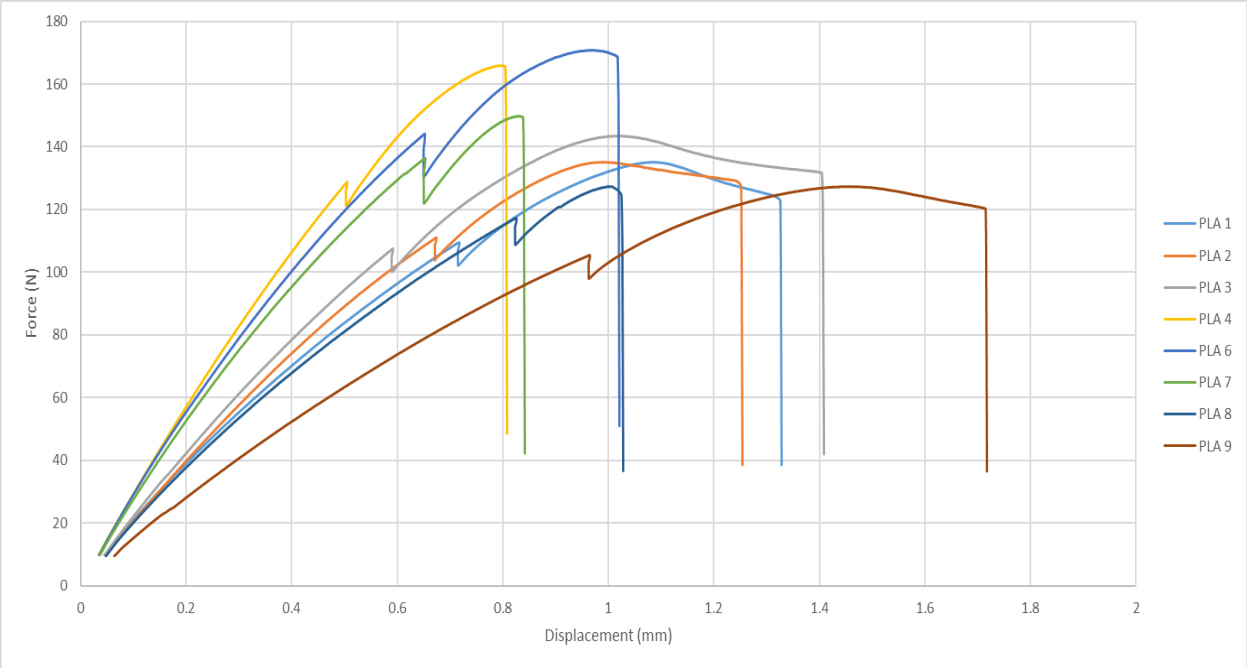

PLA + 30wt%.

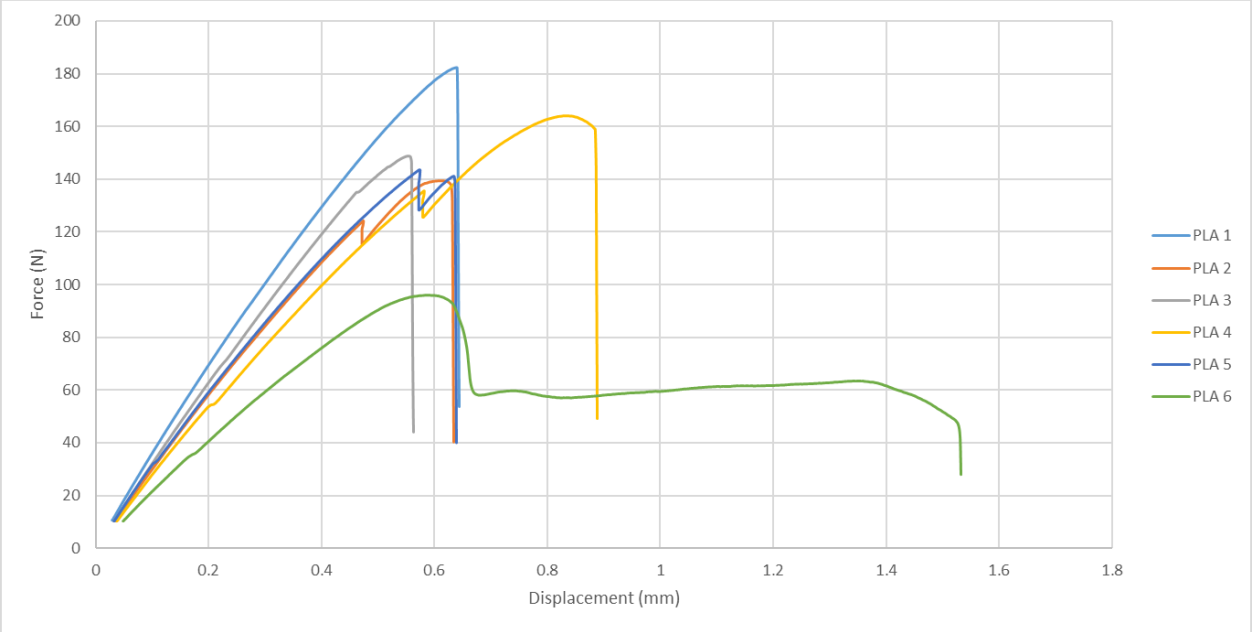

LDPE control.

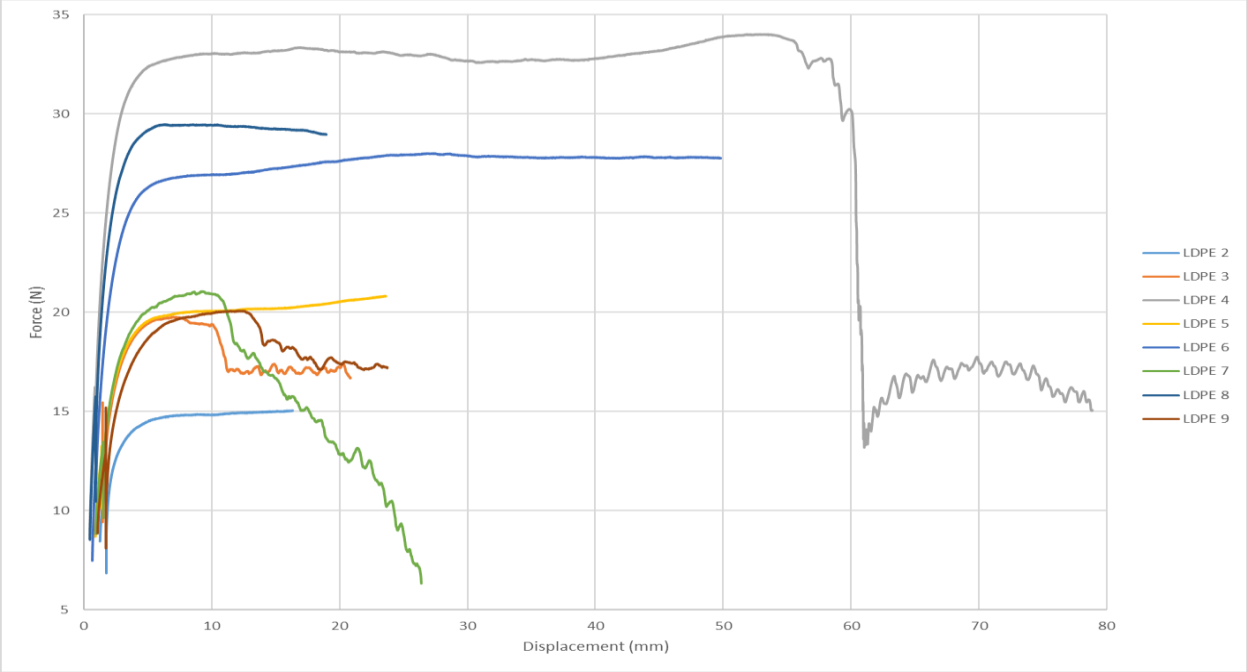

LDPE + 0.5wt%.

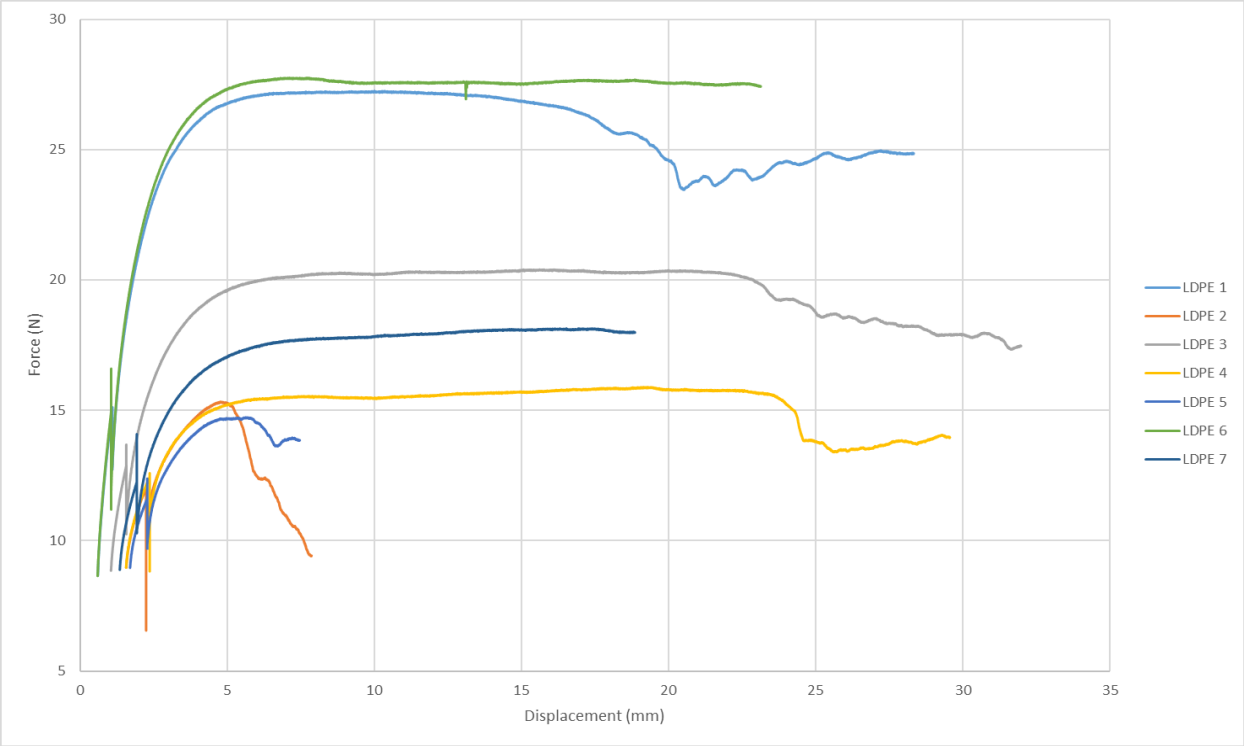

LDPE + 1wt%.

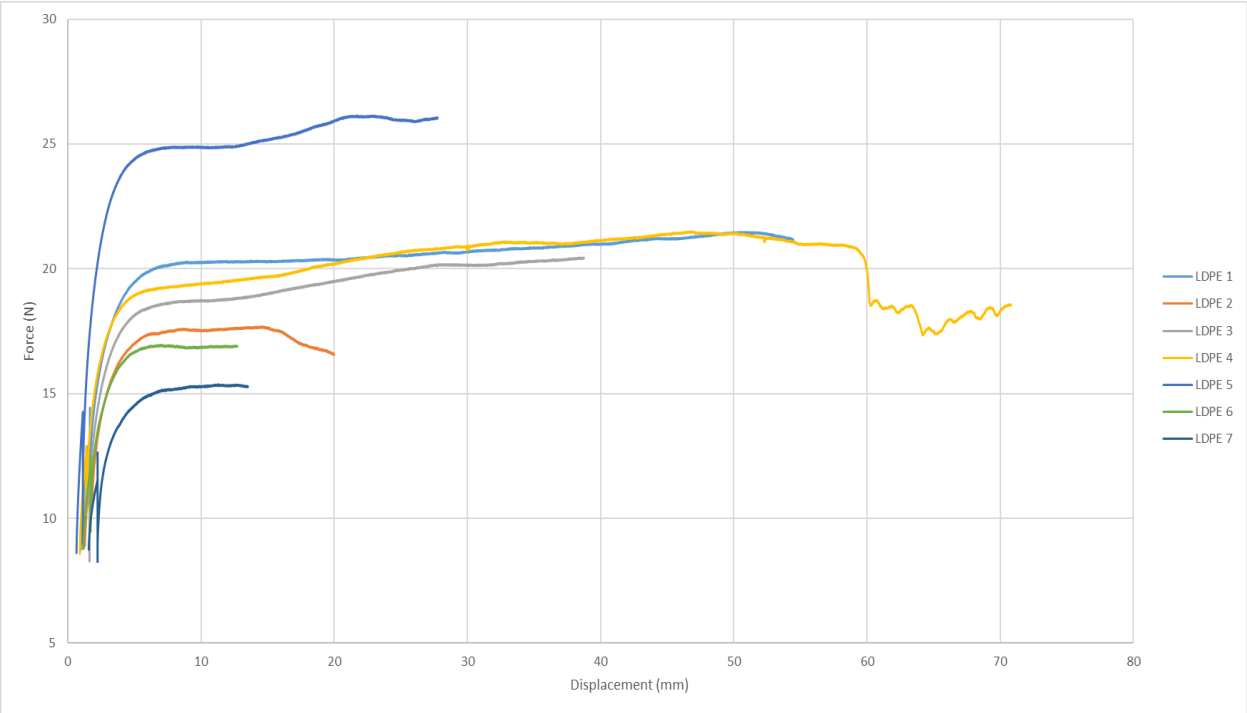

LDPE + 1.5wt%.

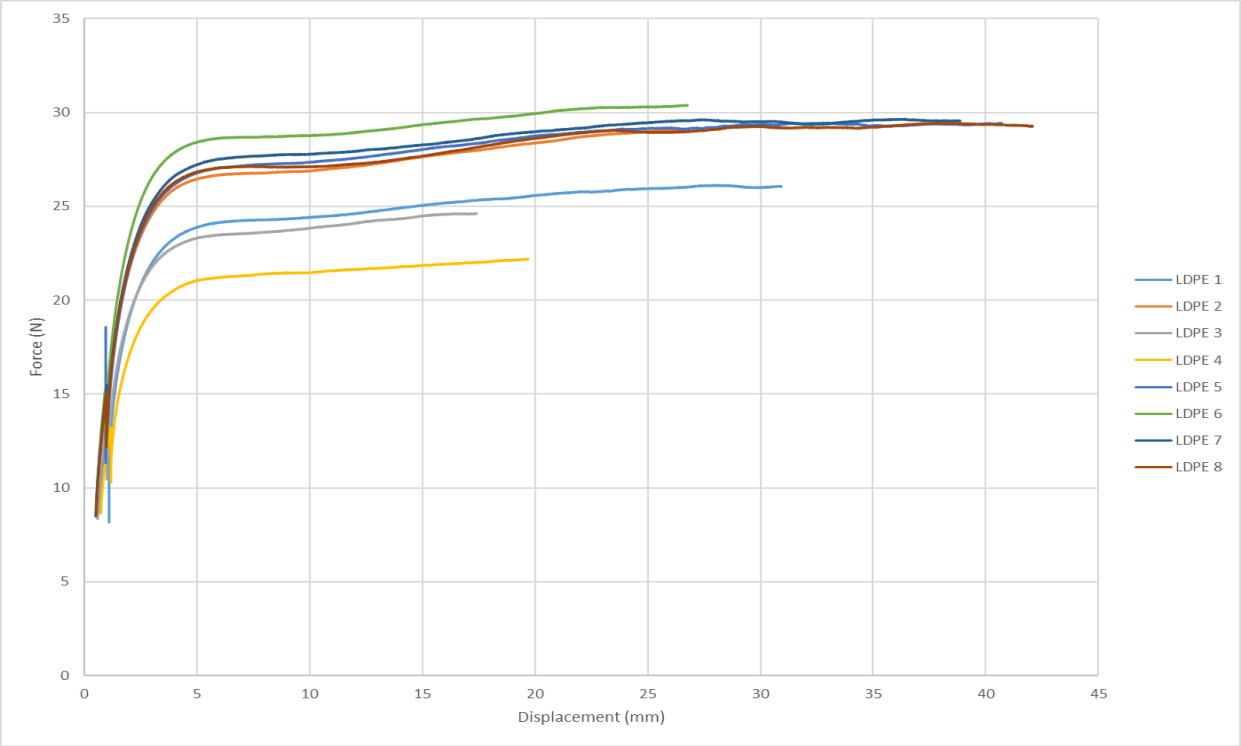

LDPE + 2wt%.

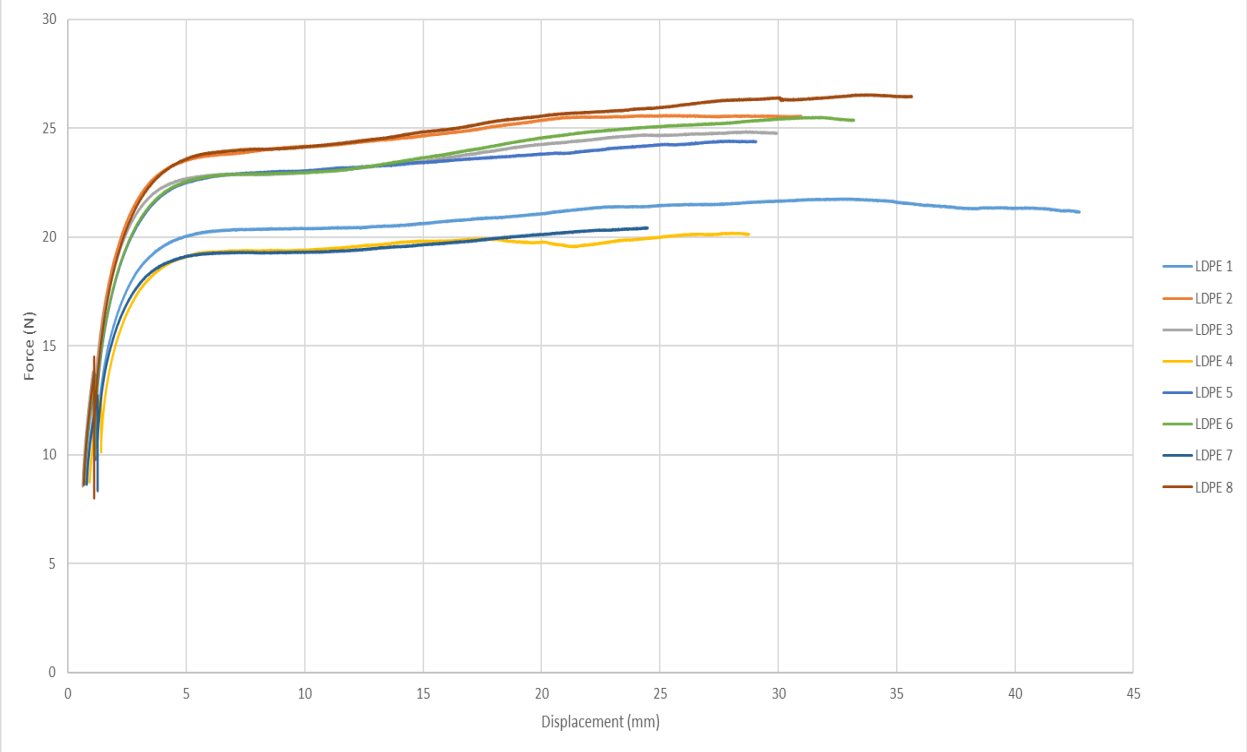

LDPE + 4wt%.

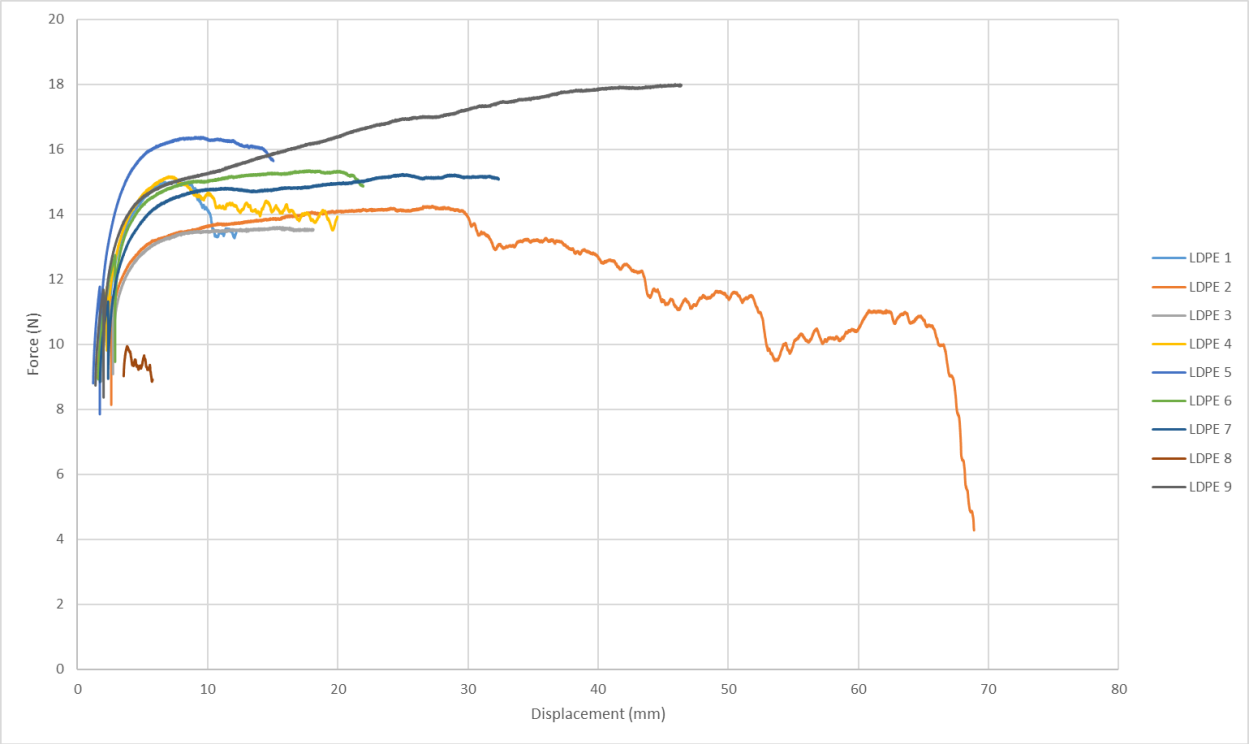

LDPE + 6wt%.

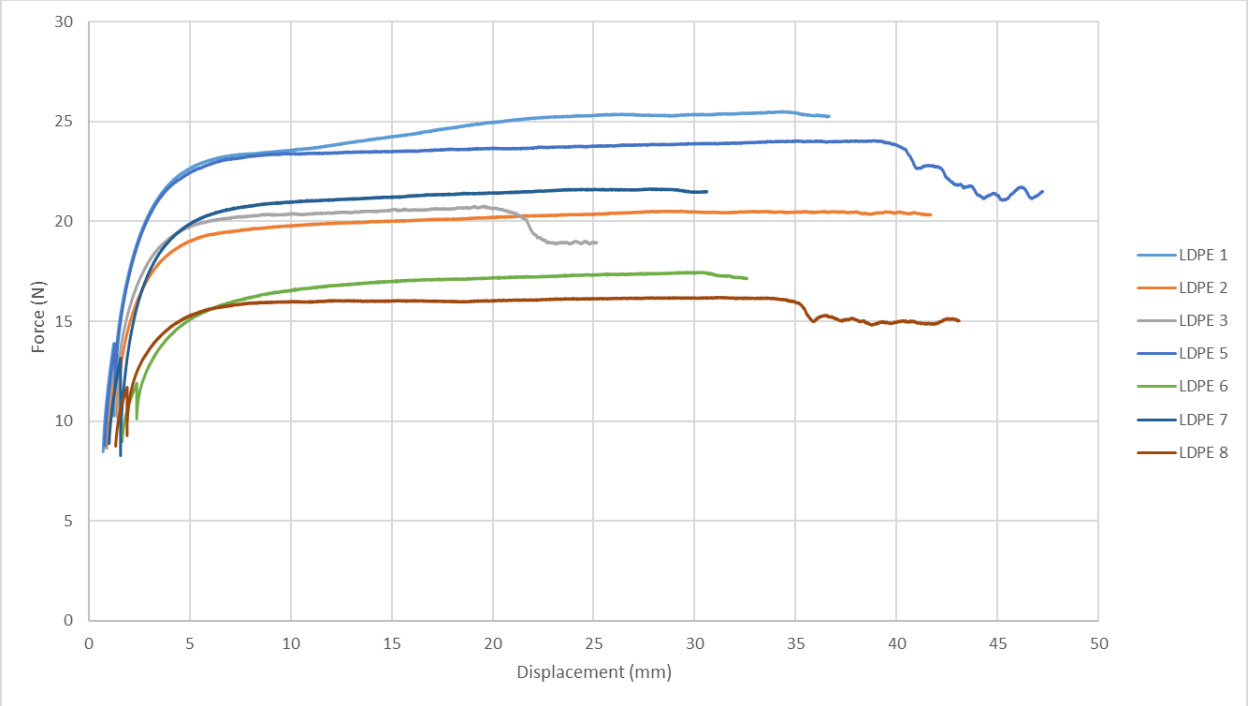

LDPE + 8wt%.

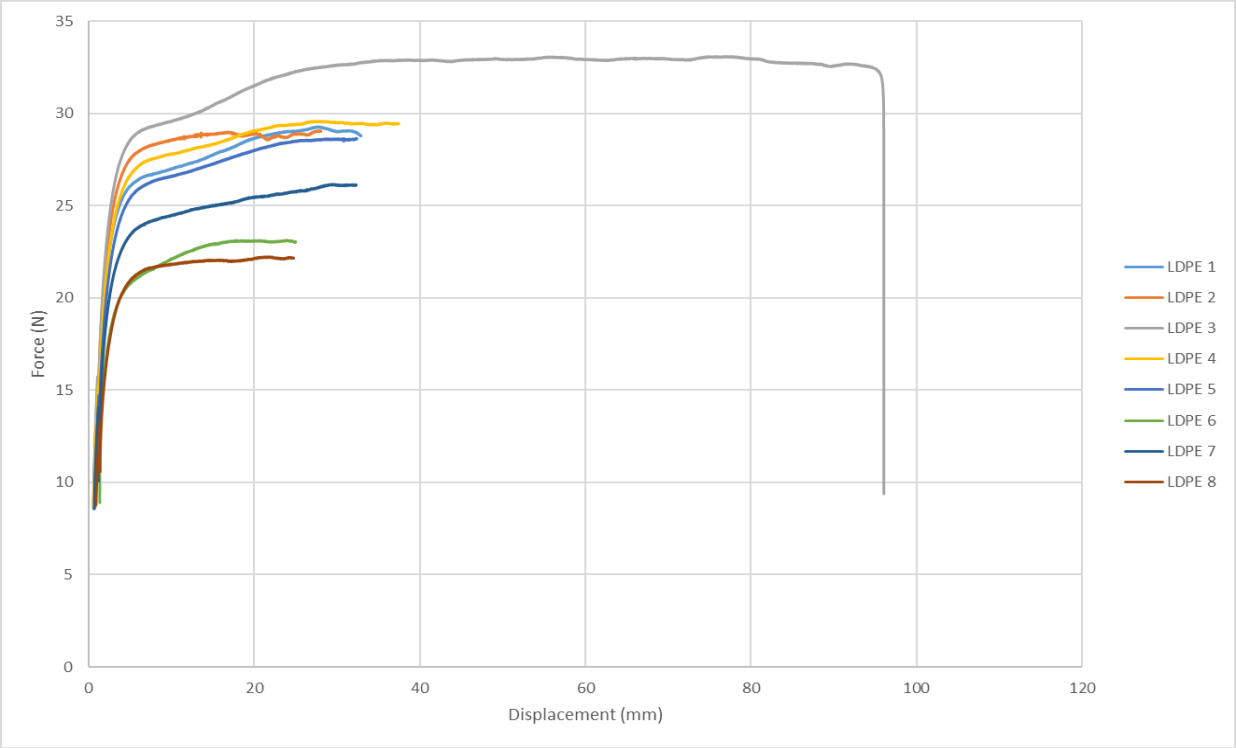

LDPE + 10wt%.

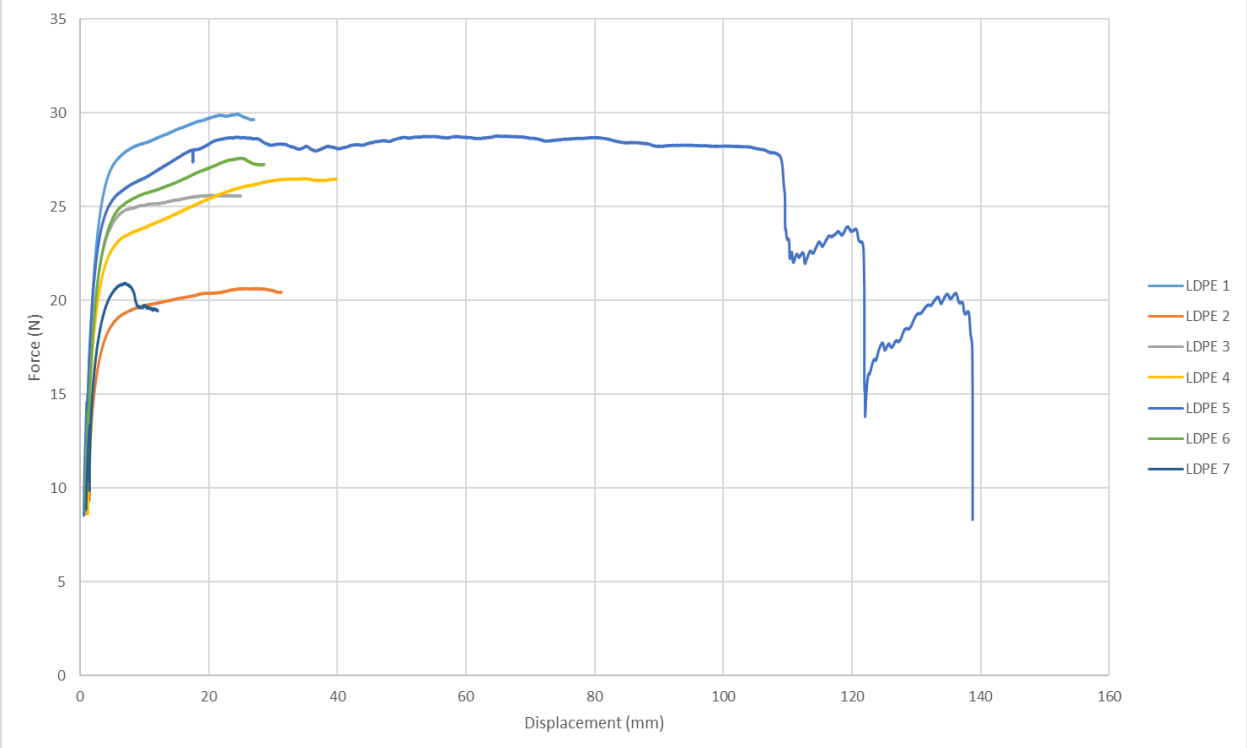

LDPE + 20wt%.

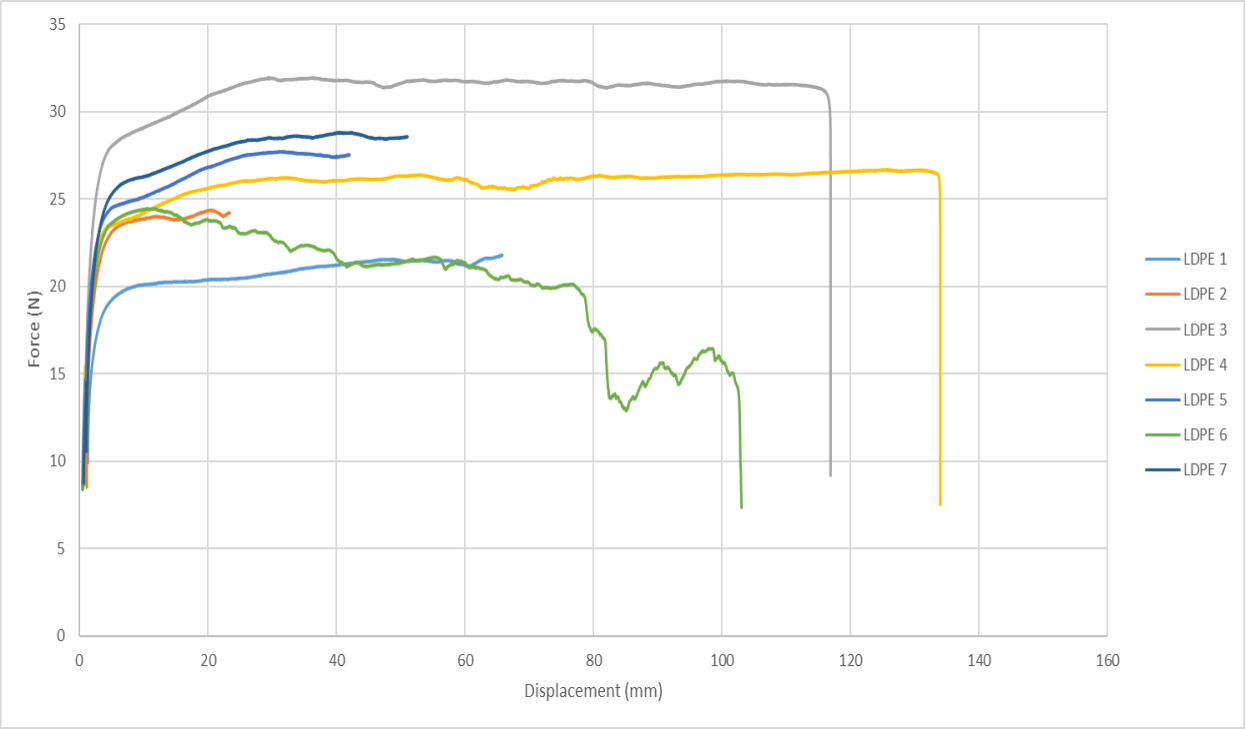

LDPE + 30wt%.

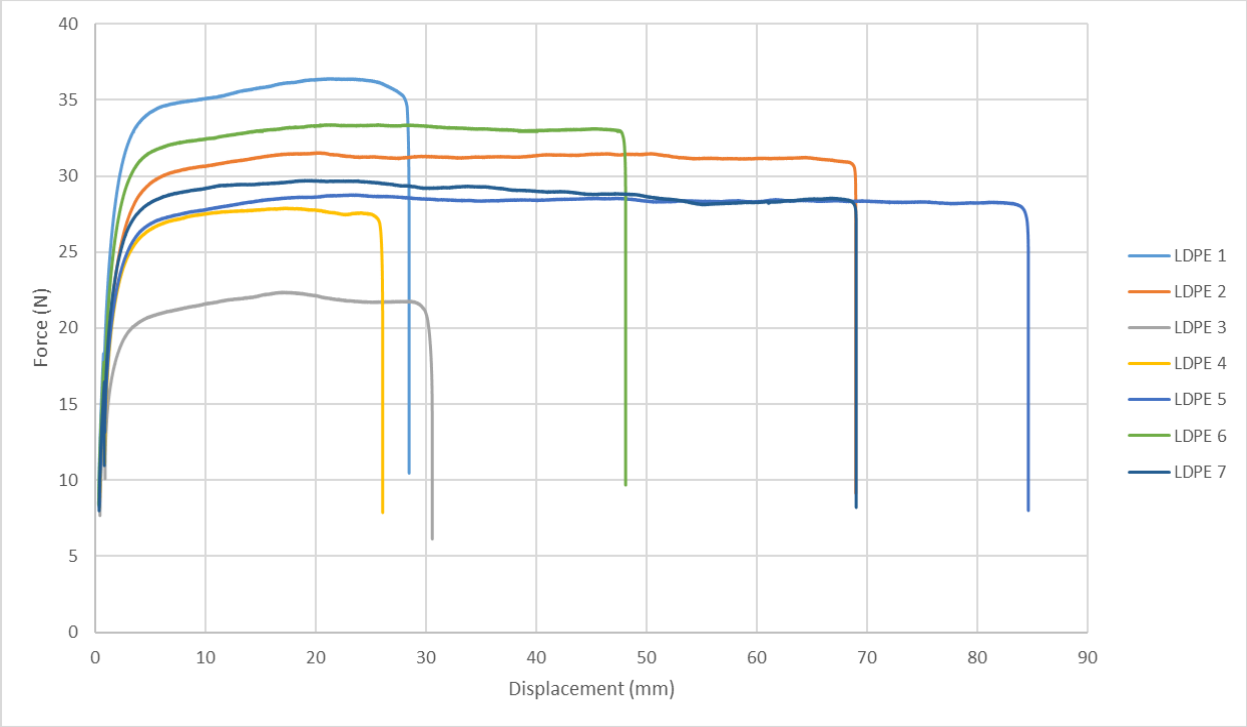

Appendix E: Compression graphs

PLA control compression.

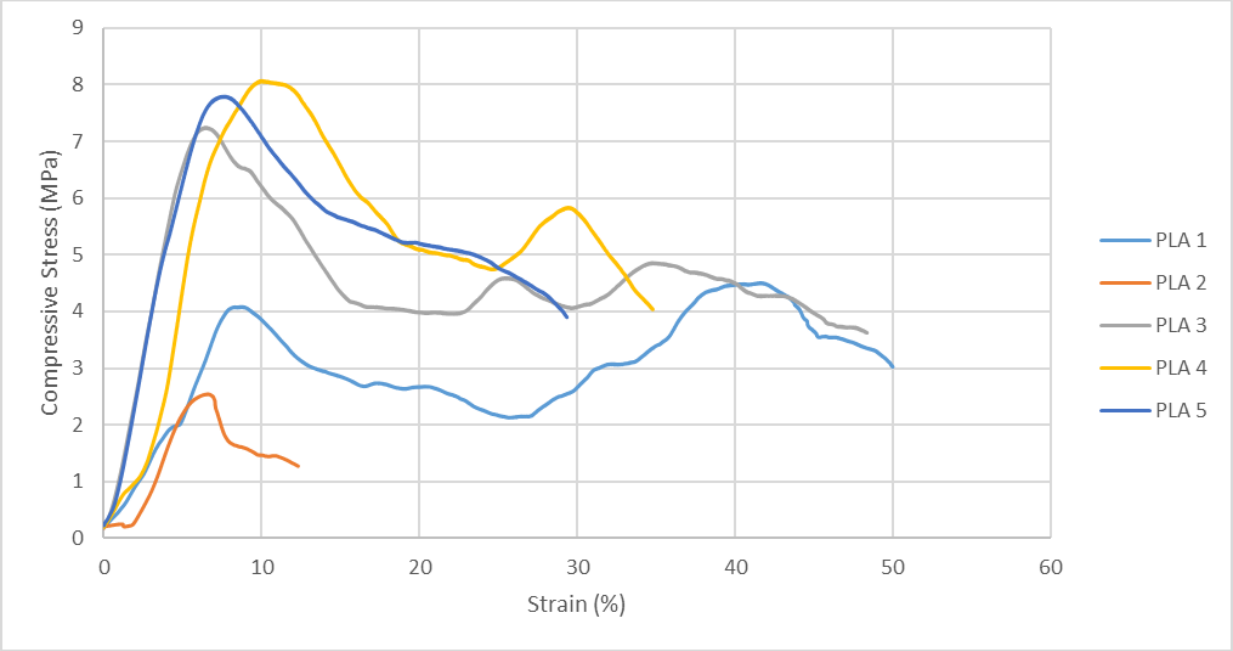

PLA control cyclic compression.

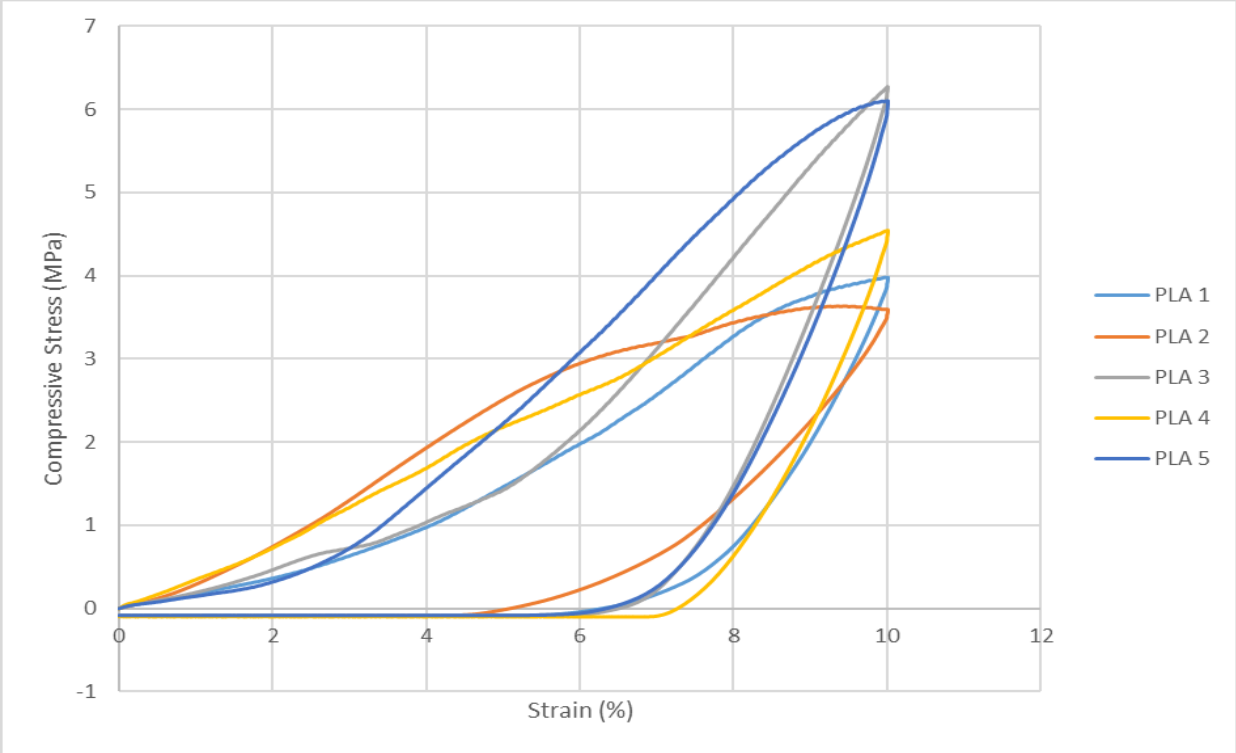

PLA + 0.5wt% compression.

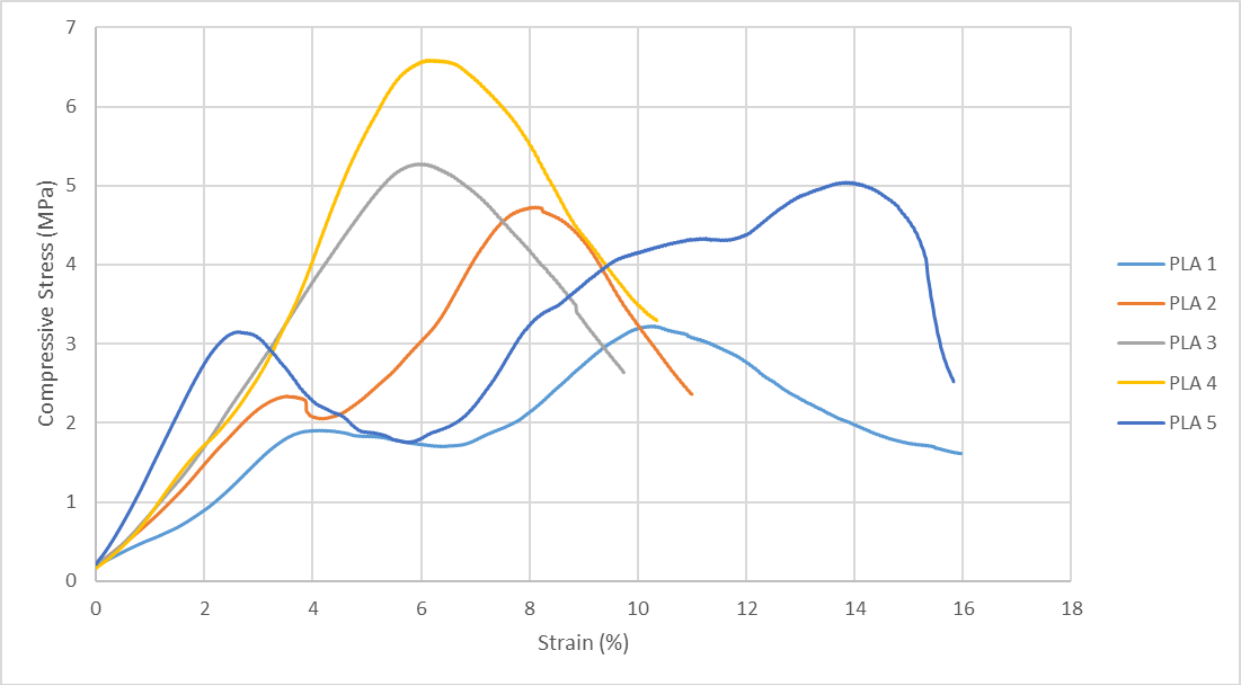

PLA + 0.5wt% cyclic compression.

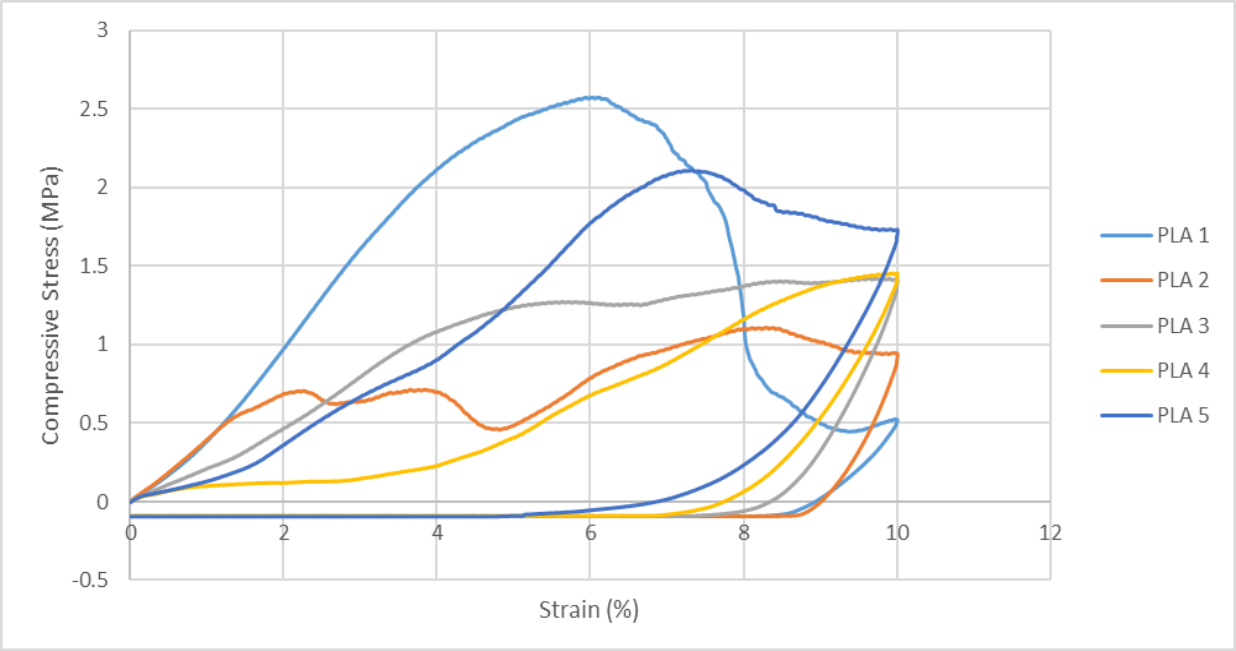

PLA + 1wt% compression.

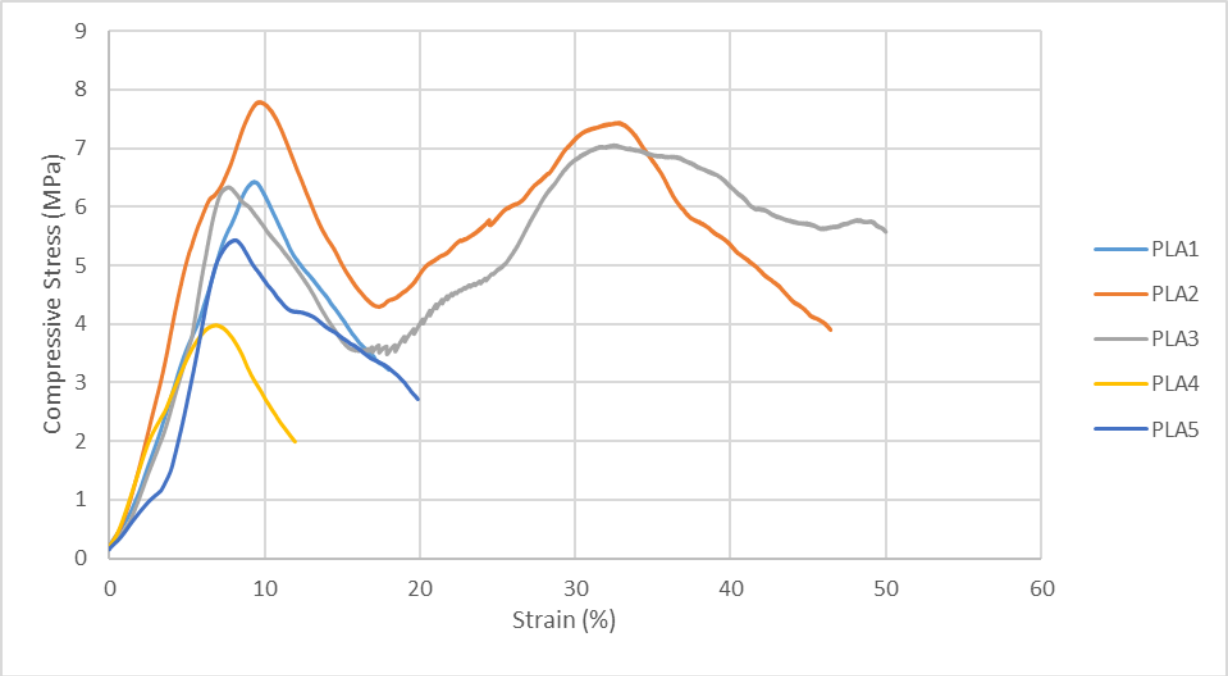

PLA + 1wt% cyclic compression.

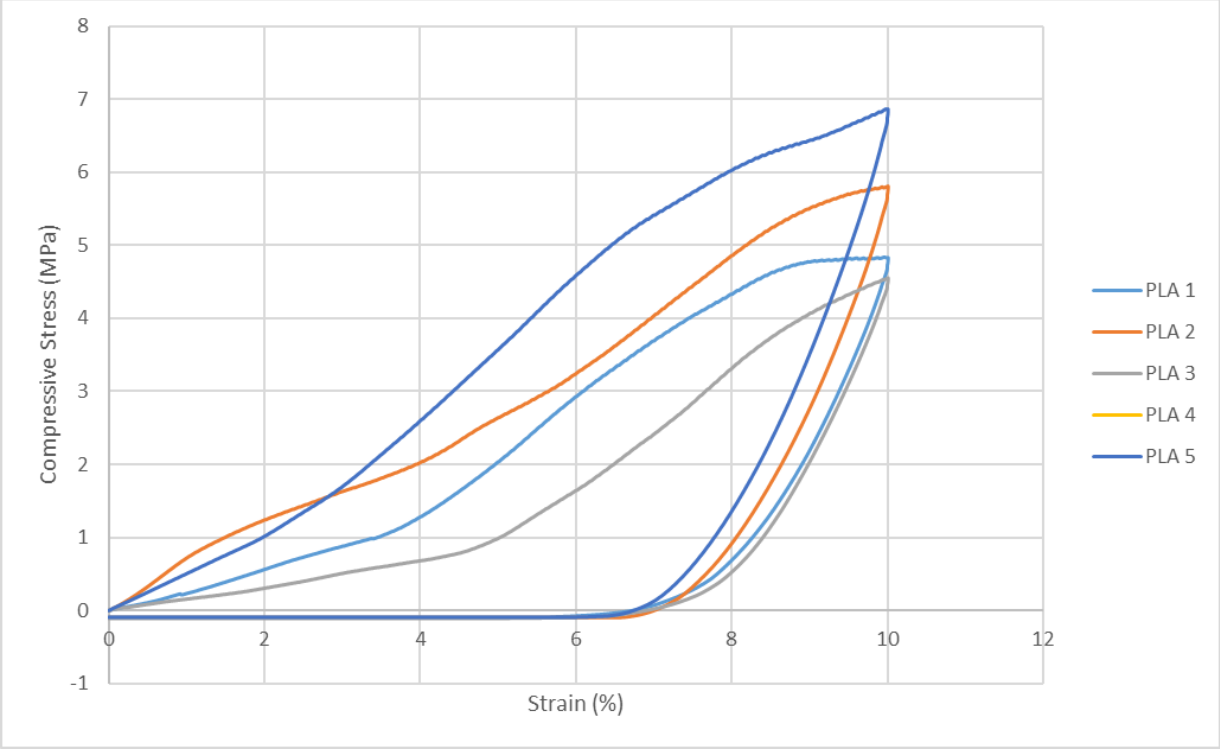

PLA + 1.5wt% compression.

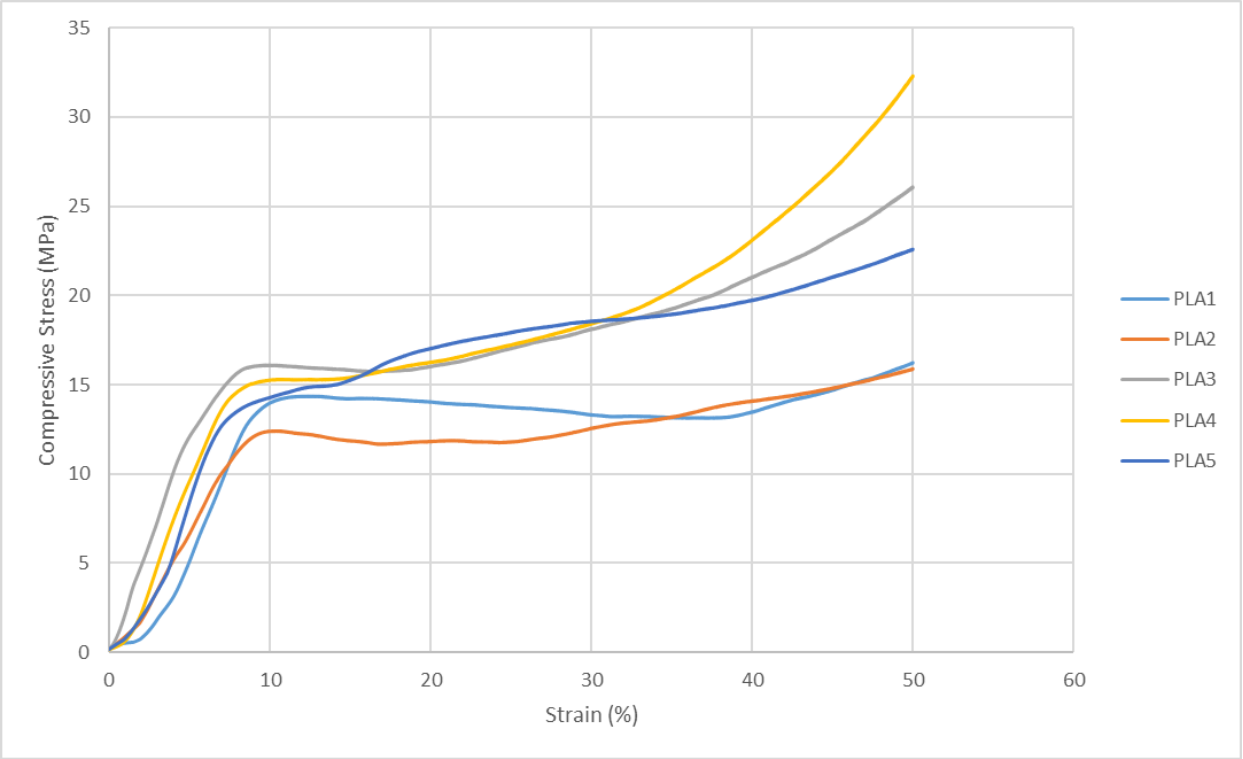

PLA + 1.5wt% cyclic compression.

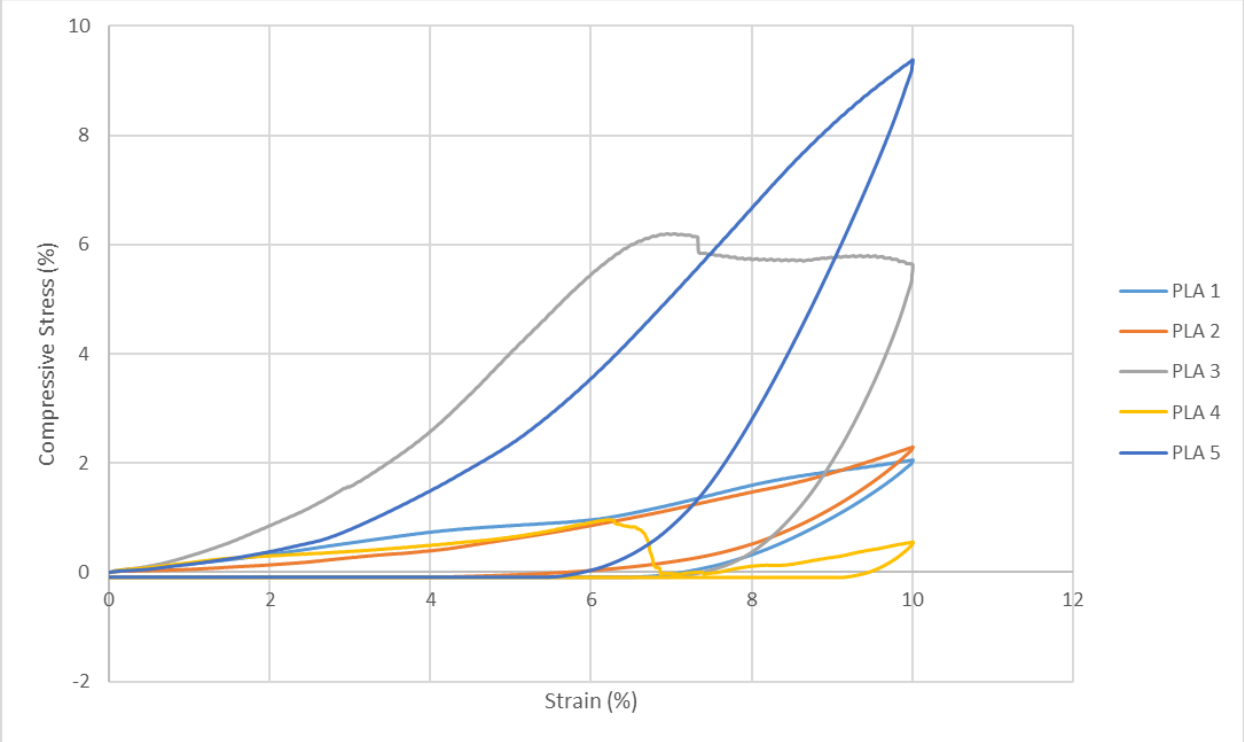

PLA + 2wt% compression.

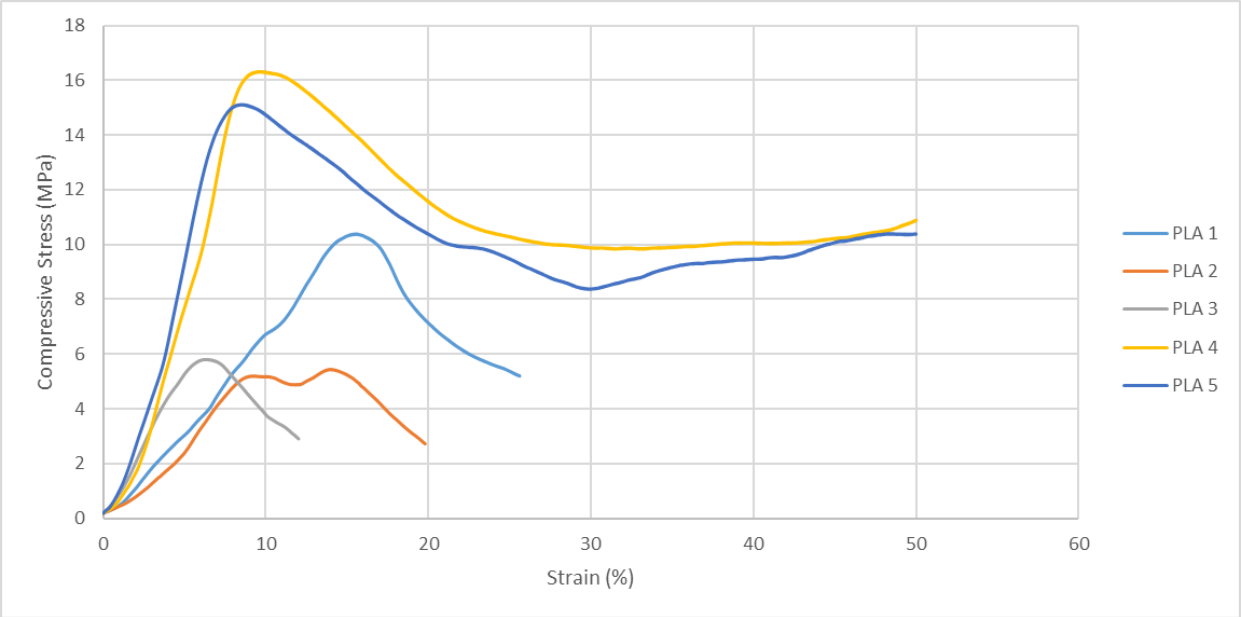

PLA + 2wt% cyclic compression.

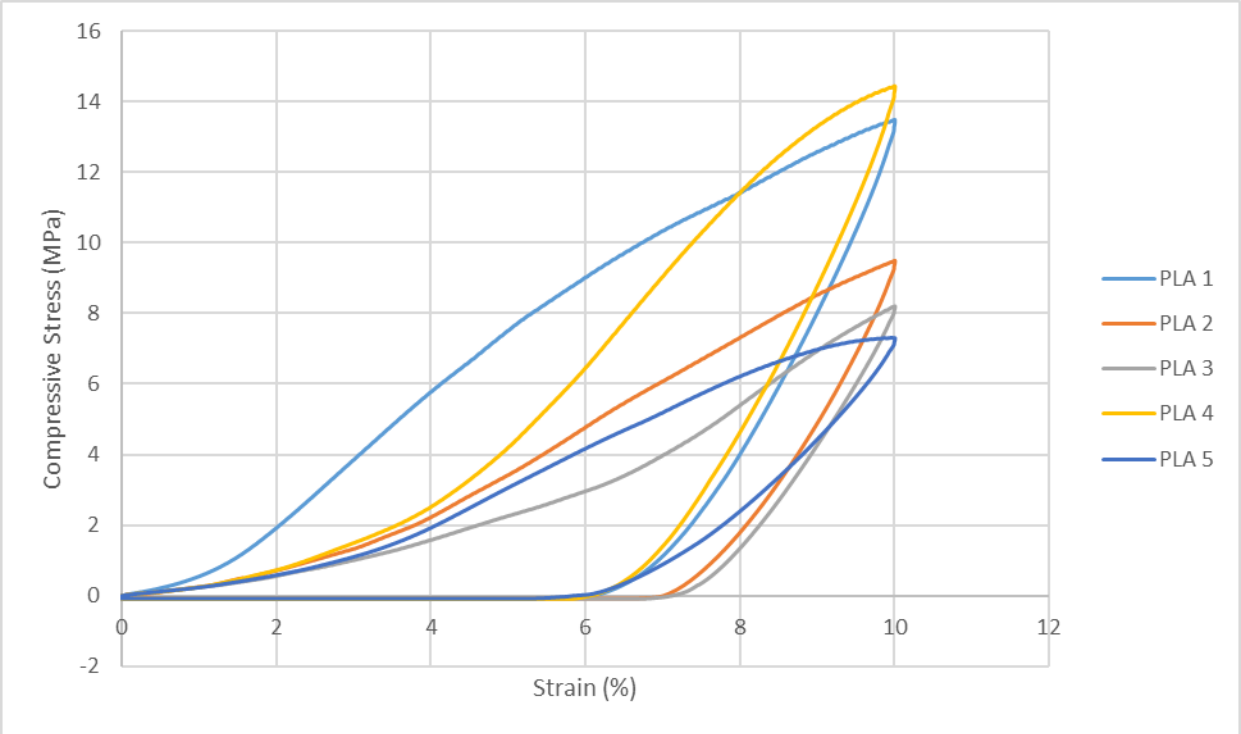

PLA + 4wt% compression.

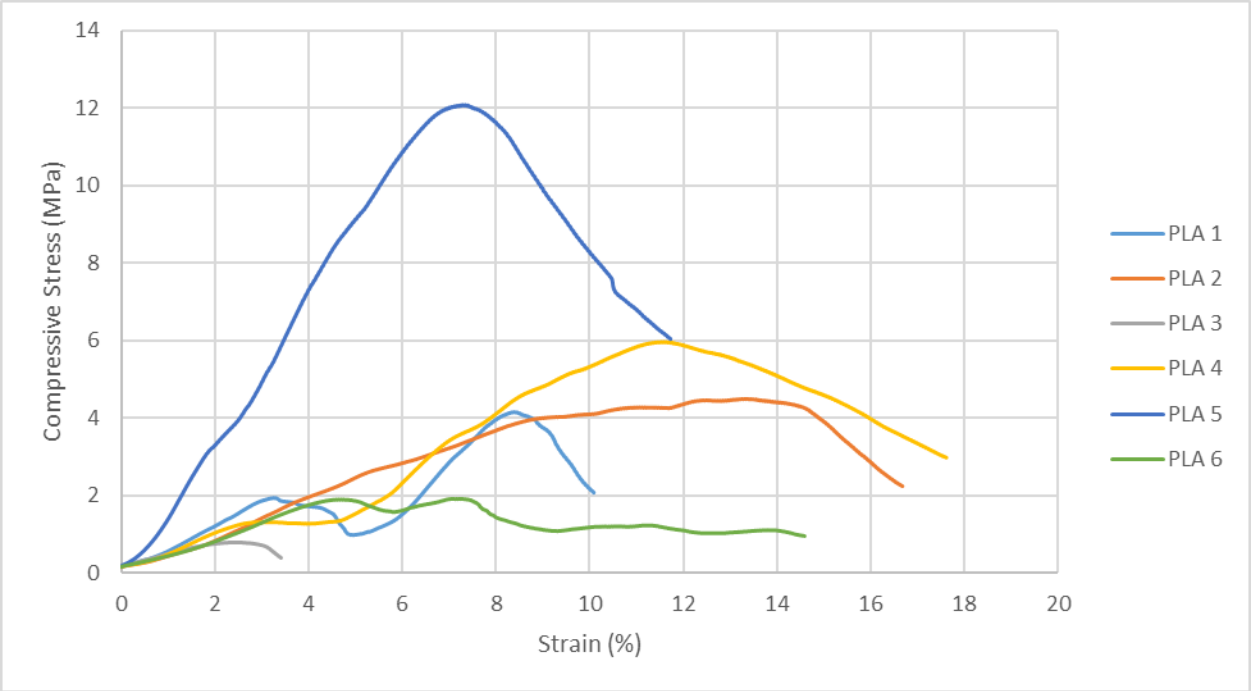

PLA + 4wt% cyclic compression.

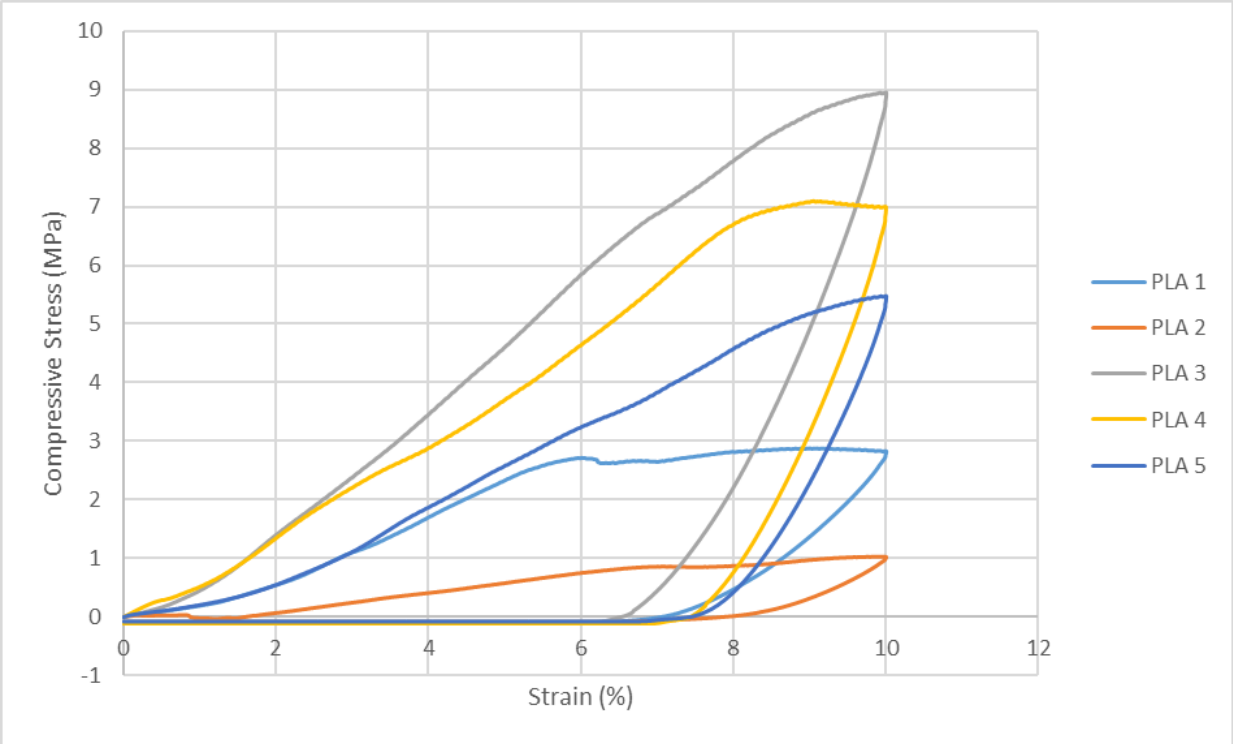

PLA + 6wt% compression.

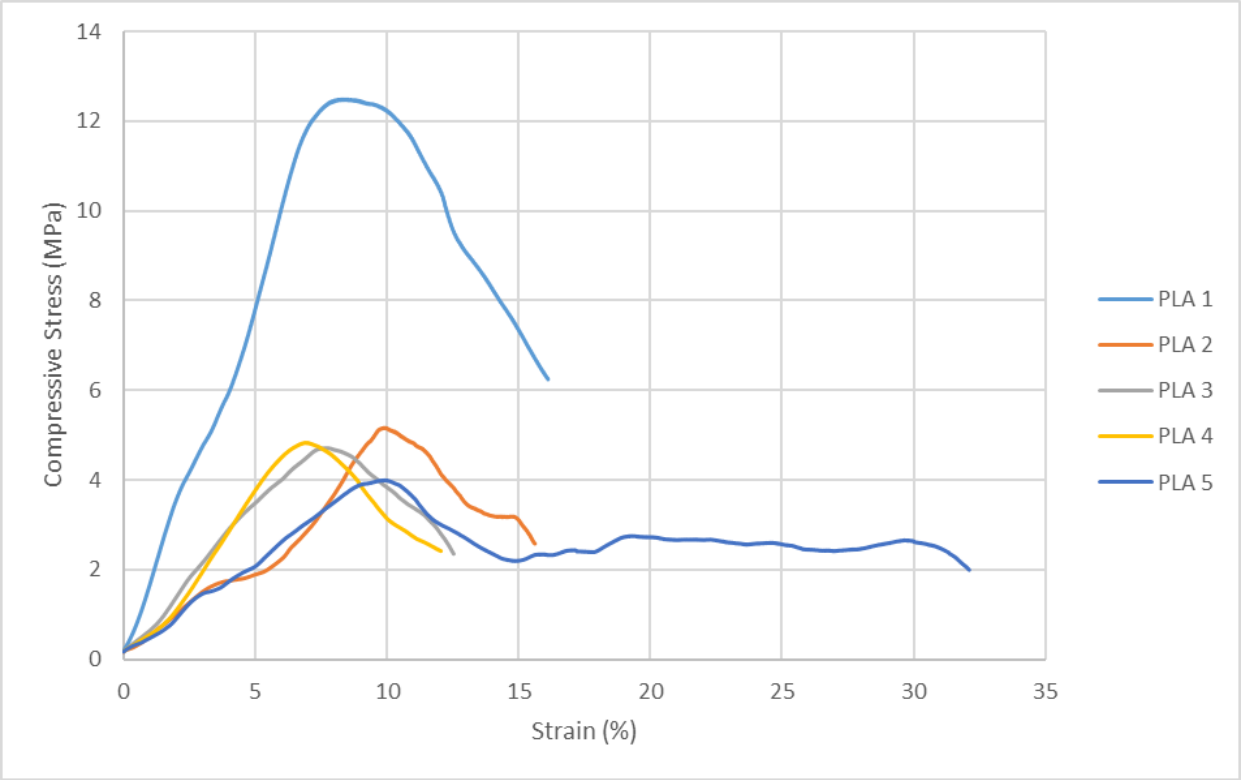

PLA + 6wt% cyclic compression.

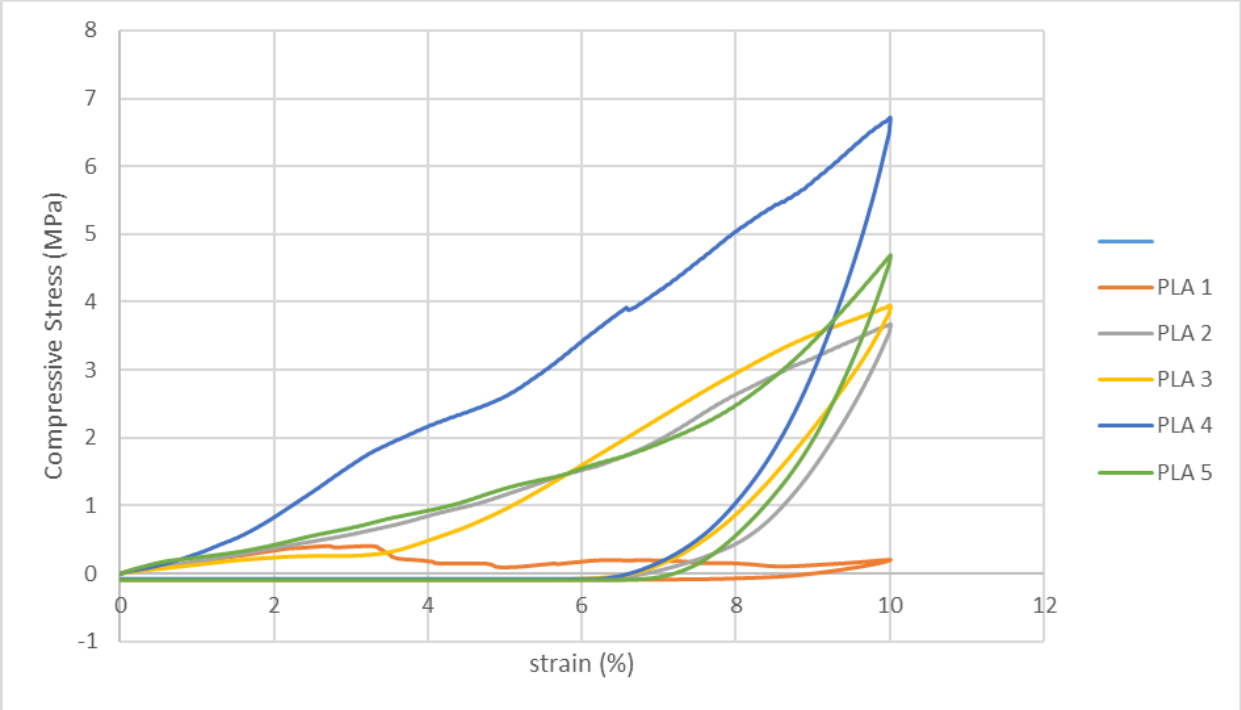

PLA + 8wt% compression.

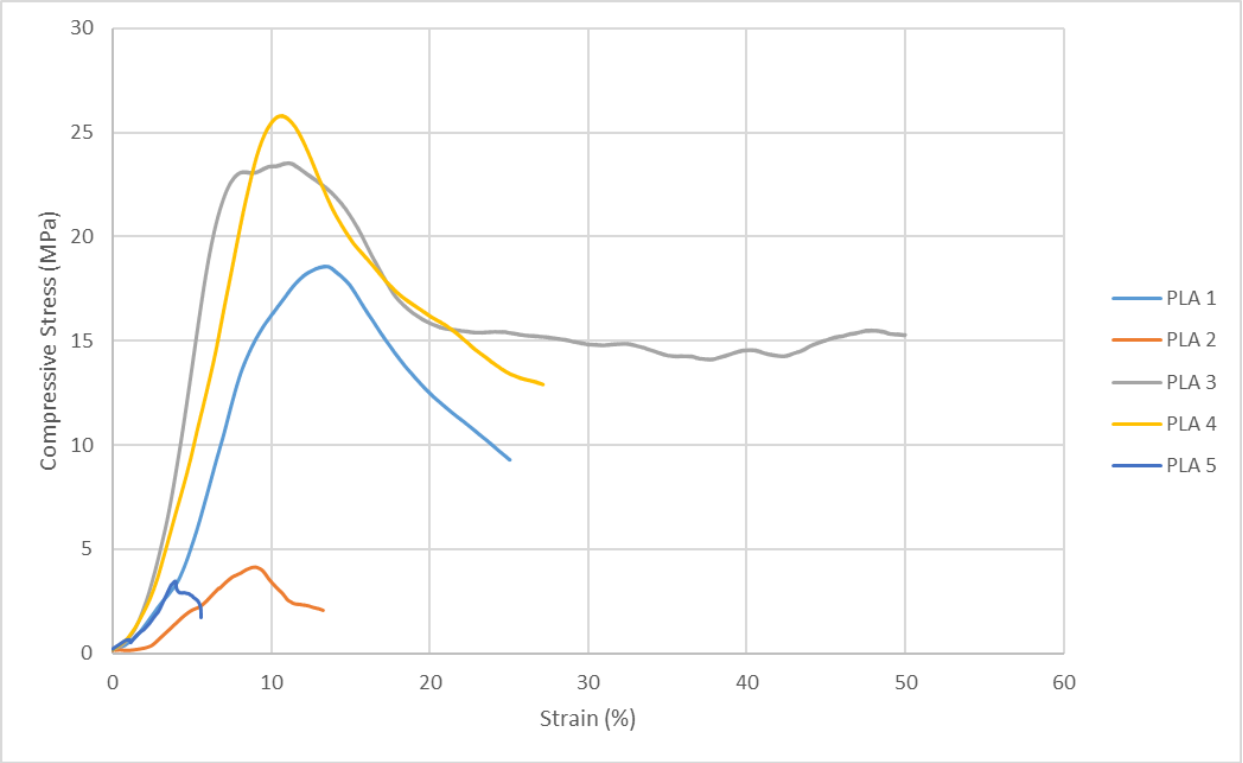

PLA + 8wt% cyclic compression.

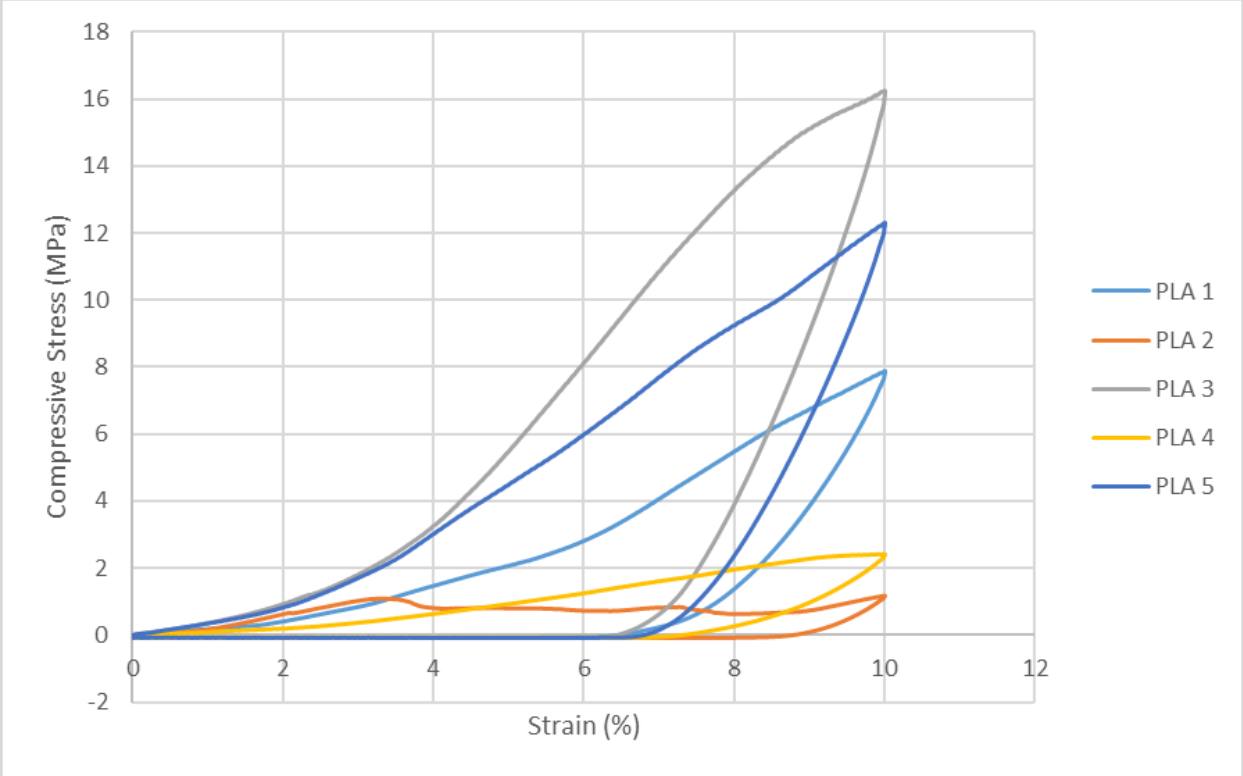

PLA + 10wt% compression.

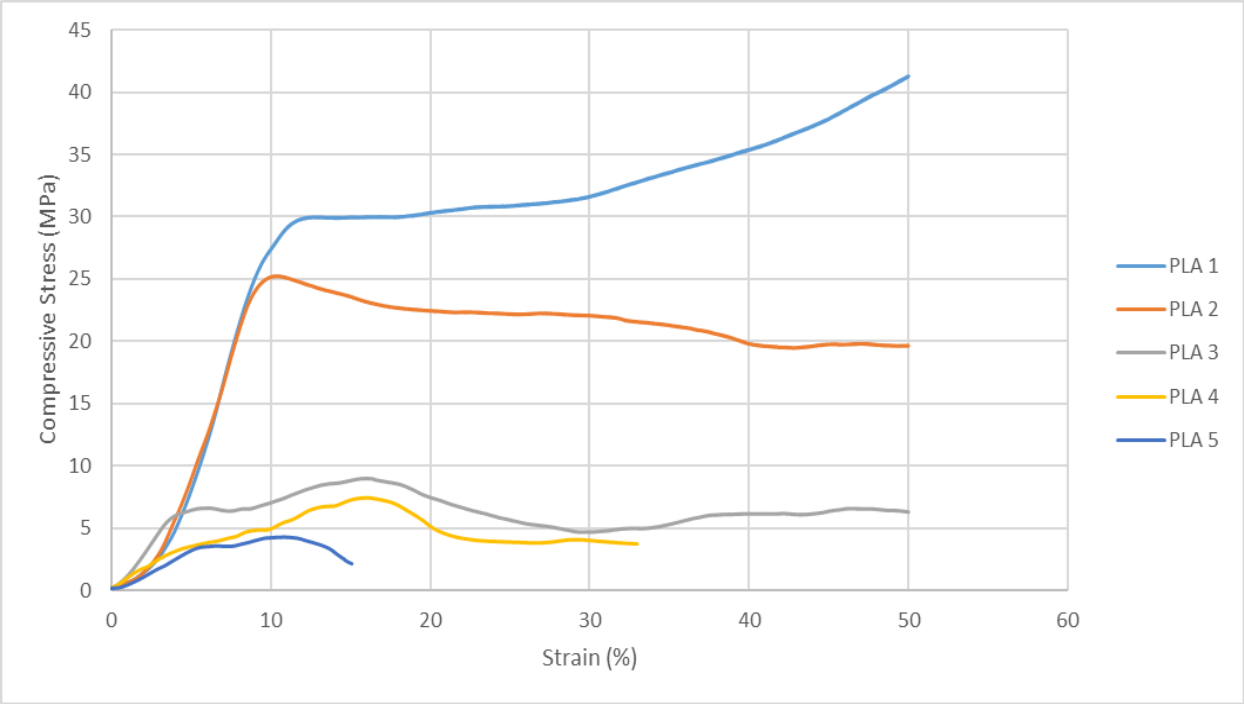

PLA + 10wt% cyclic compression.